



23182936

MICHIGAN STATE UNIVERSITY LIBRARIES



3 1293 00582 0364

**LIBRARY**  
**Michigan State**  
**University**

This is to certify that the

dissertation entitled

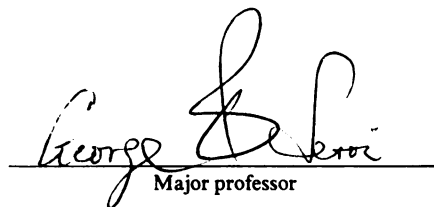
Experimental and Theoretical Studies on  
Didehydrobenzenes and Didehydropyridines

presented by

Hak-Hyun Nam

has been accepted towards fulfillment  
of the requirements for

Ph.D degree in Chemistry

  
Major professor

Date April 14, 1989

**PLACE IN RETURN BOX** to remove this checkout from your record.  
**TO AVOID FINES** return on or before date due.

<b>DATE DUE</b>	<b>DATE DUE</b>	<b>DATE DUE</b>
_____	_____	_____
_____	_____	_____
_____	_____	_____
_____	_____	_____
_____	_____	_____
_____	_____	_____
_____	_____	_____

MSU Is An Affirmative Action/Equal Opportunity Institution

**EXPERIMENTAL AND THEORETICAL STUDIES ON  
DIDEHYDROBENZENES AND DIDEHYDROPYRIDINES**

**By**

**Hak-Hyun Nam**

**A DISSERTATION**

**Submitted to**

**Michigan State University**

**in partial fulfillment of the requirements**

**for the degree of**

**DOCTOR OF PHILOSOPHY**

**Department of Chemistry**

**1989**

5680104

ABSTRACT

Experimental and Theoretical Studies on Didehydrobenzenes  
and Didehydropyridines

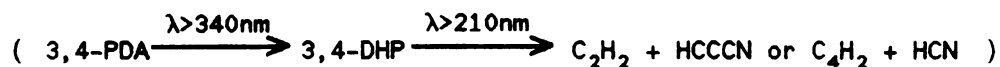
By

Hak-Hyun Nam

Experimental and theoretical investigations on the three isomers of didehydrobenzene (DHB) and the six isomers of didehydropyridine (DHP) are reported. While experimental studies were limited to vicinally didehydrogenated benzene (1,2-DHB) and pyridines (2,3- and 3,4-DHP), all possible isomers were subject to theoretical investigation.

Infrared spectra of 1,2-DHB were recorded following photolysis ( $\lambda > 210$  nm) of matrix isolated phthalic anhydride. Two new vibrational frequencies, at 1355 and 1395  $\text{cm}^{-1}$ , which agree well with our normal coordinate analysis, were identified. Successful isolation of 3,4-DHP in Ar or  $\text{N}_2$  matrices via mild photolysis ( $\lambda > 340$  nm) of 3,4-pyridine dicarboxylic anhydride (3,4-PDA) provided the first direct

evidence of any known didehydroheteroarene. Infrared spectra in the 2000 - 2300  $\text{cm}^{-1}$  region prior to and following controlled photolysis of 3,4-PDA



clearly demonstrate the formation of 3,4-DHP (2085  $\text{cm}^{-1}$ ) and its subsequent decomposition to HCN (2101  $\text{cm}^{-1}$ ) and diacetylene (2185  $\text{cm}^{-1}$ ), or cyanoacetylene (2236  $\text{cm}^{-1}$ ) and acetylene. Ten additional frequencies below 2000  $\text{cm}^{-1}$  were also attributable to 3,4-DHP. The 2,3- isomer could not be isolated under our experimental conditions. The photolysis of 2,3-PDA in  $\text{N}_2$  or Ar matrices leads to rupture of the ring structure, and infrared spectra taken at various time intervals provide no evidence of 2,3-DHP among the photolysis products.

Three different levels of *ab-initio* calculations (RHF, ROHF and GVB) with a 3-21G basis set were carried out for all DHB and DHP isomers with full geometry optimization at each level. The results for DHBs generally agree with previous GVB calculations by Noell and Newton. In contrast to the semi-empirical calculations, there are three local minima for 1,4-DHB; one diradical and two bicyclic structures. The bicyclic 1,3-DHB is located on an inflection point of the GVB potential curve. The ground states of all DHPs except the 2,6- isomer are predicted to be singlets. The stabilities decrease in the order: 3,4-(S) > 2,3-(S)  $\approx$  2,4-(S) > 2,6-(T)

$\approx 2,5-(S) \approx 3,5-(S) \approx 2,6-(S)$ , where (S) and (T) represent singlets and triplets, respectively. The DHP structures are discussed in terms of the effect of electron correlation between the two radical centers and the interaction between the nitrogen lone pair and the two radical centers.

*To My Parents  
and Sook*



## ACKNOWLEDGMENTS

I am grateful to Dr. G. E. Leroi for his support and thoughtful advice throughout my graduate work. Whenever I ran into difficulties, both in research and in personal matters, he was always willing to help me out with very generous understanding.

Without the help of Dr. J. F. Harrison, it would have been impossible to carry out the theoretical calculations presented in this dissertation. I also would like to thank Dr. A. Popov and Dr. J. Allison: they provided me an opportunity to develop my own interest in solution chemistry, signal processing and new matrix isolation techniques.

Mr. R. Haas, electronic technician, was of tremendous help whenever the FTIR spectrometer was in trouble.

Drs. J. Lopez-Garriga and L.-L. Soong were always willing to share their knowledge in science. Mr. M. Sabo spent his valuable time with me to fix the FTIR spectrometer. I am also thankful to the members of the Molecular Spectroscopy group and Theoretical Chemistry Group for their friendship and

cooperation.

Finally, I wish to thank my wife, Sook, for her patience, encouragement and love throughout my graduate career. It would have been impossible to complete this dissertation without her devotion.

Financial assistance from MSU and NSF, and fellowships from SOHIO, MOBAY and H. T. Graham are gratefully acknowledged.

## TABLE OF CONTENTS

	Page
LIST OF TABLES.....	viii
LIST OF FIGURES.....	x
CHAPTER 1 Nomenclature of Didehydrogenated Ring Systems and Methods for their Experimental and Theoretical Studies	
Introduction.....	1
1.1 Formulas and Nomenclature.....	3
1.2 Experimental Method: Matrix Isolation Spectroscopy (MIS).....	6
1.2.1 MIS of Chemical Intermediates.....	6
1.2.2 Photochemical Products of Matrices Containing Reactive Species.....	11
1.2.3 Infrared MIS.....	14
1.2.4 Identification of Photochemically Generated Reactive Species.....	15
1.2.5 Experimental Section.....	19
1.3 Theoretical Considerations: <i>Ab-Initio</i> Calculations.....	22
1.3.1 Effect of Two Electron Interactions in Didehydrobenzenes and Didehydropyridines.....	23
1.3.2 Wave Functions for DHB and DHP.....	23
1.3.3 Qualitative Discussions of Wave Functions for	

	DHB and DHP.....	28
1.3.4	Quantitative Calculation: <i>Ab-Initio</i> SCF	
	Methods.....	31
1.3.5	Computation.....	33
	References.....	37
CHAPTER 2 Didehydrobenzenes		
	Introduction.....	40
2.1	1,2-Didehydrobenzene (1,2-DHB).....	43
2.1.1	The Ground Electronic State of 1,2-DHB.....	43
2.1.2	The Ionization Energies and The Heat of Formation of 1,2-DHB.....	46
2.1.3	Electronic Spectra of 1,2-DHB.....	52
2.1.4	Vibrational Frequencies of 1,2-DHB.....	53
2.1.5	The C≡C Stretching Frequency of 1,2-DHB and Other Angle Strained Cycloalkynes.....	58
2.1.6	The Singlet Geometry of 1,2-DHB.....	61
2.1.7	The Triplet Geometry of 1,2-DHB.....	65
2.2	1,3-Didehydrobenzene (1,3-DHB).....	67
2.2.1	Experimental Studies.....	67
2.2.2	Theoretical Studies.....	68
2.3	1,4-Didehydrobenzene (1,4-DHB).....	73
2.3.1	Experimental Studies.....	73
2.3.2	Theoretical Studies.....	74
2.4	Summary and Conclusions.....	80
	References.....	84

CHAPTER 3	Didehydropyridines	
	Introduction.....	90
3.1	3,4-Didehydropyridine (3,4-DHP).....	94
3.1.1	Infrared Spectrum.....	94
3.1.2	Theoretical Calculation.....	99
3.2	2,3-Didehydropyridine (2,3-DHP).....	107
3.2.1	Infrared Spectra of The Photolyzed Products of 2,3-PDA.....	107
3.2.2	Theoretical Calculation.....	114
3.3	2,4-Didehydropyridine (2,4-DHP).....	119
3.3.1	Theoretical Calculation.....	119
3.4	2,5-Didehydropyridine (2,5-DHP).....	122
3.4.1	Theoretical Calculation.....	122
3.5	2,6-Didehydropyridine (2,6-DHP).....	127
3.5.1	Theoretical Calculation.....	127
3.6	3,5-Didehydropyridine (3,5-DHP).....	129
3.6.1	Theoretical Calculation.....	129
3.7	Summary and Conclusion.....	131
	References.....	134

1

## LIST OF TABLES

Table	Page	
2.1	45	Singlet-Triplet energy separation of 1,2-DHB
2.2	47	Experimental IEs of 1,2-DHB
2.3	48	Calculated IEs of 1,2-DHB
2.4	51	The enthalpy of formation of 1,2-DHB (298K)
2.5	57	Infrared spectrum ( $\text{cm}^{-1}$ ) of 1,2-DHB in matrices
2.6	64	Geometrical parameters of singlet 1,2-DHB
2.7	66	Geometrical parameters of triplet 1,2-DHB
2.8	71	Geometrical parameters of 1,3-DHB
2.9	72	Singlet-triplet separation of 1,3-DHB
2.10	77	Geometrical parameters of 1,4-DHB
2.11	78	The overlap population for 1,4-DHB
2.12	79	Singlet-triplet separation of 1,4-DHB
2.13	81	Relative energies (kcal/mole) of DHBs
3.1	96	Infrared bands ( $\text{cm}^{-1}$ ) resulting from photolysis of 3,4-PDA in an $\text{N}_2$ matrix at 13 K
3.2	100	Geometrical parameters of 3,4-DHP
3.3	102	Geometrical parameters of pyridine
3.4	103	Vibrational frequencies of pyridine

- 3.5        104    Comparison of calculated (RHF/3-21G) and  
              experimental frequencies ( $\text{cm}^{-1}$ ) for  
              3,4-DHP
- 3.6        106    Calculated vibrational frequencies ( $\text{cm}^{-1}$ )  
              of 3,4-DHP
- 3.7        109    Infrared bands ( $\text{cm}^{-1}$ ) resulting from  
              photolysis of 2,3-PDA in an  $\text{N}_2$  matrix at  
              13K
- 3.8        115    Geometrical parameters of 2,3-DHP
- 3.9        117    C $\equiv$ C bond length ( $\text{\AA}$ ) and vibrational  
              frequency of vicinally didehydrogenated  
              aromatic systems
- 3.10       120    Geometrical parameters of 2,4-DHP
- 3.11       123    Geometrical parameters of 2,5-DHP
- 3.12       128    Geometrical parameters of 2,6-DHP
- 3.13       130    Geometrical parameters of 3,5-DHP
- 3.14       132    Relative  $\Delta E_T$  (kcal/mole) values of DHPs  
              with respect to GVB energy of 3,4-DHP



## LIST OF FIGURES

Figure	Page	
1.1	8	Typical vacuum system for matrix isolation
1.2	9	Closed cycle cryostat
1.3	10	Typical infrared matrix isolation experiment
1.4	13	Photolysis apparatus for matrix studies
1.5	18	Typical characterization route for matrix isolated species
1.6	24	Possible configurations arising from the occupancy of two MOs by two electrons
1.7	35	Various levels of <i>ab-initio</i> calculations
2.1	60	C≡C stretching frequency of cis-bent acetylene calculated at the RHF/3-21G and GVB/3-21G level
3.1	97	IR spectra of 3,4-PDA and its photolyzed products in the 2050 - 2300 cm <sup>-1</sup> region in an N <sub>2</sub> matrix at 13 K: (a) 3,4-PDA; (b) after 100 min photolysis through water and λ>340 nm filter (The peak at 2281 cm <sup>-1</sup> is due to <sup>13</sup> CO <sub>2</sub> ); (c) following additional 30 min photolysis with λ>210nm.

- 3.2 98 Difference spectrum of 3,4-PDA before and after mild photolysis. \* indicates a band to diacetylene.
- 3.3 101 Total atomic charge of 3,4-DHP and 1,2-DHB calculated at the GVB/3-21G level.
- 3.4 108 Three types of growth-curve when 2,3-PDA is irradiated with  $\lambda > 300\text{nm}$  light.
- 3.5 112 IR spectra of the photolyzed products of 2,3-PDA in the  $2050 - 2300\text{ cm}^{-1}$  region in an  $\text{N}_2$  matrix at 13 K: (a) 10 hour photolysis through water filter and  $\lambda > 340\text{ nm}$  filter; (b) 2 hour photolysis after (a) with  $\lambda > 300\text{ nm}$  filter; (c) 1.5 hour photolysis after (b) with  $\lambda > 210\text{ nm}$  filter.
- 3.6 126 Approximate MOs of 2,5-DHP and 1,4-DHB

# CHAPTER 1

## Nomenclature of Didehydrogenated Ring Systems and Methods for Their Experimental and Theoretical Studies

### *Introduction*

Nomenclature should not only unambiguously define the function and structural formula of a molecule, but also be used consistently. Various names referring to didehydrogenated aromatic or heteroaromatic systems exist in the literature<sup>1-9</sup>. However, they are sometimes inadequate to depict their structural formula or inexplicit in characterizing their function<sup>5a</sup>. Thus it is necessary to establish a consistent nomenclature for didehydrogenated ring systems prior to the main discussion. In the first section of this chapter, merits and disadvantages of widely-used nomenclature for didehydrogenated ring systems will be compared and the nomenclature which will be used in this dissertation will be selected.

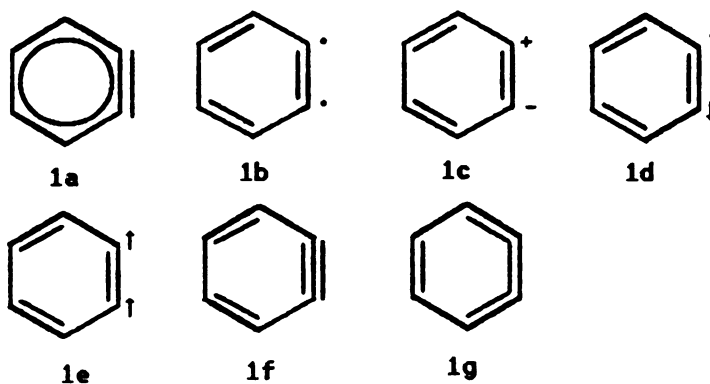
Since didehydrogenated rings are highly reactive and difficult to isolate for spectroscopic investigation<sup>1-9</sup>, few experimental techniques can be used to determine their structure. Matrix isolation, which traps a desired unstable

species in a solid inert gas via pyrolysis, electric discharge or photolysis of a precursor prior to or after codeposition with an inert gas for subsequent spectroscopic investigation, is one of the most effective experimental methods<sup>11-15</sup>. The second section is devoted to explaining the basic notions of matrix isolation spectroscopy and includes the experimental details which are only relevant to this thesis.

While experimental studies in this work are limited to vicinally didehydrogenated benzene and pyridines<sup>21</sup>, all their possible isomers are subject to theoretical investigation. These theoretical results provide valuable information regarding the structures and the detailed course of chemical reactions of those reactive intermediates where experimental evidence does not exist or is inconclusive<sup>26</sup>. However, depending on the method of calculation, results are of large variance and in some cases they lead to an entirely erroneous conclusion<sup>26</sup>. The third section will discuss the reliability and limitations of various methods of *ab-initio* molecular orbital calculations for didehydrogenated ring systems.

### 1.1. Formulas and nomenclature

In order to determine the nomenclature of didehydrogenated ring intermediates, two factors may have to be considered: (1) the representative canonical formula of a molecule and (2) the relation to its parent compound. For example, removal of two adjacent hydrogen atoms from benzene may lead to several canonical formulas of **1a - 1g**<sup>5</sup>. Certainly, all of these structures except triplet **1e** are contributors to the same resonance hybrid.



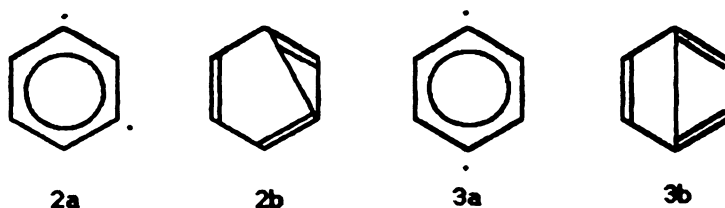
However, the name of this compound is heavily dependent on which canonical formula is regarded as a representative one. While this compound is conventionally called *benzyne*<sup>1,4</sup>, emphasizing that the parent compound is benzene and the two dehydrogenated centers may form a partial triple bond like **1a**, Chemical Abstracts names it as *1,3-cyclohexadiene-5-yne*, taking **1f** as its canonical formula. If **1g** is selected as a canonical formula, the name would be *1,2,3,5-cyclohexatetraene*. If any formula from **1b - 1e** is chosen, we might

have to use other names to represent this compound. Thus naming this compound by a certain canonical formula cannot provide a consistent nomenclature without firm theoretical and experimental justification.

Even with this complication, resonance structure 1a or Kékulé structure 1f are the most popular representations of vicinally didehydrogenated benzene<sup>2-5</sup>, and other aromatic and heteroaromatic systems are also depicted in a similar way<sup>6-9</sup>. To denote a partial triple bond in these systems, the suffix '-ene' of the parent arene or heteroarene is replaced with '-yne', namely *aryne*<sup>1</sup> and *heteroaryne*<sup>7</sup>. For example, *benzene* becomes *benzyne*, *pyridine* becomes *pyridyne* and *naphthalene* becomes *naphthalyne*, etc.

The suffix '-yne' of *aryne* or *heteroaryne* is meaningful only when two dehydrogenated centers are vicinal, whereas in much of literature the terms '*aryne*' or '*heteroaryne*' are equivalently used to imply all didehydrogenated arenes or heteroarenes<sup>5</sup>. For example, 2a or 2b is called *1,3-benzyne* or *meta-benzyne*, 3a or 3b is called *1,4-benzyne* or *para-benzyne*, etc.

However, extension of the terms '*aryne*' or '*heteroaryne*' to the non-adjacent didehydrogenated compounds, such as 2a-3b, inadequately relates the nomenclature to the structure of



those compounds.

The most consistent nomenclature for dehydrogenated ring systems seems to be *prefix-didehydro-parent*, where the prefix indicates the sites of dehydrogenation<sup>5,9</sup>. For example, instead of *1,3-benzyne* it becomes *1,3-didehydrobenzene*, *3,4-pyridyne* becomes *3,4-didehydropyridine*, etc. This nomenclature not only eliminates the unwarranted structural implication associated with the '-yne' suffix, but also includes all possible canonical resonance formulas. A further advantage of '-didehydro' nomenclature is that the name clearly indicates the bidentate reactivity of these intermediates.

In this dissertation, therefore, the most consistent '-didehydro' nomenclature will be used to denote didehydrogenated arenes or heteroarenes. For the sake of convenience, resonance or Kékulé canonical structures will represent any didehydroarenes or didehydroheteroarenes without any implication as to bonding, geometry, charge distribution, or electron multiplicity.

## ***1.2. Experimental Method: Matrix Isolation Spectroscopy (MIS)***

Since the inception of MIS by Pimentel in 1954 to study free radicals<sup>10</sup>, the technique has been widely applied to many areas of chemistry<sup>11-15</sup>. They include: intermolecular forces, conformational studies, transition metal atom chemistry in relation to its catalytic ability, molecular complexes and free radicals and unstable molecules. Spectroscopic methods used for matrix isolated samples now cover most areas of spectroscopy, namely IR, Raman, ESR, UV, magnetic circular dichroism, Mössbauer, luminescence, etc. Among the various applications of MIS listed above, vibrational spectroscopic investigation of chemical intermediates in a matrix will be discussed in this section, with focus on their photochemical generation, analysis of observed frequencies and the determination of their possible structures.

### **1.2.1. MIS of Chemical Intermediates**

In order to spectroscopically investigate an unstable chemical intermediate, we need to ensure at least two important experimental conditions: (1) the desired species should survive long enough for spectroscopic measurement, and (2) the desired species must interact minimally with its environment. MIS has been demonstrated to be one of the most



effective methods to study an unstable species. A very low concentration of a reactive species or its precursor (guest) is frozen with an excess volume of an inert gas (host) on a very cold ( $4 \sim 20$  K) spectroscopic window (e.g. alkali halide for IR, quartz for UV, sapphire rod for ESR, etc.) which maintains its low temperature by thermal contact with the cryogenic device. High host-to-guest ratios ( $100 \sim 10000$ ) are required to isolate the highly reactive intermediates, and low temperatures are necessary to prepare a rigid matrix to prohibit their intermolecular reactions and to stabilize them for routine spectroscopic measurement.

There are three basic units of instrumentation required to perform an MIS experiment: (1) vacuum system, (2) cryogenic device and (3) spectrometer. The use of a good vacuum system ( $10^{-5} \sim 10^{-6}$  Torr) is required to insulate the cryogenic temperature, to protect the matrix from contamination, and to prepare the matrix gas of high purity (Figure 1.1). Three types of cryogenic devices - double dewar cryostat, Joule-Thomson open cycle cryostat and closed cycle cryostat are widely used to maintain the cold temperature of the deposition window, through thermal contact. For most MIS experiments, a closed cycle cryostat is the most popular device because it can afford a wide range of temperature (8 - 300K) without consuming expensive liquid refrigerants (Figure 1.2). Figure 1.3 shows the schematics of an MIS experiment.

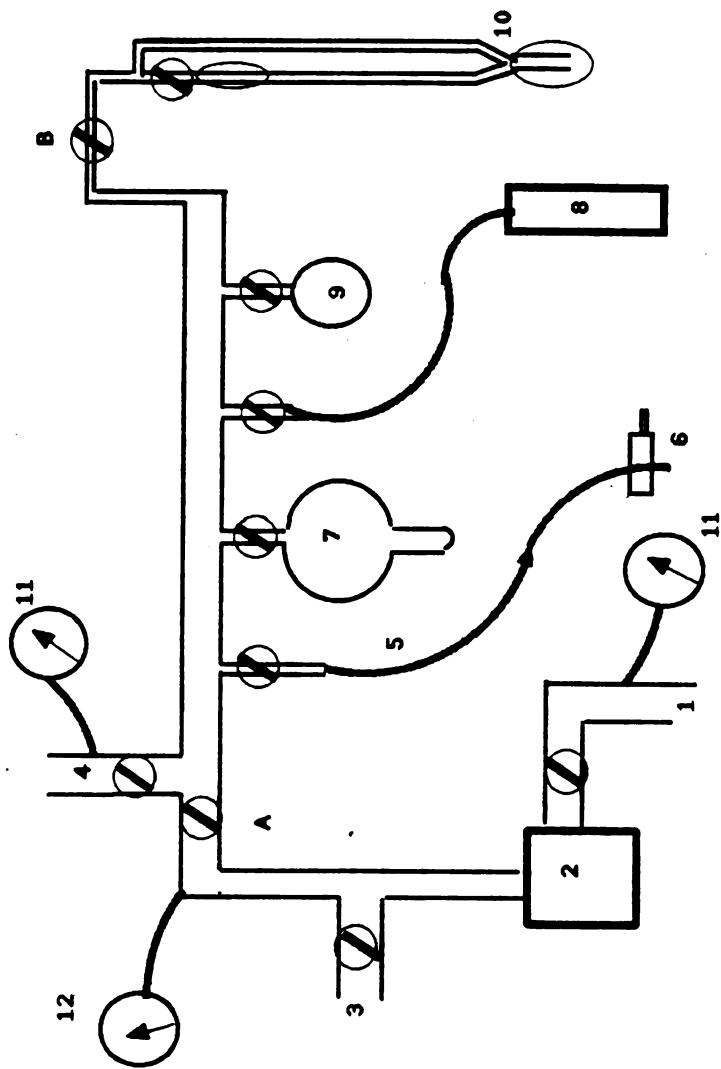


Fig. 1.1. Typical vacuum system for matrix isolation

1 to mechanical pump; 2 diffusion pump; 3 to cryostat; 4 to mechanical pump; 5 sample line; 6 needle valve; 7 3-liter bulb; 8 matrix gas tank; 9 gas or liquid sample; 10 manometer; 11 thermocouple gauge; 12 ionization gauge;  $V_{AB}$  volume between stopcocks A and B.

 denote stopcocks.

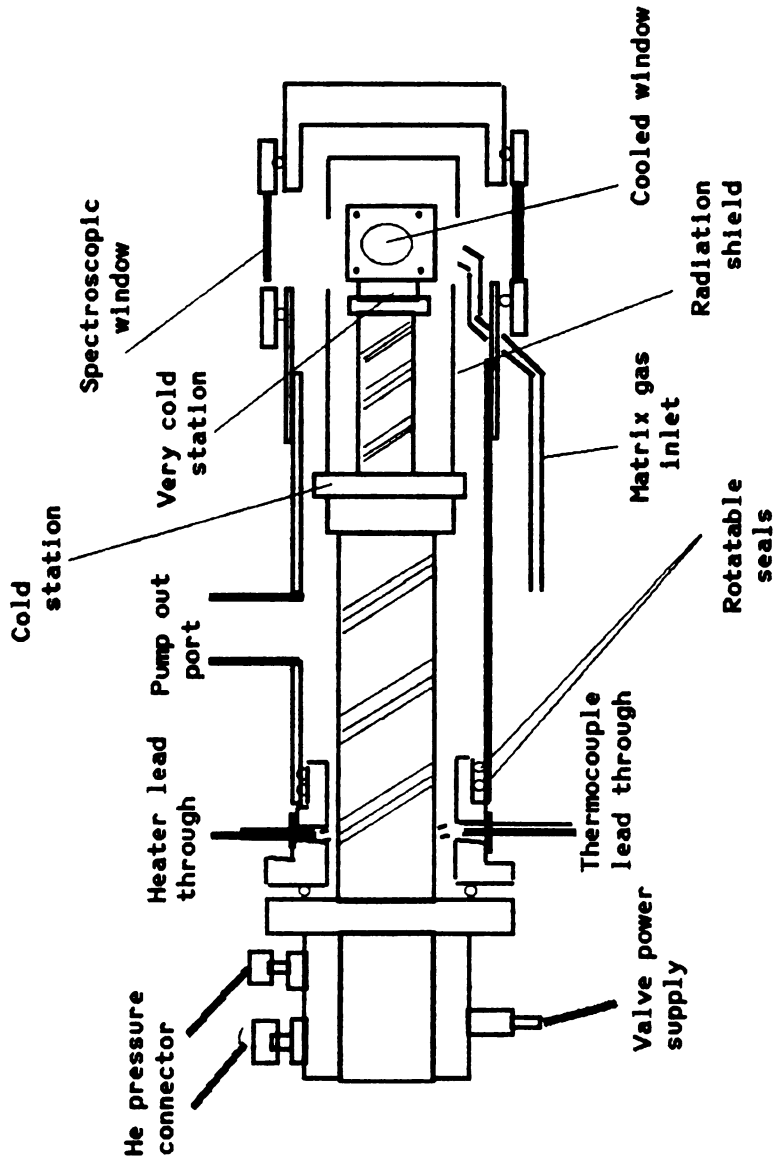


Fig. 1.2 Closed cycle cryostat

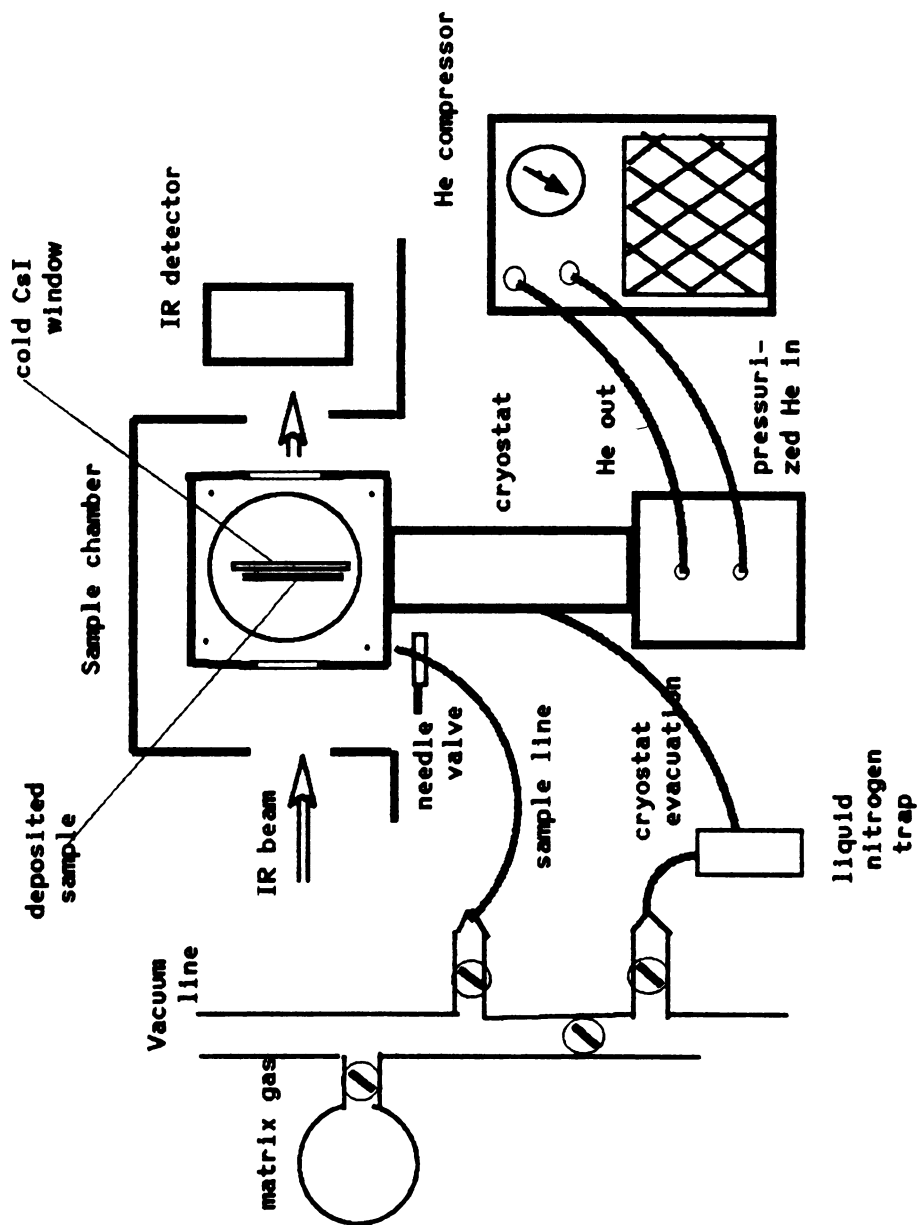


Fig. 1.3. Typical infrared matrix isolation experiment



### 1.2.2 Photochemical Production of Matrices Containing Reactive Species

Commonly used techniques for generation of the reactive species are pyrolysis, microwave discharge or mass spectrometric decomposition of the precursor prior to codeposition with inert hosts, or photolysis of relatively stable precursors after they are isolated at low temperature<sup>11,12</sup>. In this research we have employed the photolytic method because generation of the transients can be most easily controlled, and the extent of the reaction in a matrix can be most easily followed, with this technique.

To prepare the matrix isolated precursor, various sampling techniques can be used. Gaseous molecules may be premixed in the desired ratio with an inert gas in a vacuum system. This mixture is then sprayed via a needle valve onto the cold deposition window. Stable liquid or solid samples that can vaporize without decomposition are supplied to the matrix using suitable heating units. This can be done by heating the material to an appropriate temperature with some type of furnace. The heated material is then swept by an inert carrier gas to the cold deposition window through a single nozzle. Alternatively, two jets consisting of the sample vapor and an inert gas deposit the matrix simultaneously. Organic substances can be evaporated in a simple glass tube

with a heating wire; metals and other inorganic substances can be heated by the use of a Knudsen cell or high-powered Nd:YAG laser<sup>12,15</sup>.

The photolysis of a precursor can only be efficiently carried out using radiation that is strongly absorbed by the molecule, and that has sufficient energy to break chemical bonds. Except for a few colored precursors, in general ultraviolet radiation is required. As a source of ultraviolet radiation, a high pressure mercury or mercury-xenon lamp with various optical filters is most commonly used. Fig. 1.4 shows the typical photolysis apparatus for matrix studies<sup>11</sup>.

The photolytic decomposition of a precursor in general produces two or more fragments, and one of them may be the desired product. Identification of the desired species, however, is often intricate because of the possible isomerization of a precursor or the recombination of fragments which are essentially in contact in the same trapping site<sup>11</sup>. Careful selection of a precursor, which might produce small atom fragments which may diffuse out of the matrix cage, or which produces reactive fragments but leaving groups which are chemically inert to the desired species, can minimize the complication of recombination reaction. As an example, photolysis of diazoacetonitrile in an N<sub>2</sub> matrix produces HCCN free radical and N<sub>2</sub> which can

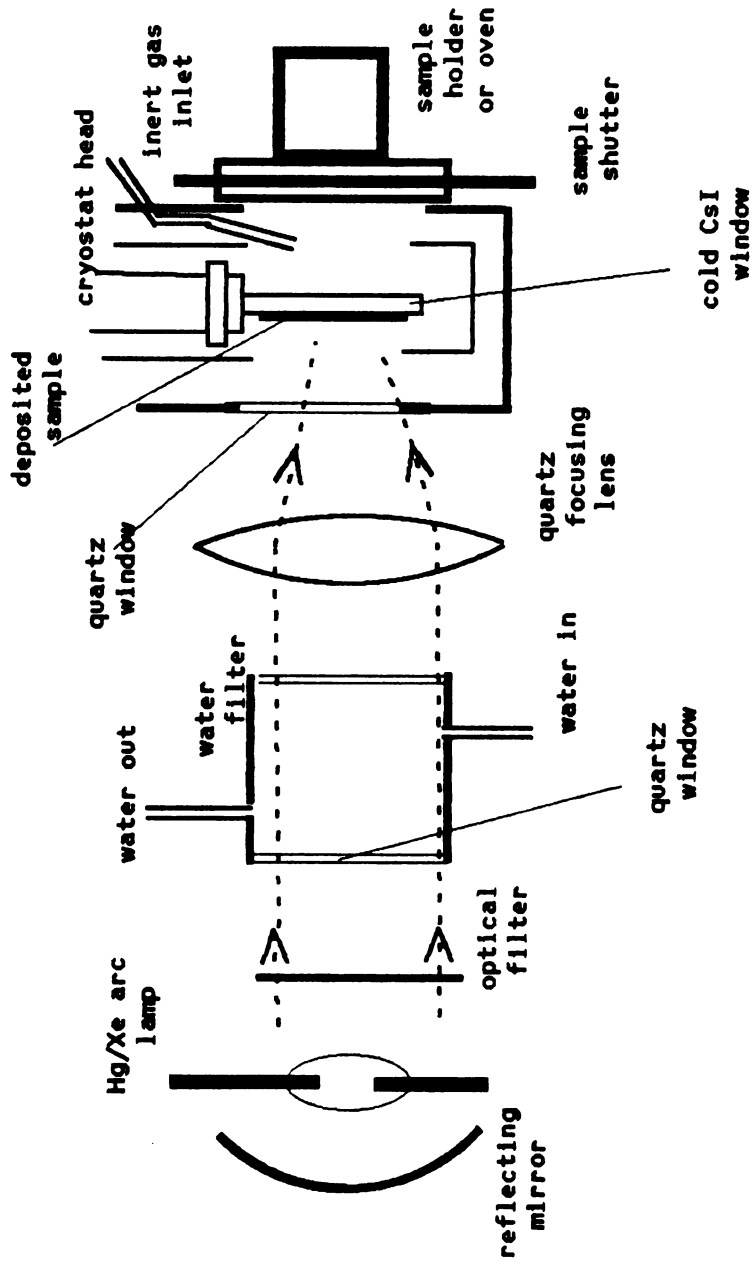


Fig. 1.4. Photolysis apparatus for matrix studies



behave as a new part of the matrix cage (HCNNCN --uv--> HCCN +N2)<sup>16</sup>.

### 1.2.3. Infrared MIS

Although many kinds of spectroscopic methods have been applied to matrix isolated species, the majority of investigations continue to rely on infrared absorption as the principal means of detection and characterization<sup>14</sup>. The absence of hot bands and rotational structure in the vibrational spectrum of most matrix isolated molecules due to the low temperature and rigid environment greatly sharpens the fundamental frequencies and allows vibrational assignments to be made with greater confidence and accuracy<sup>13</sup>. Even though host-guest interaction causes some shift of fundamental frequencies from those of the gas phase, they are usually in a tolerable range (normally within 1 percent). Uneven multiple trapping sites in a matrix will generally lead to splitting of the fundamentals<sup>11</sup>. Aggregation of the guest to multimers also complicates the matrix spectra. These problems, however, can be identified by carefully annealing the matrix (raising the temperature within 30% to 50% of the host's melting point), changing the deposition rates, or varying the host-to-guest ratios of a matrix. Moreover, the recent development of Fourier transform interferometers greatly extends the detection limit for low

concentration matrix isolated samples<sup>14</sup>.

1.2.4 Identification of Photochemically Generated Reactive species

When a matrix isolated precursor is photolyzed with an appropriate wavelength, infrared bands due to the precursor begin to decrease in intensity and new infrared bands due to product species begin to grow, as the extent of reaction increases. The assignment of new bands to a particular reactive species then can be made more or less empirically using the methods described below.

- (1) Examine the intensity of new bands versus duration of photolytic radiation. This process is particularly important when photolysis of a precursor produces more than one product. If this curve-of-growth analysis is done carefully it is possible to distinguish peaks that vary in the same way from all others.
  
- (2) Warm the matrix above 50% of its melting point (e.g. Ar: 42K, N<sub>2</sub>:32K, etc.) to allow diffusion-controlled reaction. Above about 50% of the melting point the matrix loses its rigidity and diffusion of trapped species will occur. Infrared bands of reactive species, if formed, will then disappear during this diffusion operation,

which is followed by recooling of the annealed matrix.

- (3) Examine the photochemical behavior of the products upon continued irradiation with various wavelengths. Isomerization reactions or further photochemical decomposition of the products can be induced by this process. This photochemical experiment not only helps to assign the new infrared bands to a particular species, but also elucidates the detailed photochemical mechanism of the products.
- (4) Use isotopically substituted precursors to assign the observed vibrational frequencies to the specific normal modes of the product.
- (5) Design another experiment that can produce the same reactive species with a different precursor. This may not always be possible, but is necessary to establish irrefutable evidence for the proposed reactive species.

Once we classify a group of frequencies as belonging to a certain reactive species based on the above procedures, a number of possible structures may be postulated to explain the observed vibrational frequencies. The most likely structure of the target compound is then deduced from the group frequency analysis, normal coordinate analysis and

quantum chemical calculations. Figure 1.5 summarizes schematically a typical characterization route for a matrix isolated chemical intermediate.

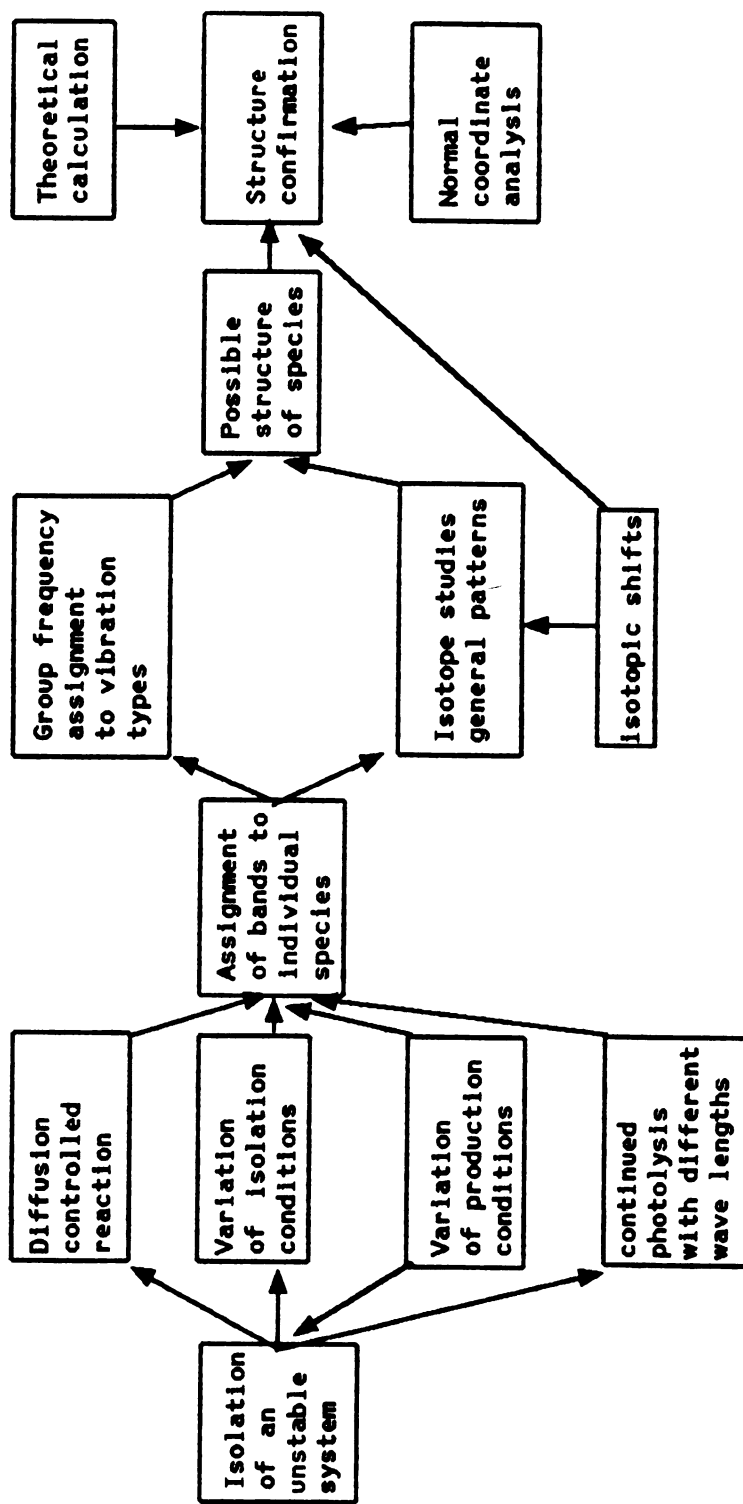
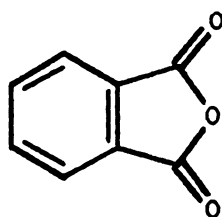


Fig. 1.5. Typical characterization route for matrix isolated species

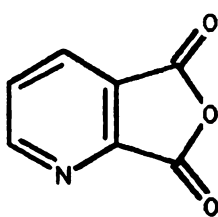


### 1.2.5 Experimental section

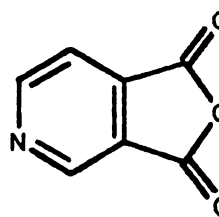
Our primary interest was to isolate and characterize the vicinally didehydrogenated benzene (*1,2-didehydrobenzene*) and pyridines (*2,3- and 3,4-didehydropyridine*)<sup>21,22</sup>. To generate these intermediates, their corresponding dicarboxylic anhydrides (4, 5 and 6) were used as precursors.



4  
phthalic  
anhydride



5  
2,3-pyridine  
dicarboxylic  
anhydride



6  
3,4-pyridine  
dicarboxylic  
anhydride

Carbon monoxide and carbon dioxide are easily fragmented out from a dicarboxylic anhydride upon pyrolysis or electron impact to form didehydrogenated compounds<sup>17-20</sup>, and the same tendency may also be expected upon photolysis. Since both carbon monoxide and dioxide have well characterized infrared bands, the appearance of their infrared bands and the variation of their intensities can be used as excellent indicators of photochemical reactions. Commercially obtained precursors (Aldrich, 95 - 97%) were further purified by vacuum sublimation before use.

Precursors were placed in an L-shaped glass tube sample holder (3/4 inch diameter) wrapped with heating tape; the heating temperature was regulated with a Variac and a thermocouple embedded underneath the heating tape. This glass tube was connected to a specially-designed shutter vacuum flange which can seal the sample holder from the cryostat cell following the deposition (Fig. 1.4).

Nitrogen or argon gas (Matheson, 99.999%) was initially collected in a 3 liter bulb which is attached to a vacuum line. The rate of deposition and the amount of host gas deposited were measured by a mercury manometer. In this measurement the ideal gas equation  $(\Delta P/\Delta t)V=(\Delta n/\Delta t)RT$  was used, where  $V$  is the total volume of that part of vacuum system ( $V_{AB}$  of Fig. 1.1) plus the sample outlet line which contains matrix gas during deposition. The rate of sample flow was controlled by means of a micrometer needle valve on the sample outlet line which leads to the cryostat (Air Products CS202 Displex cryostat). The cryostat head consists of two KBr windows for IR measurement and one quartz window perpendicular to the IR windows for photolysis (Fig. 2.3). The vacuum shroud of the cryostat is rotated for an IR measurement after the photolysis through the quartz window.

Since precursors were codeposited by sublimation (with nitrogen or argon gas (flow rate 2 mmole/min), exact



guest-to-host ratios could not be measured. Photolysis was conducted with a high pressure 200 W Hg/Xe lamp equipped with a water filter and various cutoff filters (Fig. 1.4). Infrared spectra of the precursor and photolyzed products at 13K were recorded with a BOMEM DA3.01 interferometric spectrometer (Fig. 1.3).

As summarized in section 1.2.4, growth curves for newly appearing bands, diffusion-controlled reaction studies and photochemical behavior upon continued irradiation with different wavelengths were carefully examined. The results of these experiments and their interpretations will be discussed in the following chapters.

### *1.3. Theoretical Considerations: Ab-Initio Calculations*

Although we have successfully isolated and characterized some reactive chemical intermediates in inert matrices, the data we can obtain using limited spectroscopic methods may explain only a fraction of their properties. Moreover, many reactive intermediates are too unstable to live sufficiently long for spectroscopic investigation, even with the distinctive advantages of the matrix isolation method. Another difficulty is that it is not always possible to interpret the experimental observations on certain reactive intermediates since they tend to violate the usual concept of chemical bonding. Thus, experimental studies on many chemical intermediates are rather limited or inconclusive.

Theoretical methods, such as the various levels of ab-initio molecular orbital calculation utilized in this dissertation, can provide information on various properties of a reactive intermediate beyond the limited scope of experimental observation<sup>26</sup>. For instance, geometry, electronic structure and energetics of a reactive intermediate and related transition structures and reaction paths, and molecular properties such as dipole moment, polarizability and vibrational frequencies may all be calculated using these methods. Like all experimental data, however, the reliability of the results from various levels

of ab-initio calculation must be cautiously assessed.

### 1.3.1. Effect of Two Electron Interactions in Didehydrobenzenes and Didehydropyridines

Removal of two hydrogen atoms from a parent benzene or pyridine ring systems leaves two electrons and two orbitals coplanar with the parent ring which could conceivably interact in a variety of ways. They may strongly interact to introduce a new bond between the two dehydrogenated carbon centers, or weakly interact through-space or through-bond as either a singlet or a triplet diradical<sup>30</sup>. Whatever type of interaction is involved between the two odd electrons it will deform and strain the equilibrium ring geometry of the parent compound. The reactivity of a didehydrogenated ring is often measured in terms of this ring strain energy (RSE)<sup>27b</sup>. Thus it is the interaction between the two odd electrons that primarily accounts for the physical and chemical properties - such as optimum geometry, ground state spin multiplicity and chemical reactivity - of didehydrobenzenes (DHB) and didehydropyridines (DHP).

### 1.3.2. Wave Functions for DHB and DHP

If we place all core electrons of DHB and DHP in closed shell configurations while the two odd electrons occupy two

MOs which are approximately symmetric and antisymmetric combinations of the two radical lobes  $n_1$  and  $n_2$

$$\psi_1 \approx n_1 + n_2 \quad (1)$$

$$\psi_2 \approx n_1 - n_2 \quad (2)$$

then there are six possible ways to place the two electrons in the two MOs as shown in Figure 1.6. The relative positions of  $\psi_1$  and  $\psi_2$  in Figure 1.6 are not intended to imply their actual energy levels. While  $\psi_1$  normally has lower energy than  $\psi_2$ , owing to positive overlap between two lobe orbitals ( $\langle n_1 | n_2 \rangle \geq 0$ ), through-bonding interaction can reverse this order if  $\langle n_1 | n_2 \rangle$  becomes negative (e.g. 1,4-DHB)<sup>30</sup>.

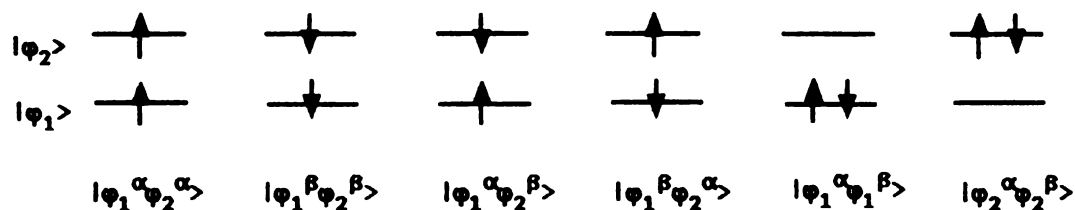


Figure 1.6. Possible configurations arising from the occupancy of two MO's by two electrons.

Of the six electronic conformations, proper combination of spatial and spin eigenfunctions give rise to one triplet and three singlet Hartree-Fock (HF) wave functions as follows:

$$|{}^3\Psi_1\rangle = \begin{cases} A [ \{\text{core}\} \varphi_1 \varphi_2 (\alpha\alpha) ] \\ A [ \{\text{core}\} \varphi_1 \varphi_2 (\alpha\beta + \beta\alpha) ] \\ A [ \{\text{core}\} \varphi_1 \varphi_2 (\beta\beta) ] \end{cases} \quad (3)$$

$$|{}^1\Psi_2\rangle = A [ \{\text{core}\} \varphi_1 \varphi_2 (\alpha\beta - \beta\alpha) ] \quad (4)$$

$$|{}^1\Psi_3\rangle = A [ \{\text{core}\} \varphi_1 \varphi_1 \alpha\beta ] \quad (5)$$

$$|{}^1\Psi_4\rangle = A [ \{\text{core}\} \varphi_2 \varphi_2 \alpha\beta ] \quad (6)$$

where  $A$  is the antisymmetrizer and the superscripts on  $\Psi$  denote the spin multiplicity. Corresponding HF energies of these states are expressed in terms of one-electron energies  $h_{ii}$  ( $=\langle\varphi_i(1)|h(1)|\varphi_i(1)\rangle$ ), Coulomb repulsion integrals  $J_{ij}$  ( $=\langle\varphi_i(1)\varphi_j(2)|r_{12}^{-1}|\varphi_j(1)\varphi_i(2)\rangle$ ) and exchange integrals  $K_{ij}$  ( $=\langle\varphi_i(1)\varphi_j(2)|r_{12}^{-1}|\varphi_j(1)\varphi_i(2)\rangle$ ):

$${}^3E_1 = E_c + h^c_{11} + h^c_{22} + J_{12} - K_{12} \quad (3')$$

$${}^1E_2 = E_c + h^c_{11} + h^c_{22} + J_{12} + K_{12} \quad (4')$$

$${}^1E_3 = E_c + 2h^c_{11} + J_{11} \quad (5')$$

$${}^1E_4 = E_c + 2h^c_{22} + J_{22} \quad (6')$$

where

$$h^c_{ii} \equiv h_{ii} + \sum_p^{\text{closed}} (2J_{pi} - K_{pi}) \quad (7)$$

and

$$E_c \equiv 2 \sum_p^{\text{closed}} h_{pp} + \sum_{p,q}^{\text{closed}} (2J_{pq} - K_{pq}) \quad (8)$$

For geometries where  $|^1\Psi_3\rangle$  and  $|^1\Psi_4\rangle$  are allowed to interact, which is the general case for DHB and DHP, these MOs can be mixed by appropriate linear combinations<sup>23,24</sup>:

$$|^1\Psi_5\rangle = c_1|^1\Psi_3\rangle - c_2|^1\Psi_4\rangle \quad (9)$$

$$|^1\Psi_6\rangle = c_1|^1\Psi_3\rangle + c_2|^1\Psi_4\rangle \quad (10)$$

with corresponding energies

$${}^1E_5 = E_c + c_1^2(2hc_{11} + J_{11}) + c_2^2(2hc_{22} + J_{22}) - 2c_1c_2K_{12} \quad (9')$$

$${}^1E_6 = E_c + c_1^2(2hc_{11} + J_{11}) + c_2^2(2hc_{22} + J_{22}) + 2c_1c_2K_{12} \quad (10')$$

where  $c_1^2 + c_2^2 = 1$ .  $|^1\Psi_2\rangle$  is not incorporated in equations (9) and (10) because it has spin symmetry different from the other two singlets. Equation (9) introduces the correlation between the two electrons (last term in equation (9')) and is often referred to as a two configuration (TC) wave function. This TC wave function can be further factored into

$$\begin{aligned} &|^1\Psi_5\rangle \\ &= A[\{\text{core}\}(c_1\phi_1\phi_1 - c_2\phi_2\phi_2)\alpha\beta] \end{aligned} \quad (13)$$

$$= A[\{\text{core}\}(c_1^{1/2}\phi_1 + c_2^{1/2}\phi_2)(c_1^{1/2}\phi_1 - c_2^{1/2}\phi_2)(\alpha\beta - \beta\alpha)] \quad (13')$$

which involves two singly occupied, non-orthogonal MO's,

$$\phi_1' = (c_1^{1/2}\phi_1 + c_2^{1/2}\phi_2)/(c_1 + c_2)^{1/2} \quad (14)$$

$$\varphi_2' = (c_1^{1/2}\varphi_1 - c_2^{1/2}\varphi_2) / (c_1 + c_2)^{1/2} \quad (15)$$

with overlap integral value

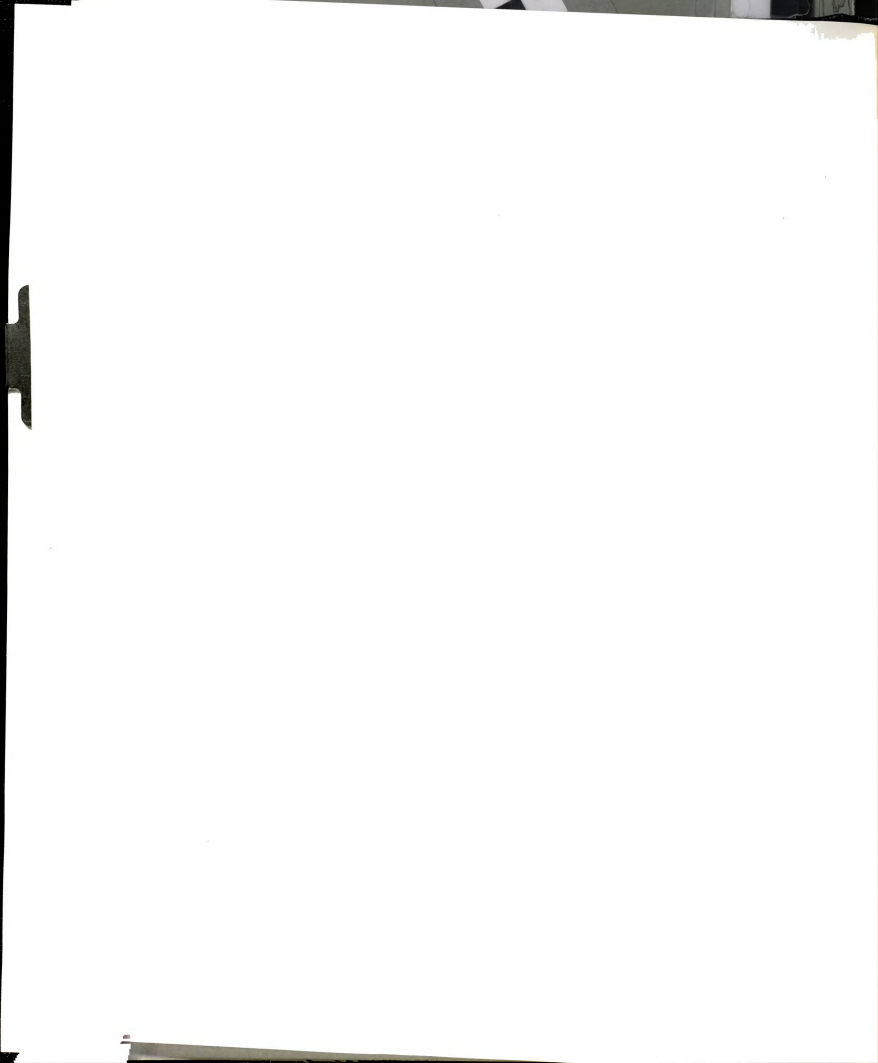
$$S = (c_1 - c_2) / (c_1 + c_2) \quad (16).$$

The MOs in equation (14) and (15) are often referred to as general valence bond (GVB) orbitals<sup>25</sup> and equation (13) is their natural orbital expression. Thus, two-term one-pair GVB wave functions and the TC wave function are equivalent in their functional form. However, the conceptual basis for TC and GVB wave functions do not coincide, in that the TC wave function is a linear combination of two doubly occupied singlet configurations while the GVB wave function is a product of two localized non-orthogonal MOs:  $\varphi_1'$  and  $\varphi_2'$ .

From equation (13) written in natural orbital form, we see that another way of obtaining the GVB wave function from the usual HF closed shell wave function is<sup>25</sup>:

$$\varphi_1\varphi_1\alpha\beta \rightarrow (c_1\varphi_1\varphi_1 - c_2\varphi_2\varphi_2)\alpha\beta, \quad \langle\varphi_1|\varphi_2\rangle = 0 \quad (17)$$

That is, an electron pair normally described by a HF closed shell orbital is instead described by a geminal expansion consisting of two orthogonal doubly occupied orbitals. This pair correlation description can in fact be extended to an





arbitrary length  $m$  to include any amount of correlation between the two singlet coupled electrons<sup>25</sup>:

$$\varphi_1\varphi_1\alpha\beta \rightarrow \sum_{q=1}^m c_q\varphi_q\varphi_q\alpha\beta, \quad \langle\varphi_p|\varphi_q\rangle = \delta_{pq} \quad (18)$$

If the nitrogen lone pair orbital  $\varphi_3$  in DHP plays an important role correlating two singlet coupled orbitals  $\varphi_1$  and  $\varphi_2$ , we may incorporate  $\varphi_3$  using equation (18), i.e.,

$$|{}^1\Psi_7\rangle = A[\{\text{core}\}(c_1\varphi_1\varphi_1+c_2\varphi_2\varphi_2+c_3\varphi_3\varphi_3)\alpha\beta] \quad (19)$$

where  $c_1^2+c_2^2+c_3^2=1$ . While  $c_1$  and  $c_2$  of equation (13) are taken to be positive, coefficients of (18) and (19) can be either positive or negative.

Thus, the appropriate wave functions for DHB or DHP are: equation (3) for a triplet, and equations (4), (9) and (10) for three singlet states. In the case of DHP, equation (19) will be further examined in order to account for the role of the nitrogen lone pair orbital in the correlation between the two singlet coupled electrons.

### 1.3.3. Qualitative Discussion of Wave Functions for DHB and DHP

In order to understand the qualitative aspects of DHB or

1875

1876

DHP wave functions developed in section 1.3.2, we will consider two restricted cases assuming that the same set of known MOs are used to construct the wave functions given in equation (3) - (10). They are: (1) MOs  $\varphi_1$  and  $\varphi_2$  are degenerate with no conceivable interaction between the two radical lobes (i.e.,  $\langle n_1 | n_2 \rangle$  has small values), and (2) MOs  $\varphi_1$  and  $\varphi_2$  are split in energy either by interaction with themselves or with other levels.

In the first case, we may predetermine the mixing coefficients  $c_1$  and  $c_2$  of equation (9) to be equal. Under this condition, the relative energies of wave functions (3), (4), (9) and (10) can be expressed in terms of only Coulomb and exchange integrals:

$$\Delta^3 E_1 = J_{12} - K_{12} \quad (3'')$$

$$\Delta^1 E_2 = J_{12} + K_{12} \quad (4'')$$

$$\Delta^1 E_5 = (J_{11} + J_{22})/2 - K_{12} = J_{11} - K_{12} \quad (9'')$$

$$\Delta^1 E_6 = (J_{11} + J_{22})/2 + K_{12} = J_{11} + K_{12} \quad (10'')$$

These  $\Delta E$ 's then predict that the triplet state is the lowest in energy, obeying Hund's rule. This is owing to the fact that the Coulomb repulsion integral between two electrons in the same MO is always greater than that between two electrons in different MOs ( $J_{ij} < J_{ii}$ ). Equation (10'') shows that the totally symmetric singlet,  $2^{-1/2}(|^1\Psi_3\rangle + |^1\Psi_4\rangle)$ , will be the

highest in energy. However, it is less clear whether (4") is greater or less than (9"). Thus, the lowest singlet state can be specified only after we carry out the calculation for  $J_{ij}$  and  $K_{ij}$  with known functional form of  $\phi_1$  and  $\phi_2$ .

It is unlikely that the radical lobes do not interact, as presumed in the previous case. When the two levels are not degenerate, variational optimization of  $c_1$  and  $c_2$  in equation (9') can bring this singlet energy level down, below that of the triplet. One of the closed shell singlet wave functions ( $|^1\Psi_3\rangle$  or  $|^1\Psi_4\rangle$ ) could also be a ground state if the MOs  $\phi_1$  and  $\phi_2$  are significantly split in energy. In this case, equation (9) and (10) are not relevant; the mixing coefficient belonging to the higher energy configuration in equation (9') approaches zero, resulting in a singlet energy of either (5') or (6'). A sufficient condition for a closed shell singlet ground state is then assured if the low-lying singlet energy (5') or (6') is less than triplet energy (3'), i.e.,

$$h_{ii} - h_{jj} > J_{ii} - J_{ij} + K_{ij} + \sum_p^{\text{closed}} \{ (2J_{jp} - K_{jp}) - (2J_{ip} - K_{ip}) \} \quad (20)$$

where  $i, j = 1$  or  $2$  and  $p$  denotes the MO's in core shells. Interpreted physically, equation (20) requires that the difference in one-electron energies be large enough to overcome the greater Coulomb repulsion energy associated with

having two electrons in the same MO, rather than in different MOs with parallel spin.

In conclusion, if two odd electrons occupy a pair of degenerate or nearly degenerate MOs, the normal consequence is a triplet ground state. If the two levels are significantly split in energy, by interaction with themselves or with other levels, then the possibility of a thermodynamically and kinetically stabilized singlet state arises<sup>30</sup>.

#### 1.3.4. Quantitative Calculation: *ab-initio* SCF Methods

In the previous section, we could draw some useful qualitative conclusions from a known set of MOs for all wave functions. However, to obtain these MOs, it is necessary to carry out various level of self-consistent field (SCF) calculations (see Figure 1.7).

The restricted Hartree-Fock (RHF) calculation, in which the MOs occupied by electrons of  $\alpha$  and  $\beta$  spin are restricted to be the same, results in one of the low-lying doubly occupied singlets (equation (5) or (6)) as its solution. The other two singlet states will not be specified by the RHF method. As was discussed in sections 1.3.1 and 1.3.2, a

single configuration doubly occupied singlet wave function cannot properly describe the ground singlet state of DHB and DHP.

Correlated wave functions for pure spin states require linear combinations of electron configurations. Such multiconfigurational wave functions can be obtained directly by multiconfigurational SCF (MCSCF) calculations, provided one knows for which orbitals electron correlations will be most important. The two configuration wave function, a restricted form of the MCSCF wave function, correctly accounts for the most important correlations between the two odd electrons of DHB and DHP. Thus TCSCF, or equivalently the one-pair GVB calculation, yields an appropriate description of the singlet ground state of DHB and DHP<sup>27,28</sup>.

The energy and wave function of the triplet state can be found by either unrestricted Hartree-Fock (UHF) or restricted open shell Hartree-Fock (ROHF) SCF calculation. While the UHF method, which allows different spatial orbitals for electrons of  $\alpha$  and  $\beta$  spin, computes a favorable triplet energy in an open shell system, the resultant wave function is mixed with higher spin states (spin contamination). That is, the UHF wave function is not an eigen function of the spin operator. In order to maintain the correct functional form for the triplet state of DHB and DHP (equation (3)), a ROHF

1900-1910

1910-1920

1920-1930

1930-1940

1940-1950

1950-1960

calculation is necessary. However, the difference in energy between the two methods is not significant when the spin contamination of the UHF wave function is small<sup>26</sup>.

The triplets of DHB and DHP can be adequately described with a single configuration ROHF calculation. However, the singlets require correlation of the in-plane electron pair through the TCSCF calculation. Of course, both these calculations will recover only a small fraction of the total electron correlation energy, and yet this singlet TCSCF/triplet ROHF approach should account for the major correlation difference between the singlet and the triplet states<sup>23-27</sup>.

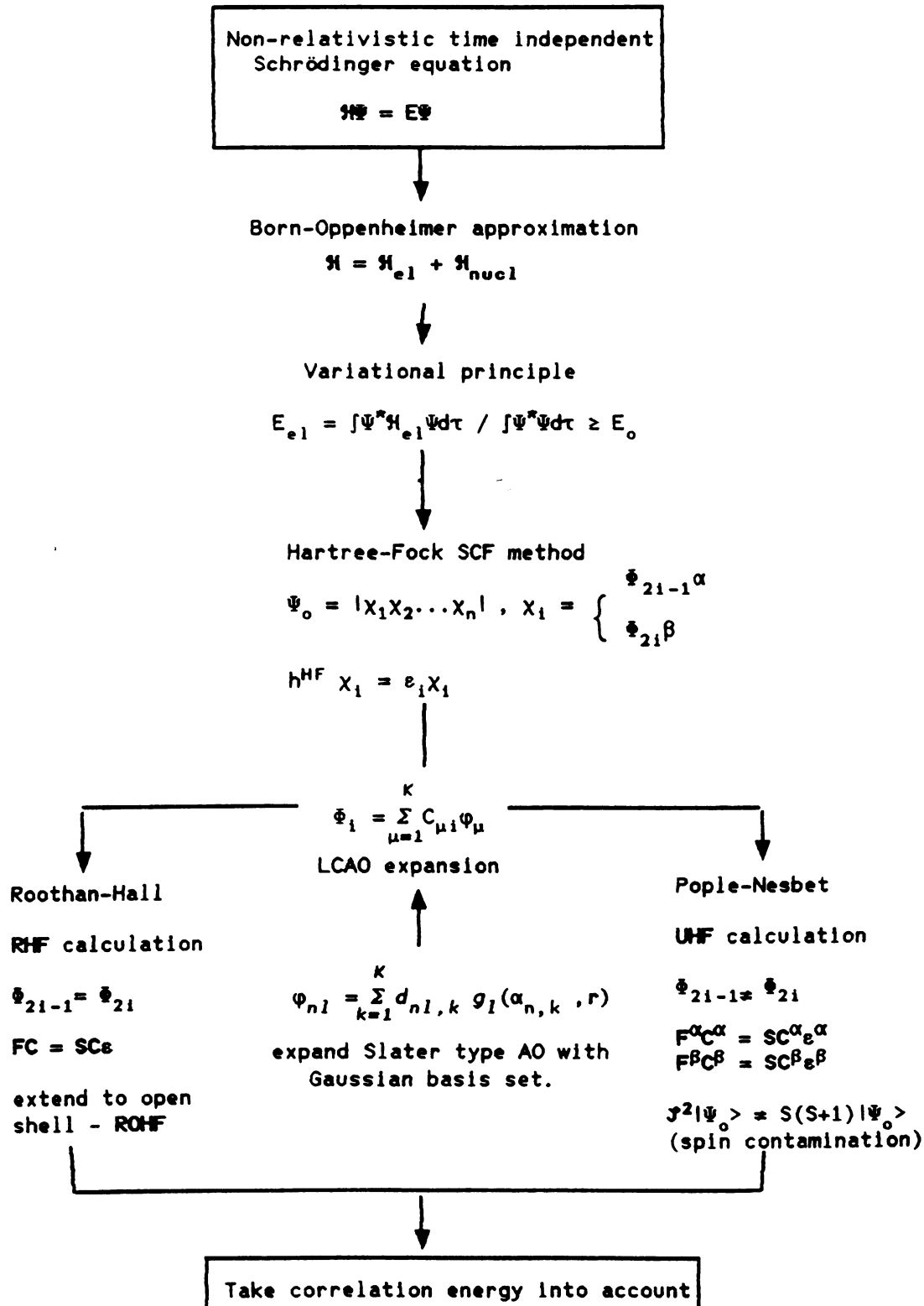
In order to recover the total electron correlation energy, a configuration interaction (CI) calculation is required. Another popular way of obtaining this correlation energy is the Möller-Plesset (MP) perturbation treatment. However, the CI or MP calculations on DHB or DHP systems could not be done in this dissertation because of the limitations in existing computing facilities.

#### 1.3.5. Computation

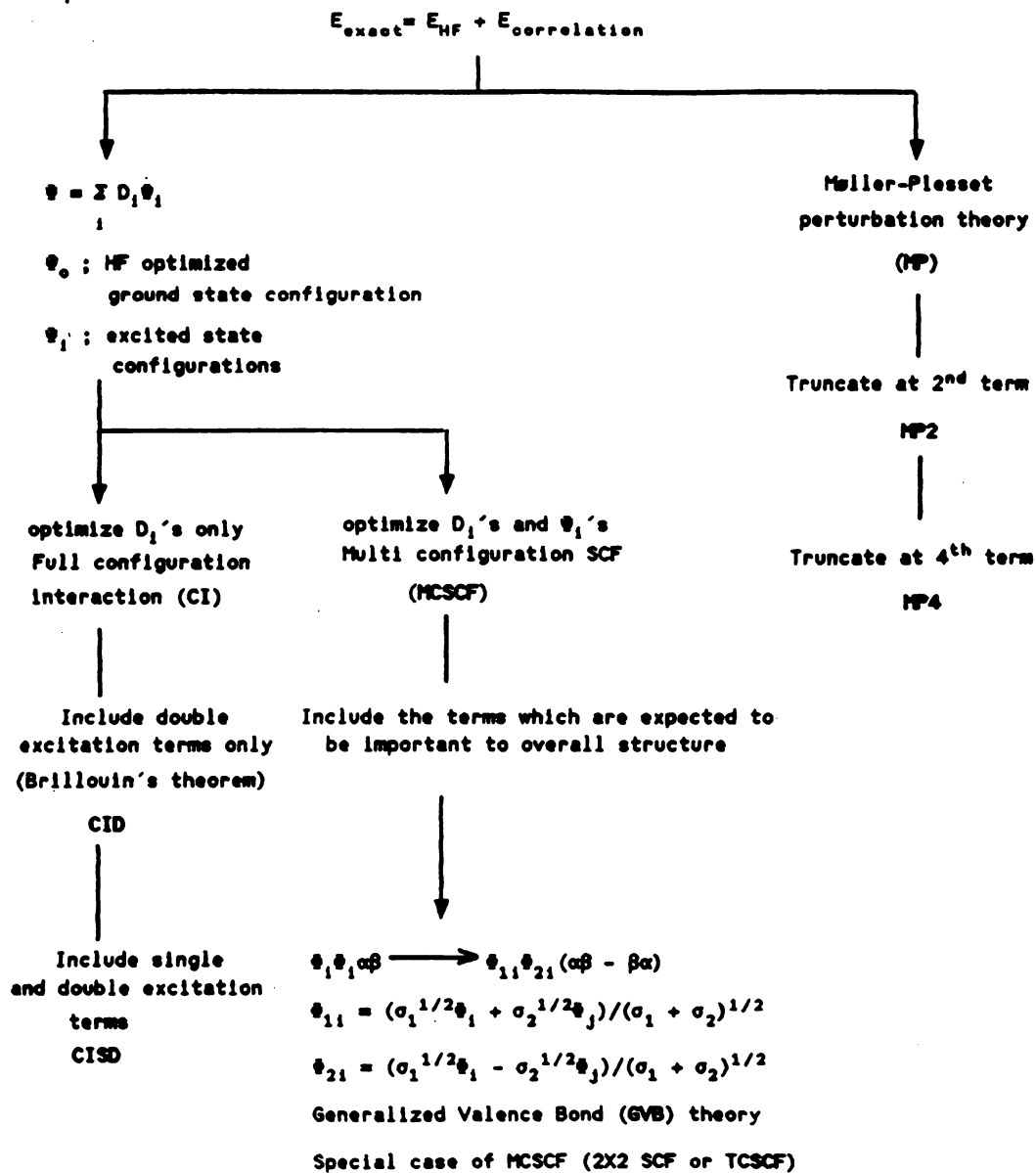


Three different levels of ab-initio calculations (RHF, ROHF and GVB) have been carried out using the GAUSSIAN86 program<sup>29</sup> which is installed on a Micro-VAX II in the Chemistry Department and an IBM 3090 system in the Michigan State University Computer Center. The singlet and triplet energies of all isomers of DHB and DHP have been obtained from fully optimized geometries. In addition, vibrational frequencies have been calculated for vicinally didehydrogenated systems (1,2-DHB, 2,3- and 3,4-DHP), using either the finite difference or the analytic second derivative method at the RHF, ROHF and GVB levels. All calculations are done with the 3-21G basis set. The effect of adding a polarization function to the basis set has not been extensively investigated.

In order to examine the characteristics of the strained triple bond in 1,2-DHB and 3,4-DHP, various properties of cis-bent acetylene ( $0^{\circ}$ ~ $80^{\circ}$ ) have been calculated at the RHF, ROHF and GVB levels.









## REFERENCES

1. Roberts, J. D.; Simmons, H. E.; Carlsmith, L. A. *J. Am. Chem. Soc.* 1953, 75, 3290.
2. (a) Hoffman, R. W. "*Dehydrobenzene and Cycloalkynes*"; Academic Press, New York 1967.; (b) Hoffman, R. W. In "*Chemistry of Acetylenes*"; Viehe, H. G., Ed.; Marcel Dekker, New York 1969.
4. (a) Field, E. K. In "*Organic Reactive Intermediates*"; McManus, S. P., Ed.; Academic Press, New York 1973; Chapter 7.; (b) Field, E. K.; Meyerson, S. *Adv. Phys. Org. Chem.* 1968, 6, 1.
5. (a) Reinecke, M. G. In "*Reactive Intermediates, vol 2.*"; Abramovitch, R. A., Ed.; Plenum Press, New York 1981; Chapter 5.; (b) Reinecke, M. G. *Tetrahedron* 1982, 38, 427.
6. den Hertog, H. J.; van der Plas, H. C. *Advan. Het. Chem.* 1965, 4, 121.
7. Kauffmann, Th. *Angew. Chem. (Intern. Ed. Engl.)* 1965, 4, 543.
8. Kauffmann, Th.; Wirthwein, R. *Angew. Chem. (Intern. Ed. Engl.)* 1971, 10, 20.
9. van der Plas, H. C.; Roeterdink, F. in "*The Chemistry of Functional Groups, Supplement C: The Chemistry of Triple Bonded Functional Groups*" Patai, S.; Rapport, Z., Eds.; John Wiley and Sons, New York 1983.
10. Whittel, E.; Dows, D. A.; Pimentel, G. C. *J. Chem. Phys.* 1954, 22, 1943.
11. Craddock, S.; Hinchcliff, A. J. "*Matrix Isolation*";

Cambridge University Press, Cambridge 1975.

12. Barnes, A. J.; Orville-Thomas, W. J.; Muller, A.; Gaufres, R. "*Matrix Isolation Spectroscopy*"; D. Reidel Publishing Co., Dordrecht 1981.
13. Jodl, H. J. In "*Vibrational Spectra and Structure, vol. 13*" Durig, J. R., Ed.; Elsevier Science Publishers, Amsterdam 1984.
14. Green, D. W.; Reedy, G. T. In "*Fourier Transform Infrared Spectroscopy, vol. 3.*" Ferraro, J. R.; Basile, L. J., Eds.; Academic Press, New York 1982.
15. Knight, L. B. *Acc. Chem. Res.* 1986, 19, 313.
16. Dendramis, A.; Leroi, G. E. *J. Chem. Phys.* 1977, 66, 4334.
17. Brown, R. F. C.; Crow, W. D.; Solly, R. K. *Chem. Ind. (London)* 1966, 343.
18. Cava, M. P.; Mitchel, M. J.; Dejongh, D. C.; van Fossen, R. Y. *Tetrahedron Letters*, 1966, 2947.
19. Reinecke, M. G.; Newsom, J. G.; Chen, L.-J., *J. Am. Chem. Soc.* 1981, 103, 2706.
20. Dewar, M. J. S.; Tien, T.P. *J. Chem. Soc. Chem. Comm.* 1985, 1243.
21. Nam, H.-H.; Leroi, G. E. *J. Am. Chem. Soc.* 1988, 110, 4096.
22. Nam, H.-H.; Leroi, G. E. *J. Mol. Struct.* 1987, 157, 301.
23. "*Diradicals*"; Borden, W. T. Ed.; John Wiley and Sons, 1982.; Chapter 1 and 2.
24. Salem, L.; Rowland, C. *Angew. Chem. Int. Ed. Engl.* 1972, 11, 92.



25. Bobrowicz, F. W.; Goddard III, W. A. In *"Methods of Electronic Structure Theory"*; Schaefer III, H. F. Ed.; Plenum Press: New York, 1977.; Chapter 4.
26. Hehre, W. J.; Radom, L.; Schleyer, P. v. R.; Pople, J. A. *"Ab-Initio Molecular Orbital Theory"*; John Wiley and Sons, 1986.
27. (a) Newton, M. D.; Noell, J. O. *J. Am. Chem. Soc.* 1979, 101, 51. (b) Newton, M. D. In *"Applications of Electronic Structure Theory"*; Schaefer III, H. F., Ed.; Plenum Press, New York 1977; Chapter 6.
28. (a) Hiller, I. H.; Vincent, M. A.; Guest, M. F.; von Nissen, W. *Chem. Phys. Lett.* 1987, 134, 403. (b) Rigby, K.; Hiller, I. H.; Vincent, M. A. *J. Chem. Soc. Perkin Trans. II.* 1987, 117.
29. Frisch, M. J.; Binkley, J. S.; Schlegel, H. B.; Raghavachari, K.; Melius, C. F.; Martin, R. L.; Stewart, J. J. P.; Bobrowicz, F. W.; Rohlfing, C. M.; Kahn, L. R.; Defrees, D. J.; Seeger, R.; Whiteside R. A.; Foc, D. J.; Fleuder, E. M.; Pople, J. A. *"GAUSSIAN 86"*; Carnegie-Mellon Quantum Chemistry Publishing Unit, Pittsburg PA, 1984.
30. Hoffman, R. *Acc. Chem. Res.* 1971, 4, 1.

## CHAPTER 2

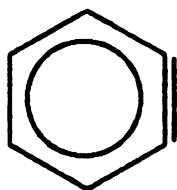
### Didehydrobenzenes (DHB)

#### *Introduction*

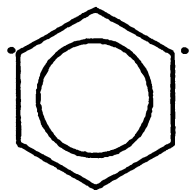
Since the pioneering experiments of Wittig *et al.* in the 1940s and of Roberts, Huisgen and their coworkers in the early 1950s, a large volume of work has substantiated the intermediacy of 1,2-DHB in many organic reactions<sup>1-6</sup>. This interesting intermediate has attracted widespread attention, as demonstrated by numerous review articles<sup>1<sup>b</sup>, 3-7</sup>, including a monograph<sup>1<sup>a</sup></sup> and two periodical reports<sup>2</sup>. However, although many of its chemical properties are well known, the physical properties of 1,2-DHB, such as its geometry, electronic structure and ionization energy, are still being debated.

Related, but much less studied intermediates are the 1,3- and 1,4- isomers. Berry *et al.* first brought them to attention from their observation of an  $m/z=76$  peak in the time-of-flight mass spectrum when benzenediazonium-3- or -4-carboxylate were decomposed by flash vacuum photolysis<sup>4,2</sup>. Further experimental evidence of these intermediates has been provided by the groups of Bergman (1,4-DHB)<sup>6<sup>9</sup>, 7<sup>1</sup></sup>, Washburn (1,3-DHB)<sup>6<sup>6</sup></sup> and Billups (1,3-DHB)<sup>6<sup>7</sup></sup>.

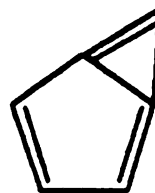
The structures of these DHBs are commonly depicted as follows:



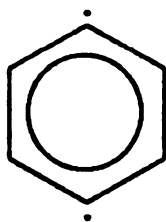
(1)



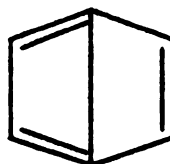
(2a)



(2b)



(3a)

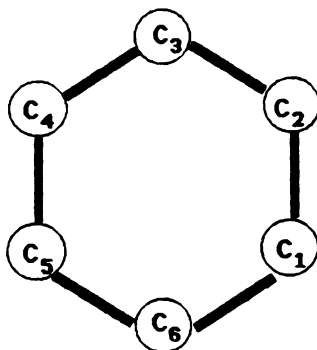


(3b)

Structure (1) represents one possible resonance form of 1,2-DHB. The 1,3- and 1,4- isomers have two types of structure: diradical (2a) and (3a), and bicyclic (2b) and (3b). Numerous theoretical calculations concerning the geometries, nature of ground electronic states and the relative stabilities of all these DHBs have been published<sup>8-28</sup>.

While the chemistry of the DHBs has been thoroughly reviewed<sup>1-7</sup>, the physical data, both experimental and theoretical, have not been critically examined to date. Considering the amount of accumulated information regarding

the physical properties of these intermediates, it seems appropriate to review them now and to indicate the direction of future research in this area. Included also are the results of our own theoretical calculations (GVB/3-21G level) on all DHB isomers. The C-C bonds of the six-membered ring are specified with the subscripted carbon numbers as shown below (e.g. C<sub>1</sub>-C<sub>2</sub>),



where the number 1 always corresponds to the first dehydrocarbon center.



## 2.1. 1,2-Didehydrobenzene (1,2-DHB)

### 2.1.1. The ground electronic state of 1,2-DHB

For triplet 1,2-DHB ( $^3B_2$ ), a good qualitative description of the electronic structure is provided by the single configuration (there are 40 electrons in this system and  $10a_1$  is the 20<sup>th</sup> orbital)

$$\sim 2b_1^2 1a_2^2 10a_1^1 8b_2^1 (\alpha\alpha) \quad (1)$$

where the  $10a_1$  and  $8b_2$  orbitals approximately correspond to symmetric and antisymmetric combinations of the two in-plane  $\sigma$  radical lobes left behind by didehydrogenation of benzene. The triplet wave function can be found by either restricted open-shell or unrestricted Hartree-Fock (ROHF or UHF) methods.

Two low energy singlet states are possible<sup>9</sup>. In the higher energy one the electrons are arranged as in the triplet, but with their spins opposed to form a  $^1B_2$  wave function:

$$\sim 2b_1^2 1a_2^2 10a_1^1 8b_2^1 (\alpha\beta - \beta\alpha) \quad (2)$$

In the lower energy singlet both electrons are in the same orbital, but a second configuration of this type makes a large contribution. Thus the  $^1A_1$  closed-shell SCF function

$$\sim 2b_1^2 1a_2^2 10a_1^2 \quad (3)$$

is considerably less accurate than the two-configuration SCF

1950-1951

1950-1951

1950-1951

1950-1951

1950-1951

1950-1951

1950-1951

(TCSCF) function<sup>75</sup>

$$\sim 2b_1^2 1a_2^2 (c_1 10a_1^2 - c_2 8b_2^2), \quad (4)$$

where the coefficients  $c_1$  and  $c_2$  are variationally optimized and their values are often used to describe the relative diradical character of this molecule<sup>20,25,28</sup>.

Therefore, in order to make a reliable prediction for the 1,2-DHB singlet-triplet energy separation,  $\Delta E(S-T)$ , the ROHF and TCSCF ( or equivalently one pair GVB) wave functions are required<sup>75</sup>. Wilhite and Whitten performed rather extensive configuration interaction calculations for the three DHB isomers under the constraint that their carbon skeletons retain a benzene configuration<sup>15a</sup>. Even with this severe geometrical limitation they could show that the ground state of 1,2-DHB is a singlet at the two-determinant CI level, while this order is reversed at the single determinant SCF level. Noell and Newton performed GVB calculations for 1,2-DHB with a partially optimized singlet geometry at the RHF/4-31G level<sup>20</sup>. They predicted that the singlet is 28.1 kcal/mole more stable than the triplet. The  $\Delta E(S-T)$  values calculated with the fully optimized singlet (GVB/3-21G and GVB/6-31G\*) and triplet (ROHF/3-21G and ROHF/6-31G\*) geometries are 29.9 (3-21G) and 27.6 kcal/mole (6-31G\*), respectively. More extensive CI calculation would increase the  $\Delta E(S-T)$  gap further<sup>15</sup>. In general, semi-empirical calculations, such as MINDO/3 and MNDO methods, predict much



1900 (1900)

1901 (1901)

1902 (1902)

1903 (1903)

1904 (1904)

1905 (1905)

1906 (1906)

1907 (1907)

smaller  $\Delta E(S-T)$  values than *ab-initio* TCSCF/ROHF comparisons (see Table 2.1).

Table 2.1 Singlet-triplet energy separation of 1,2-DHB

Methods	$\Delta E(S-T)$ kcal/mole	Comments
2-det. CI <sup>15</sup>	13.0	benzene geometry
many-det. CI <sup>15</sup>	16.6	
GVB/ROHF <sup>20</sup>	28.1	singlet; RHF/4-31G partial geometry optimization <sup>20</sup> triplet; MINDO/3 optimized <sup>18</sup>
GVB/ROHF <sup>**</sup>	29.9	GVB/3-21G <sup>28</sup> , ROHF/3-21G
GVB/ROHF <sup>**</sup>	27.6	GVB/6-31G <sup>*27, 28</sup> , ROHF/6-31G <sup>*</sup>
INDO <sup>13</sup>	12.5	benzene geometry
MINDO/3 <sup>18</sup>	8.6	MINDO/3 optimized geometries
MINDO RHF/ RHF/HE <sup>23</sup>	3.8	MINDO optimized geometries
LINDO/S PERTCI <sup>40</sup>	33.2	MINDO optimized geometries <sup>23</sup>

\*\* This work

Lineberger and coworkers have attempted to measure  $\Delta E(S-T)$  from the photoelectron spectrum of the  $^2B_2$  state of  $C_6H_4^-$ ; their result, 37.7 kcal/mole<sup>54</sup>, is about 30% larger than the predictions from GVB/ROHF calculations<sup>20</sup>. There have been some attempts to trap the triplet 1,2-DHB in 1,2-cycloaddition reactions with various olefins<sup>56-62</sup>. Jones and Levin, however, provided convincing evidence against the

possibility of a triplet intermediate from the stereochemical analysis of the [2+2] and [2+4] cycloaddition reactions of 1,2-DHB with appropriately substituted *cis*- or *trans*- olefins or with some dienes<sup>57</sup>. An attempt to generate triplet 1,2-DHB via the photolytic decomposition of triplet phthaloyl peroxide in benzophenone medium failed because of the rapid triplet-singlet interconversion in the intermediate steps<sup>56</sup>.

From the above evidence, the ground electronic state of 1,2-DHB is undoubtedly a singlet. However, other electronic properties, such as the ionization energy and the relative energy levels of valence shells, are not yet clearly elucidated.

#### 2.1.2. The ionization energy and the heat of formation of 1,2-DHB

The experimental values reported for the ionization energy (IE) of 1,2-DHB are collected in Table 1.2. Three bands, at 9.24, 9.75 and 9.87 eV, were observed in the photoelectron (PE) spectra of the products from the flash vacuum thermolysis of phthalic anhydride or indantrione by Dewar and Tien<sup>53</sup>. With the help of MNDO calculations, the authors have interpreted these as the first three ionization energies of 1,2-DHB.

Table 2.2 Experimental IEs of 1,2-DHB

PE <sup>53</sup>	mass <sup>46</sup>	mass <sup>48</sup>
9.24	9.75	9.45
9.75		
9.87		

Before Dewar and Tien's experiment, the IEs of 1,2-DHB were obtained from mass spectrometry<sup>46,48</sup>. Fisher and Lossing pyrolyzed o-diiodobenzene in a reactor coupled to a mass spectrometer and detected 1,2-DHB with a vertical IE of 9.75 eV which is 0.25 eV higher than that of benzene (9.50 eV in their experiment)<sup>46</sup>. Subsequently, Grützmacher and Lohmann reported 9.45 eV as the IE of 1,2-DHB by measuring the appearance energy of the  $m/z=76$  peak resulting from the pyrolysis of bis-2-iodophenyl<sup>48</sup>. Rosenstock *et al.* corrected this value to 8.95 eV based on the fact that the average IE of the linear  $C_6H_4$  isomers is  $9.09 \pm 0.02$  eV<sup>50</sup>; no substantial experimental evidence for this adjustment has been provided. Nevertheless, this correction suggests that the IE of 1,2-DHB might be much lower than the previously reported values from the mass spectrometric measurements.

Based on the MNDO calculation, Dewar and Tien assigned the first two bands of the PE spectrum to the  $a_2$  and  $b_1$  orbitals, which are benzene-like  $\pi$  orbitals, and the third to the

Table 2.3 Calculated IEs of 1,2-DHB

RHF <sup>a</sup> (3-21G)	RHF <sup>27</sup> (DZ+P)	OVGF <sup>27</sup> (DZ+P)	2ph-TDA <sup>27</sup> (DZ+P)	CI <sup>27</sup> (6-31G*)	MNDO <sup>53</sup>	assignment
9.73	9.75	9.55	9.54	9.07	9.83	1a <sub>2</sub>
9.81	9.77	9.57	9.54	9.06	9.57	2b <sub>1</sub>
10.21	10.23	9.77	9.65	8.98	9.93	10a <sub>1</sub>

<sup>a</sup> This work

in-plane a<sub>1</sub> orbital which corresponds to the symmetric combination of the two σ radical lobes. This assignment, however, has been challenged by Hiller *et al.* on the basis of *ab-initio* CI, OVGF (outer valence Green Function method) and extended 2ph-TDA (two-particle-hole Tamm-Dancoff approximation) calculations<sup>27</sup>. The first two IEs of 1,2-DHB are predicted to be nearly degenerate in these calculations (see Table 2.3). Since the first IE in the PE spectrum, 9.24 eV, is substantially separated from the other two rather closely spaced IEs, Hiller *et al.* suggested that the bands at 9.75 and 9.87 eV are attributable to the 2b<sub>1</sub> and 1a<sub>2</sub> orbitals of 1,2-DHB and the band at 9.24 eV may originate from some contaminant. Wentrup *et al.* also seriously questioned the attribution of the PE spectrum to 1,2-DHB<sup>41</sup> because other possible intermediates, such as cyclopentadienylidene ketene, could have been formed in Dewar and Tien's experiment<sup>53</sup>. According to the analysis by Hiller *et al.*, if we discard the first band of the PE spectrum, the first IE of 1,2-DHB is 9.75 eV and this value agrees well with the previous mass

spectrometric measurement by Fisher and Lossing.

The above MNDO and *ab-initio* analyses (except the CI calculation) place the in-plane  $10a_1$  orbital below the out-of-plane  $\pi$ -orbitals,  $1a_2$  and  $2b_1$ . Considering that the vast amount of experimental results have been interpreted on the assumption that the  $10a_1$  orbital is the highest occupied MO (HOMO) of 1,2-DHB<sup>1-7</sup>, the MNDO or *ab-initio* energy level ordering of the valence shell orbitals disagrees with the conventional description of 1,2-DHB. However, the recent UV/VIS spectrum of 1,2-DHB by Münzel and Schweig shows that the in-plane MO  $10a_1$  is indeed the HOMO of 1,2-DHB<sup>45</sup>.

This discrepancy arises from the fact the closed-shell SCF procedure overestimates the strength of the  $C_1-C_2$  bond, and thus lowers the energy of the  $10a_1$  orbital below those of the out-of-plane  $\pi$ -orbitals. However, inclusion of electron correlation at the CISD level reverses this order<sup>27</sup> (see Table 2.3). Thus, a simple application of Koopman's theorem without considering the effect of electron correlation may not correctly account for the IEs of 1,2-DHB, and it may be premature to conclude that the PE spectrum band at 9.24 eV is not due to 1,2-DHB. On the other hand, Dewar and Tien's experiments also include some refutable ambiguities as have been pointed out by Wentrup *et al*<sup>41</sup>. Thus, in our opinion, the first IE of 1,2-DHB is still not well established.

With the known IEs, the heat of formation ( $\Delta H_f$ ) of 1,2-DHB could be derived from the mass spectrometrically determined  $\Delta H_f$  of the  $C_6H_4^+$  ion, which is one of the principal fragments of various phenyl derivatives. Several groups have calculated the  $\Delta H_f$  of 1,2-DHB from such measurements<sup>47-50,52</sup>. Their values range from 100 to 120 kcal/mole, depending on the estimated  $\Delta H_f$  of the  $C_6H_4^+$  ion and the IEs of 1,2-DHB used. These results are collected in Table 2.4. As one may note from the entries, there are large variances in both  $\Delta H_f(C_6H_4^+)$  and the IE of 1,2-DHB. Thus, the estimated values of  $\Delta H_f(1,2-DHB)$  from mass spectrometry should be cited cautiously.

Pollack and Hehre employed ion cyclotron resonance (ICR) spectroscopy to determine the  $\Delta H_f$  of 1,2-DHB<sup>51</sup>. They measured the proton affinities of the unstable neutral molecule  $C_6D_4$  (9.5 kcal/mole) by abstracting a deuteron from the phenyl- $d_5$  cation with bases of varying strengths, and combined with these values the  $\Delta H_f$  of 1,2-DHB ( $118 \pm 5$  kcal/mole) could be derived from the previously known  $\Delta H_f$  of  $C_6D_5^+$  ( $270 \pm 3$  kcal/mole), of  $H^+$  (367.3 kcal/mole) and the enthalpy of protonation of ammonia (205 kcal/mole).

Theoretically calculated enthalpies of formation of 1,2-DHB range from 107 to 138.2 kcal/mole (see Table 2.4).

Table 2.4. The enthalpy of formation of 1,2-DHB (298 K)

<i>Mass spectrometry</i>				
source of $C_6H_4^+$	$\Delta H_f(C_6H_4^+)$	IE( $C_6H_4^+$ )	$\Delta H_f(1,2-DHB)$	ref.
benzene	345	9.75	120	47
electron impact				
bis-2-iodophenyl	336	9.45	118	48
pyrolysis				
benzene	318	9.45	100	49
photo ionization				
benzonitrile	313	8.95	107	50
photo ionization				
<i>o</i> -dibromobenzene	308	8.95	101	52
photo ionization				
<i>Ion Cyclotron Resonance Spectroscopy (ICR)</i>				
measurement of electron affinities of $C_6D_4$			118	51
<i>Theoretical calculations</i>				
MINDO/2			107	14
RHF/STO-3G			120	17a
MINDO/3			118	18
MINDO/3-CI			114	18
MINDO/SCF			138	23
MINDO/3x3CI			126	23
MINDO/UHF			120	23

$\Delta H_f$ ; kcal/mole, IE; eV



1957

1958

1959

1960

1961

1962

1963

1964

1965

1966

1967

1968

1969

1970

1971

1972

1973

1974

1975

1976

1977

1978

1979

1980

1981

1982

1983

1984

1985

1986

1987

1988

1989

1990

1991

1992

1993

1994

1995

1996

1997

1998

1999

However, the quality of each theoretical method may not be judged merely on the basis of numerical coincidence with the experimental  $\Delta H_f(1,2\text{-DHB})$  values, since in our opinion the reported values have not achieved the desired accuracy.

### 2.1.3. Electronic spectra of 1,2-DHB

Berry *et al.* reported the first UV spectrum of gaseous 1,2-DHB<sup>42</sup>, which showed a broad absorption with the maximum at 243 nm<sup>42,43</sup>. They suggested that the absorption may be due to the transition of an electron either from the in-plane  $\sigma$  MO ( $10a_1$ ) to the  $\sigma^*$  MO ( $8b_2$ ) or from the out-of-plane  $\pi$  MO ( $1a_2$ ) to the  $\sigma^*$  MO ( $8b_2$ ). Yonezawa *et al.* calculated the electronic transition energies of 1,2-DHB in the semi-empirical ZDO approximation; they predicted that the  $\sigma \rightarrow \sigma^*$  transition would lie at longer wavelengths (411 nm) and suggested that the maximum observed by Berry *et al.* might correspond to the  $\pi \rightarrow \pi^*$  transition<sup>11</sup>. On the other hand, Wilhite and Whitten predicted that the  $\sigma \rightarrow \sigma^*$  transition would occur at shorter wavelengths than the  $\pi \rightarrow \pi^*$  or  $\pi \rightarrow \sigma^*$  transitions, based on *ab-initio* CI calculations<sup>15</sup>. However, this prediction presents some incomprehensible problems because it contradicts the orbital energy levels of 1,2-DHB in their own calculation.

1900  
1901  
1902  
1903  
1904  
1905  
1906  
1907  
1908  
1909  
1910  
1911  
1912  
1913  
1914  
1915  
1916  
1917  
1918  
1919  
1920  
1921  
1922  
1923  
1924  
1925  
1926  
1927  
1928  
1929  
1930  
1931  
1932  
1933  
1934  
1935  
1936  
1937  
1938  
1939  
1940  
1941  
1942  
1943  
1944  
1945  
1946  
1947  
1948  
1949  
1950  
1951  
1952  
1953  
1954  
1955  
1956  
1957  
1958  
1959  
1960  
1961  
1962  
1963  
1964  
1965  
1966  
1967  
1968  
1969  
1970  
1971  
1972  
1973  
1974  
1975  
1976  
1977  
1978  
1979  
1980  
1981  
1982  
1983  
1984  
1985  
1986  
1987  
1988  
1989  
1990  
1991  
1992  
1993  
1994  
1995  
1996  
1997  
1998  
1999  
2000

Kolc photolyzed the precursor benzocyclobutenedione, isolated in an EPA matrix at 77K, and obtained the UV spectrum of 1,2-DHB in the 270 - 380 nm range<sup>44</sup>. Only featureless broad absorption, which may correspond to a tail of the previously reported spectrum<sup>42</sup>, was observed.

Recently, Münzel and Schweig reported the UV/VIS spectrum of 1,2-DHB in an Ar matrix, obtained via photolysis of either 3-diazobenzofuranone or benzocyclobutenedione<sup>45</sup>. Five bands, at 380, 293, 246, 214 and 199 nm, were attributed to 1,2-DHB, and assigned with the help of LNDO/S PERTCI calculations. The lowest energy band at 380 nm corresponds to a  $\sigma \rightarrow \sigma^*$  transition, and its broad band shape indicates lengthening of the  $C\equiv C$  bond following the HOMO-LUMO excitation. The following four bands, corresponding to  $\pi \rightarrow \pi^*$  transitions, originate from the splitting of the three benzene UV bands ( $^1L_b \leftarrow ^1A$ ,  $^1L_a \leftarrow ^1A$  and  $^1B \leftarrow ^1A$ ) due to the lowered symmetry of 1,2-DHB ( $C_{2v}$ ) from that of benzene ( $D_{6h}$ ). Thus, they concluded that 1,2-DHB can be considered as benzene with an additional  $\sigma$  bond.

#### 2.1.4. Vibrational frequencies of 1,2-DHB

The first IR spectrum of 1,2-DHB was reported by Chapman and coworkers in 1973<sup>37a</sup>. They photolyzed the precursors

1912  
1913  
1914  
1915  
1916  
1917  
1918  
1919  
1920  
1921  
1922  
1923  
1924  
1925  
1926  
1927  
1928  
1929  
1930  
1931  
1932  
1933  
1934  
1935  
1936  
1937  
1938  
1939  
1940  
1941  
1942  
1943  
1944  
1945  
1946  
1947  
1948  
1949  
1950  
1951  
1952  
1953  
1954  
1955  
1956  
1957  
1958  
1959  
1960  
1961  
1962  
1963  
1964  
1965  
1966  
1967  
1968  
1969  
1970  
1971  
1972  
1973  
1974  
1975  
1976  
1977  
1978  
1979  
1980  
1981  
1982  
1983  
1984  
1985  
1986  
1987  
1988  
1989  
1990  
1991  
1992  
1993  
1994  
1995  
1996  
1997  
1998  
1999  
2000  
2001  
2002  
2003  
2004  
2005  
2006  
2007  
2008  
2009  
2010  
2011  
2012  
2013  
2014  
2015  
2016  
2017  
2018  
2019  
2020  
2021  
2022  
2023  
2024  
2025

phthaloyl peroxide or benzocyclobutenedione, isolated in an Ar matrix at 8K, with UV light to obtain eight bands in the 400 - 1700  $\text{cm}^{-1}$  range which were attributable to 1,2-DHB. One additional acetylenic band at 2085  $\text{cm}^{-1}$  was found two years later by the same group<sup>37b</sup>, following short wavelength photolysis of 3-diazobenzofuranone under similar matrix conditions.

On the basis of those results, Laing and Berry proposed a cycloalkyne-like structure and a set of force constants for 1,2-DHB<sup>35</sup>. Badger's rule and Coulson's bond-order/bond-length relationship were used to deduce the  $C_{2v}$  symmetry geometry, and the complete vibrational spectra of the normal and perdeuterated molecules ( $C_{2v}$  symmetry:  $9a_1 + 4a_2 + 3b_1 + 8b_2$  normal modes) were calculated with Wilson's GF matrix method (normal coordinate calculation). Among the significant predictions was the expectation of two  $C\equiv C$  ring stretching modes of  $A_1$  symmetry in the 2000 - 2500  $\text{cm}^{-1}$  region for each isotopomer.

Subsequently, Dunkin and MacDonald obtained improved IR spectra of 1,2-DHB and tetradeuterio-1,2-DHB by UV photolysis of phthalic anhydride and its perdeuterated analog, isolated in  $N_2$  matrices at 12 K<sup>38</sup>. The  $C_6H_4$  spectrum reported by Chapman *et al.* was generally confirmed, with the addition of a C-H stretch at 3088  $\text{cm}^{-1}$  and the exception of a band

1910  
1911  
1912  
1913  
1914  
1915  
1916

previously observed at  $1627\text{ cm}^{-1}$ . Eleven bands were reported for  $\text{C}_6\text{D}_4$ ; agreement between observed and predicted frequencies was quite reasonable below  $2000\text{ cm}^{-1}$ , but rather poor in the critical higher wavenumber region. Reevaluation of the 1,2-DHB force field was suggested<sup>38</sup> and the normal coordinate analysis by Laing and Berry was criticized in an independent MNDO study by Dewar *et al*<sup>21</sup>.

Nam and Leroi indeed found a fundamental mistake in Laing and Berry's calculation<sup>36</sup>: the proposed  $\text{C}_{2v}$  planar ring structure was not closed with the given geometrical parameters, which resulted in an incorrect formulation of the G matrix<sup>76</sup>. This error progressively accumulated throughout their calculation. Hence, Nam and Leroi carried out a new normal coordinate analysis of 1,2-DHB<sup>36</sup> with the theoretically calculated structure<sup>20</sup> and the additional frequencies of  $\text{C}_6\text{D}_4$ <sup>38</sup>. From this calculation, the following conclusions were drawn: (1) the bond-length/bond-strength correlation (Badger's rule) is not applicable to 1,2-DHB, which is explicable in terms of alternating  $\pi$ -electron overlap population around the ring.; (2) only one  $\text{C}\equiv\text{C}$  stretching frequency over  $2000\text{ cm}^{-1}$  is predicted.

Two additional IR frequencies ( $1355, 1395\text{ cm}^{-1}$ ) of 1,2-DHB were reported by Nam and Leroi<sup>40</sup>, which agree well with their previous calculation<sup>36</sup>. However, attempts to obtain the Raman



frequencies of 1,2-DHB have not been successful to date<sup>40</sup>. Brown *et al.* obtained the IR spectra of 1,2-DHB from various precursors<sup>39</sup>, but no additional peaks were identified.

Lineberger and his coworkers reported photoelectron spectra of gaseous  $C_6H_4^-$  and  $C_6D_4^-$ , from which three vibrational intervals in each of the corresponding ground state neutral species were inferred ( $C_6H_6$ : 1860, 1040 and 605  $cm^{-1}$ ;  $C_6D_4$ : 1860, 980 and 585  $cm^{-1}$ )<sup>54</sup>. The highest frequency mode was attributed to the acetylenic  $C\equiv C$  bond stretch, which is noticeably smaller than the previously observed values in matrices. They suggested that this mode may have not been detectable in the previous experiments. The recent scaled GVB/3-21G calculation by Rigby *et al.* obtains 1859  $cm^{-1}$  as the  $C\equiv C$  stretching frequency of 1,2-DHB. However, as the authors have pointed out, this low frequency is due to an artifact of their scaling method. Thus, there are no available experimental or theoretical results that support a  $C\equiv C$  stretching frequency below 2000  $cm^{-1}$ , as suggested by Lineberger *et al.*

Three quantum mechanical calculations of the vibrational spectrum of 1,2-DHB have been published; one MNDO<sup>21</sup> and two *ab-initio* (RHF/3-21G<sup>25</sup> and GVB/3-21G<sup>28</sup>) calculations. The MNDO calculation by Dewar *et al.* is in poor agreement with the known experimental frequencies, although it correctly

1900

1901

1902

1903

Table 2.5. Infrared spectrum ( $\text{cm}^{-1}$ ) of 1,2-DHB in matrices

Wentrup <i>et al.</i> (phthalic- anhydride) <sup>41</sup>	Nam and Lerol ( $\text{N}_2$ ) <sup>40</sup>	Dunkin and MacDonald ( $\text{N}_2$ ) <sup>38</sup>	Chapman <i>et al.</i> (Ar) <sup>37</sup>	Normal mode calculation <sup>36</sup>
	470	472	469	482 ( $b_2$ )
720	739	743	735	743 ( $b_1$ )
815	848	847	849	845 ( $b_1$ )
1020	1038	1039	1038	1039 ( $b_1$ )
1045	1056	1055	1053	1052 ( $a_1$ )
	1355			1360 ( $b_2$ )
	1395			1391 ( $a_1$ )
1440	1448	1448	1451	1450 ( $b_2$ )
	1596	1598	1607	1599 ( $a_1$ )
			1627	1657 ( $a_1$ )
2080	2082	2084	2085	2091 ( $a_1$ )
		3088		3081 ( $a_1$ )

1944  
1945  
1946  
1947  
1948  
1949  
1950  
1951  
1952  
1953  
1954  
1955  
1956  
1957  
1958  
1959  
1960  
1961  
1962  
1963  
1964  
1965  
1966  
1967  
1968  
1969  
1970  
1971  
1972  
1973  
1974  
1975  
1976  
1977  
1978  
1979  
1980  
1981  
1982  
1983  
1984  
1985  
1986  
1987  
1988  
1989  
1990  
1991  
1992  
1993  
1994  
1995  
1996  
1997  
1998  
1999  
2000  
2001  
2002  
2003  
2004  
2005  
2006  
2007  
2008  
2009  
2010  
2011  
2012  
2013  
2014  
2015  
2016  
2017  
2018  
2019  
2020  
2021  
2022  
2023  
2024  
2025  
2026  
2027  
2028  
2029  
2030

reproduces the  $C\equiv C$  stretching. The scaled RHF/3-21G calculation by Radom *et al.* more closely fits the IR data than does the MNDO calculation, but two strong IR bands are mis-assigned to an infrared inactive  $a_2$  mode in this report<sup>40</sup>. The more recent scaled GVB/3-21G calculation by Rigby *et al.* presents no improvement over the RHF results; rather the calculated  $C\equiv C$  stretching frequency ( $1859\text{ cm}^{-1}$ ) is in poorer agreement with the observed frequency ( $2085\text{ cm}^{-1}$ ). The scaling factors utilized were obtained by comparing the calculated (RHF/3-21G) and experimental frequencies of benzene and were applied to the force constants of 1,2-DHB obtained from their GVB/3-21G calculation. The vibrational frequencies of 1,2-DHB were then obtained from the normal coordinate calculation using these scaled force constants. Rigby *et al.* pointed out that the transfer of scaling factors from one molecule to another may not always be appropriate, especially when the RHF scaling factors are applied to the force constants derived from a correlated wave function.

#### 2.1.5. The $C\equiv C$ stretching frequencies of 1,2-DHB and other angle strained cycloalkynes

1,2-DHB is often referred to as a strained cycloalkyne<sup>1</sup>. The physical and chemical properties of the angle-strained

C≡C bond in cycloalkynes have been explained with a *cis*-bent acetylene model<sup>29-34</sup>. For example, it was shown that the increased reactivity of 1,2-DHB and other cycloalkynes toward nucleophiles is due to the large decrease in LUMO energy compared to the small increase in HOMO energy upon *cis* bending of the acetylenic bond<sup>29</sup>. The expected lowering of LUMO energies with decreasing ring size was indeed observed from the electron transmission spectra of a few selected cycloalkynes<sup>30-32</sup>. Recent MNDO and MNDOC/BWEN studies on the [2+2] cycloaddition reaction paths of 1,2-DHB with ethylene found no special electronic effects due to the aromatic conjugation of the true cyclic structure in 1,2-DHB relative to the bent acetylene model<sup>34</sup>. In this section, we will also employ the *cis*-bent acetylene model to explain the C≡C stretching frequencies of 1,2-DHB and other cycloalkynes.

Figure 2.1 shows the C≡C stretching frequencies of *cis*-bent acetylene ( $\nu_{C\equiv C}(\alpha)$ ;  $\alpha$  denotes the bond angle H-C≡C) calculated at the RHF and GVB level with 3-21G basis set. While the GVB  $\nu_{C\equiv C}$  dramatically shift to lower wavenumber as the angle  $\alpha$  decreases ( $\nu_{C\equiv C}(180^\circ) - \nu_{C\equiv C}(120^\circ) \approx 200 \text{ cm}^{-1}$ ), the RHF  $\nu_{C\equiv C}$  is quite rigid upon bending. The RHF method allows the angle  $\alpha$  to decrease less than  $60^\circ$  (i.e.  $\alpha > 120^\circ$ ) before an imaginary frequency results. On the other hand, *cis*-bent acetylene suffers bending more resiliently when it is allowed to have diradical character with the GVB method, and all of

1900  
1901  
1902  
1903

its normal modes remain real when  $\alpha > 100^\circ$ .

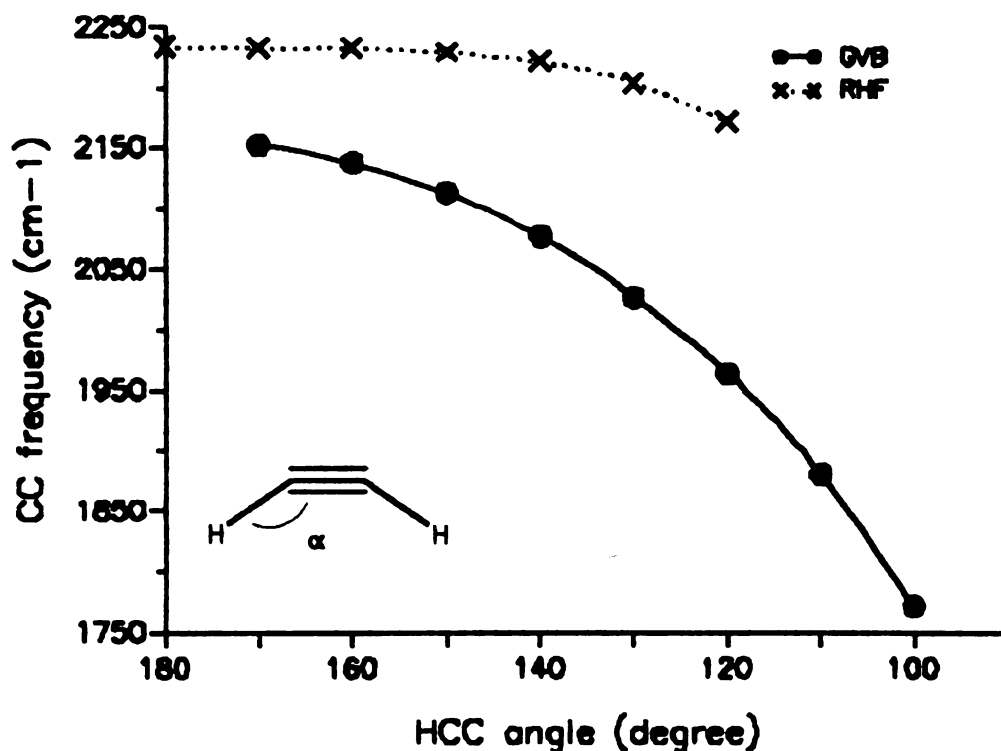


Figure 2.1.  $\text{C}\equiv\text{C}$  stretching frequency of *cis*-bent acetylene calculated at the RHF/3-21G (x---x) and GVB/3-21G (—) level.

Meier *et al.* found a linear correlation between the  $\nu_{\text{C}\equiv\text{C}}$  and  $\alpha(\text{C}-\text{C}\equiv\text{C})$  by comparing the experimentally observed  $\nu_{\text{C}\equiv\text{C}}$  of various cycloalkynes with respect to their  $\text{C}-\text{C}\equiv\text{C}$  bond angles, and the  $\nu_{\text{C}\equiv\text{C}}$  of 1,2-DHB agrees well with the predicted relationship<sup>33</sup>. The slope  $\Delta\nu_{\text{C}\equiv\text{C}}/\Delta\alpha(\text{C}-\text{C}\equiv\text{C})$  of this linear correlation ( $\nu_{\text{C}\equiv\text{C}}(180^\circ) - \nu_{\text{C}\equiv\text{C}}(130^\circ) \approx 150 \text{ cm}^{-1}$ ) is qualitatively concordant with the GVB calculation. The RHF method fails to describe this relationship. These results indicate that as far as the vibrational structure is concerned the  $\text{C}_1-\text{C}_2$  bond of 1,2-DHB is a true strained triple bond with appreciable diradical character.



1900-1901

1901-1902

1902-1903

1903-1904

1904-1905

1905-1906

1906-1907

1907-1908

1908-1909

1909-1910

1910-1911

1911-1912

1912-1913

1913-1914

1914-1915

1915-1916

1916-1917

1917-1918

1918-1919

1919-1920

1920-1921

1921-1922

1922-1923

1923-1924

1924-1925

1925-1926

1926-1927

1927-1928

1928-1929

1929-1930

1930-1931

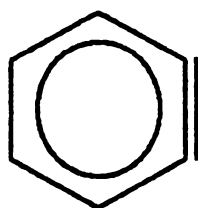
1931-1932

1932-1933

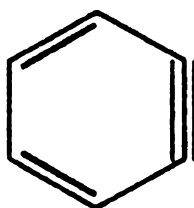
1933-1934

2.1.6. The singlet geometry of 1,2-DHB

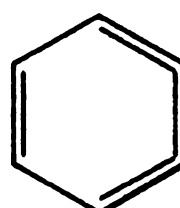
Numerous theoretical studies on the geometry of 1,2-DHB have been reported in the last three decades<sup>8-28</sup>; their results are collected in Table 2.6. While all calculations agree that the C<sub>1</sub>-C<sub>2</sub> bond is the shortest bond in the ring, the degree of alternation from an equilibrium geometry of benzene in the remaining bonds is still in dispute<sup>7</sup>. The calculated geometrical parameters are often used to determine the most significant resonance structure of 1,2-DHB, namely the aromatic (1a), cycloalkyne-like (1b) or cumulene-like (1c) structures of 1,2-DHB.



(1a)



(1b)



(1c)

The geometrical parameters from an early  $\pi$ -electron calculation by Coulson<sup>8</sup> and a normal coordinate analysis by Laing and Berry<sup>35</sup> are consistent with structure (1b). However, the former should be regarded as having at best a crudely qualitative significance as was warned by the author, and the latter does not conform a cyclic structure<sup>36</sup>. Thus, practically no theoretical calculation provides geometrical

parameters suitable to structure (1b)<sup>17</sup>. The RHF/STO-3G equilibrium geometry is somewhat close to structure (1b), but with a negligible bond length alternation between the C<sub>2</sub>-C<sub>3</sub> and C<sub>3</sub>-C<sub>4</sub> bonds. The absence of lengthening in the bonds adjacent to C<sub>1</sub>-C<sub>2</sub> was explained in terms of an *ab-initio* hybrid orbital analysis<sup>17</sup>. On the other hand, the total overlap populations do alternate in the sense of structure (1b)<sup>17</sup>.

EHT calculations on 1,2-DHB employing the benzene geometry suggest a sizable contribution from structure (1c), *i.e.*, the total overlap population for the C<sub>4</sub>-C<sub>5</sub> bond is larger than that for the adjacent C<sub>3</sub>-C<sub>4</sub> and C<sub>5</sub>-C<sub>6</sub> bonds, and the  $\pi$ -electron overlap population alternates around the ring in the sense of (1c)<sup>9</sup>. Haselbach supported this prediction with the MINDO/2 calculation<sup>11</sup>. However, these calculations are at too rudimentary a level to draw any definitive conclusion.

Most other calculations provide geometries which are characterized by short C<sub>1</sub>-C<sub>2</sub> acetylenic bond lengths (1.22 - 1.30 Å) and progressively increasing C<sub>2</sub>-C<sub>3</sub> (1.38 - 1.39 Å), C<sub>3</sub>-C<sub>4</sub> (1.39 - 1.42 Å) and C<sub>4</sub>-C<sub>5</sub> (1.40 - 1.43 Å) bond lengths around the ring<sup>17-28</sup>, structure (1a). Except for the C<sub>1</sub>-C<sub>2</sub> bond, the bond lengths are quite close to the benzene value (1.40 Å). Through a comparison of calculated bond lengths,  $\pi$ -charge transfer, and  $\pi$ -electron overlap population for

1,2-DHB, benzene, and acyclic molecules, Bock *et al.* concluded that 1,2-DHB possesses a highly strained aromatic structure<sup>24</sup>.

The IR spectrum of 1,2-DHB favors the cycloalkyne-like structure with cumulene-like  $\pi$ -electron system<sup>37a</sup>. On the other hand, the UV/VIS spectrum clearly shows that the  $\pi \rightarrow \pi^*$  transitions are from the benzenoid structure<sup>45</sup>. Recently, Brown *et al.* reported the microwave transitions of 1,2-DHB from which rotational constants were derived (A: 6990, B: 5707 and C: 3140 MHz)<sup>55</sup>. The calculated rotational constants using the HF 6-31G\* optimized geometry by Bock *et al.* show a good agreement with the observed values<sup>55</sup>.

Combining all currently available experimental and theoretical results, we conclude that the true structure of 1,2-DHB is an aromatic system with an acetylenic C<sub>1</sub>-C<sub>2</sub> bond. There is no substantial experimental or theoretical evidence supporting a cumulene-like structure. A cycloalkyne-like structure seems to be the most significant resonance contribution, as is reflected by the  $\pi$ -electron population<sup>17,20,24</sup>, but the absence of bond length alternation around the ring is inconsistent with this structure. At this time, the geometry optimized at the GVB/6-31G\* level by Rigby *et al.* seems to be the best, since among all structures in Table 2.8, its rotational constants

Table 2.6. Geometrical parameters of 1,2-DHB

Parameter method	R <sub>1</sub>	R <sub>2</sub>	R <sub>3</sub>	R <sub>4</sub>	S <sub>1</sub>	S <sub>2</sub>	α <sub>1</sub>	α <sub>2</sub>	α <sub>3</sub>	β <sub>1</sub>	β <sub>2</sub>	ref.
π-electron	1.22	1.44	1.37	1.42								8
ZDO, semi- empirical	1.29	1.39	1.41	1.39								11
MINDO/2	1.256	1.344	1.399	1.402	1.084	1.084	130.0	106.0	124.0	128.0	119.0	14
MINDO/3	1.279	1.385	1.416	1.424			127.4	109.7	122.9			18,19
MINDO/3-CI	1.291	1.384	1.417	1.419			127.2	109.8	123.0			18
MINDO	1.252	1.382	1.424	1.434	1.082	1.090	129.0	107.8	123.2	127.6	118.5	21
MINDO/CI	1.298	1.381	1.421	1.425								23
MINDOC/SCF	1.243	1.381	1.409	1.425								22
MINDOC/2x2CI	1.243	1.381	1.409	1.425								22
MINDOC/BMEN1	1.281	1.388	1.418	1.452								22
RHF/STO-3G	1.218	1.392	1.389	1.421	1.084	1.084	127.6	109.9	122.5	127.4	119.3	17, **
RHF/3-21G	1.225	1.383	1.396	1.408	1.068	1.072	127.3	110.3	122.4	126.9	119.0	25, 26
GVB/3-21G	1.261	1.382	1.392	1.403	1.069	1.072	125.6	112.6	121.8	125.2	119.3	27
RHF/4-31G	1.226	1.389	1.389	1.420	1.080	1.080	127.2	110.5	122.3	124.8	118.9	20
RHF/6-31G	1.232	1.385	1.398	1.410	1.069	1.073	127.2	110.2	122.4	126.8	118.9	24
RHF/6-31G*	1.223	1.382	1.391	1.410	1.073	1.076	127.3	110.2	122.4	126.9	118.9	24
GVB/6-31G*	1.260	1.383	1.389	1.404	1.073	1.076	125.7	112.4	121.9	125.3	119.3	27, 28
Normal Coord. Analysis	1.349	1.401	1.387	1.405			124.0	118.0	118.0			30

R<sub>1</sub>=C<sub>1</sub>C<sub>2</sub>, R<sub>2</sub>=C<sub>2</sub>C<sub>3</sub>, R<sub>3</sub>=C<sub>3</sub>C<sub>4</sub>, R<sub>4</sub>=C<sub>4</sub>C<sub>5</sub>, S<sub>1</sub>=C<sub>3</sub>H<sub>1</sub>, S<sub>2</sub>=C<sub>4</sub>H<sub>2</sub>, α<sub>1</sub>=∠C<sub>1</sub>C<sub>2</sub>C<sub>3</sub>, α<sub>2</sub>=∠C<sub>2</sub>C<sub>3</sub>C<sub>4</sub>, α<sub>3</sub>=∠C<sub>3</sub>C<sub>4</sub>C<sub>5</sub>.

β=∠C<sub>2</sub>C<sub>3</sub>H<sub>1</sub>, β=∠C<sub>3</sub>C<sub>4</sub>H<sub>2</sub>.

are in best agreement with the experimentally observed values.

#### 2.1.8. The triplet geometry of 1,2-DHB

Since the lowest triplet state of 1,2-DHB is known not to be the ground state and is not likely to be observed experimentally, its structure has attracted less interest. However, our knowledge of 1,2-DHB would not be complete without an adequate description of its triplet state.

The geometrical parameters of triplet 1,2-DHB, calculated at the ROHF/3-21G level are listed in Table 2.7 along with the previously reported MINDO/3 results. Both calculations agree that the  $C_1-C_2$  bond distance will be considerably elongated in the triplet state, with the consequent loss of triple bond character, but they predict very different bond length alternation for the other three bonds around the ring. While the MINDO/3 geometry is somewhat close to a cumulene-like structure, the ROHF/3-21G geometry corresponds to a Kékulé benzene structure.

11 111  
111111

Table 2.7. Geometrical parameters of triplet 1,2-DHB

parameter method	R <sub>1</sub>	R <sub>2</sub>	R <sub>3</sub>	R <sub>4</sub>	S <sub>1</sub>	S <sub>2</sub>	α <sub>1</sub>	α <sub>2</sub>	α <sub>3</sub>	β <sub>1</sub>	β <sub>2</sub>	Ref.
MINDO/3	1.376	1.384	1.410	1.406	1.080	1.080	122.4	116.6	120.0			18
ROHF/ 3-21G	1.381	1.371	1.394	1.383	1.071	1.072	120.9	118.6	121.5	120.6	119.6	This work



## 2.2. 1,3-Didehydrobenzene (1,3-DHB)

### 2.2.1. Experimental studies

Berry *et al.* observed a transient species at  $m/z=76$  by means of time-of-flight mass spectrometry following the flash vacuum photolysis of benzenediazonium-3-carboxylate<sup>63a</sup>. The kinetic UV spectrum of this compound shows a continuous absorption from 220 to 290 nm and perhaps two maxima at 328 and 339 nm. They attributed this spectrum to 1,3-DHB whose structure is represented by either 1,3-diyl (2a) or bicyclo[3.1.0]hexatriene (2b).

Experimental evidence for the intermediacy of both (2a) and (2b) has been obtained. Washburn and his coworkers firmly established the involvement of (2b) as a reaction intermediate in the dehalogenation of *exo,exo*-4,6-dibromobicyclo[3.1.0]hexene and related compounds with lithium dimethylamide at  $-75^{\circ}\text{C}$ <sup>66</sup>. Experimental results by Billups *et al.* (isolation of the substituted naphthalenes from the dehydrohalogenation of benzo-6,6-dichloro-5-bromobicyclo[3.1.0]hex-2-ene)<sup>67</sup>, by Bergman *et al.* (high temperature pyrolysis of disubstituted 1,5-hexadiyne-3-enes)<sup>68</sup> and by Gaviña *et al.* (thermal decomposition of diaryliodonium-3-carboxylate with trapping resins)<sup>74</sup> strongly support the intermediacy of (2a) in their reaction mechanisms.

1950-1951

1952-1953

1954

1955

1956

1957

1958

These experimental results indicate that the occurrence of (2a) or (2b) depends largely on the method of generation. At low temperature, from a precursor that already contains the 1-3 bridge bond, bicyclic (2b) can be generated and trapped by very reactive reagents before ring opening to diradical. On the other hand, high temperature thermal rearrangement or decomposition produces diradicals (2a), which subsequently exhibit free radical properties.

No direct spectroscopic observation has yet been reported for this interesting isomer.

### 2.2.2. Theoretical studies

The results from various theoretical calculations for the 1,3- isomer are as controversial as those from experimental studies. Hoffman *et al.* pointed out that there exists substantial 1-3 bonding in 1,3-DHB, based on the EHT population analysis<sup>9</sup>. Hess and Schaad estimated the REPEs (resonance energy per  $\pi$ -electron) for the bicyclic, diradical and zwitterionic structure of 1,3-DHB, from which they found that the bicyclic structure (2b) ( $0.055\beta$ ) retains the most aromatic character (e.g. benzene;  $0.065\beta$ )<sup>65</sup>. Subsequently, based on the MINDO/3-SCF and MINDO/3-CI calculations, Dewar

and Li predicted that 1,3-DHB exists as a singlet bicyclic structure with ground state energy comparable to 1,2-DHB<sup>18</sup>. Washburn also reported that the RHF/STO-3G geometry optimization leads to a closed-shell bicyclic structure (2b)<sup>66a</sup>.

Noell and Newton performed a limited geometry optimization for 1,3-DHB at the GVB level with a 4-31G basis set<sup>20</sup>. They concentrated their efforts on the C<sub>1</sub>-C<sub>3</sub> separation while each C-C bond length in the six-membered ring was held fixed at the corresponding MINDO/3-SCF equilibrium value. From this calculation, they concluded that 1,3-DHB exists as a singlet diradical. However, no attempt was made to ascertain if the GVB level would yield a local minimum for a bicyclic geometry. Thiel carried out MNDOC/SCF, MNDOC/2x2CI and MNDOC/BWEN1 calculations on all three DHB isomers<sup>22</sup>. It was found that the SCF geometry of 1,3-DHB corresponds to a closed-shell bicyclic structure, and the 2x2CI and BWEN1 to a diradicaloid. Dewar *et al.* reexamined the structures and energetics of DHBs using MNDO/SCF, MNDO/3x3CI and UMNDO calculations<sup>23</sup>. While the MNDO/SCF method failed to obtain the diradical structure, both structures were MNDO/3x3CI at the local minima with (2a) being more stable than (2b) by 5.7 kcal/mole.

Since the *ab-initio* calculations on 1,3-DHB by Noell and

Newton were somewhat limited, we have reexamined the structures and energetics of this molecule with the fully optimized geometry at the RHF and GVB levels with a 3-21G basis set. The results of these calculations are collected in Table 2.8 along with the previously reported results. Except the C-C bond length alternation around the ring, the results are in good accord with those from the GVB/4-31G calculations.

The bicyclic structure is found to be a local minimum on the RHF potential surface, but is located on an inflection point of the GVB potential curve ( $E_T^{\text{GVB}}$  vs.  $R_{\text{C}_1-\text{C}_3}$ ) at a  $\text{C}_1-\text{C}_3$  distance of 1.54 Å, which lies 33.2 kcal/mole above the equilibrium diradical structure. The MNDOC /2x2CI and /BWEN1 geometry optimization also failed to find the bicyclic minimum for 1,3-DHB. On the other hand, the barrier to conversion of (2b) to (2a) is substantially large (~ 9 kcal/mole) in the MNDO/3x3CI calculation, which indicates that (2b) must exist as a stable reaction intermediate. If the failure to describe bicyclic 1,3-DHB at the GVB/3-21G level stems from the overestimation of ring strain energy by the use of a small split basis set, this problem may be corrected by employing a larger basis set including polarization functions. However, as discussed further in the next section, this is not likely to be the case because the GVB/3-21G calculation could successfully optimize the

Table 2.8. Geometrical parameters of 1,3-DNB

Method	para- Meters				ref.	
	R <sub>1</sub>	R <sub>2</sub>	R <sub>3</sub>	R <sub>4</sub>		
<sup>1</sup> A <sub>1</sub> MINDO/3	1.360	1.389	1.412	1.955	91.9 142.4 115.0 113.3	18
MINDO/3-CI	1.373	1.389	1.411	2.120	101.1 134.6 117.1 115.2	18
MINDO/SCF	1.372	1.379	1.420	1.582	70.4	22 <sup>22</sup>
MINDO/2x2CI	1.377	1.377	1.406	2.204	106.3	22
MINDO/BIENI	1.379	1.382	1.415	2.186	104.9	22
MINDO-CI	1.382	1.382	1.428	1.628	72.2	23 <sup>23</sup>
	1.381	1.381	1.412	2.202	105.0	
RHF/STO-3G	1.364	1.391	1.389	1.500	66.7 163.3 107.7 111.4	66a <sup>66</sup>
RHF/3-21G	1.352	1.381	1.413	1.514	68.1 163.5 106.2 112.4	This work <sup>22</sup>
GVB/3-21G	1.377	1.372	1.390	2.242	109.0 128.4 118.3 117.7	This work
GVB/4-31G	1.360	1.389	1.412	2.208	108.5 129.6 117.5 116.8	20 <sup>20</sup>
<sup>3</sup> B <sub>2</sub> MINDO/3	1.389	1.383		2.306	112.2 128.0	18
RONF/3-21G	1.376	1.374	1.392	2.326	115.4 124.3 117.6 120.8	This work
RONF/4-31G	1.360	1.389	1.412	2.295	115.1 124.2 120.9 114.7	20 <sup>20</sup>

R<sub>1</sub>=C<sub>1</sub>C<sub>2</sub>, R<sub>2</sub>=C<sub>3</sub>C<sub>4</sub>, R<sub>3</sub>=C<sub>4</sub>C<sub>5</sub>, R<sub>4</sub>=C<sub>1</sub>C<sub>3</sub>, α<sub>1</sub>=∠C<sub>1</sub>C<sub>2</sub>C<sub>3</sub>, α<sub>2</sub>=∠C<sub>2</sub>C<sub>3</sub>C<sub>4</sub>, α<sub>3</sub>=∠C<sub>3</sub>C<sub>4</sub>C<sub>5</sub>, α<sub>4</sub>=∠C<sub>4</sub>C<sub>3</sub>C<sub>2</sub>  
 x partially optimized with respect to R<sub>4</sub> from the MINDO/3 geometry.

<sup>22</sup>bicyclic structure

extremely strained bicyclic ring structure of 1,4-DHB (butalene). Thus, our GVB calculations on 1,3-DHB suggest that the bicyclic form (2b) is not a stable intermediate, but exists as a transient species.

Early INDO and *ab-initio* CI calculations on 1,3-DHB with the equilibrium geometry of benzene predict that the ground electronic state of 1,3-DHB is a triplet. More recent calculations, however, show that the singlet state is 5 - 18 kcal/mole below the triplet state (see Table 2.9).

Table 2.9. Singlet-Triplet separation of 1,3-DHB

method	$\Delta E(S-T)$	comments	ref.
INDO	-26.5	benzene geometry	13
2-Det. CI	- 1.8	benzene geometry ROHF triplet	15
many-Det. CI	- 1.6	benzene geometry	15
MINDO/3	6.2	MINDO/3 singlet	18
GVB/ROHF	17.8	4-31G, partially optimized geometry	20
GVB/ROHF	10.5	3-21G	This work

Director  
General  
and  
Secretary  
of  
the  
Board  
of  
Education



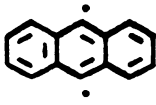
### 2.3. 1,4-Didehydrobenzene (1,4-DHB)

#### 2.3.1. Experimental studies

Like the 1,2- and 1,3- isomers, Berry *et al.* ascribed the species at  $m/z=76$  obtained during the flash vacuum photolysis of benzenediazonium-4-carboxylate to 1,4-DHB<sup>63</sup>. Based on the appearance and decay patterns of this species measured by kinetic UV and time-of-flight mass spectrometry, they proposed two most likely structures, (3a) and (3b), for 1,4-DHB.

Bergman and his coworkers reported that the gas phase thermal equilibration of *cis*-1,6- and *cis*-3,4-dideuterio-1,5-hexadiyne-3-ene takes place via (3a)<sup>69,71</sup>. When these molecules were heated in solution, aromatic products consistent with the trapping of the (3a) were obtained. Recently, Gaviña *et al.* found evidence of (3a) as a reaction intermediate in the thermal decomposition of diaryliodonium-4-carboxylate with trapping resins<sup>74</sup>. On the other hand, Breslow *et al.* presented evidence for the intervention of (3b) as a stable intermediate in the reaction of lithium dimethylamide with 1-chlorobicyclo[2.2.0]hexa-2,5-diene<sup>72</sup>.

The spin state of 1,4-DHB has been inferred as a singlet from the fact that no ESR signal could be observed for matrix

isolated 9,10-didehydroanthracene (  )<sup>70</sup>. From CIDNP (chemically induced dynamic nuclear polarization) and cage-escape reaction studies on diradical 2,3-dipropyl-1,4-DHB produced in the solution thermolysis of *Z*-4,5-diethynyl-4-octene, Bergman and his coworkers concluded that the reactive state of the diradical is a singlet<sup>71</sup>.

Thus, the experimental results indicate that 1,4-DHB can exist in both diradical (3a) and bicyclic (3b) forms, and that the most probable ground electronic state is a singlet diradical. As in the case of 1,3-DHB, no direct spectroscopic observations of 1,4-DHB have been reported. An attempt to obtain the IR spectrum of 1,4-DHB in an N<sub>2</sub> matrix via UV photolysis of the precursor 1,4-diiodobenzene has not been successful<sup>73</sup>.

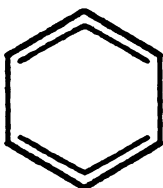
### 2.3.2. Theoretical studies

In contrast to previously published results<sup>18,22,23</sup>, the GVB/3-21G geometry optimization for singlet 1,4-DHB finds three local minima; two bicyclic and one diradical structure. The first bicyclic structure (3b) (hereafter simply termed butalene-A) lies 81.3 kcal/mole above the lowest diradical structure with long transannular bond (C<sub>1</sub>-C<sub>4</sub>; 1.698 Å). The second bicyclic structure (3b') (butalene-B) lies 10.7 kcal/mole above butalene-A (92.0 kcal/mole above the

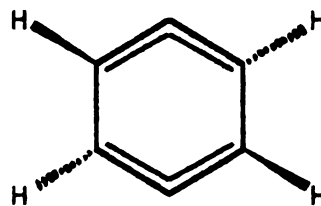
diradical 1,4-DHB) with a rather short  $C_1-C_4$  bond distance (1.454 Å). The energy differences for these two bicyclic structures with respect to the lowest diradical 1,4-DHB (3a) are much higher than those from the semi-empirical calculations. As Noell and Newton pointed out<sup>20</sup>, these values may be too large by as much as a factor of 2. The detailed structures of these three 1,4-DHBs are listed in Table 2.10 along with the previously reported values.



(3b')



(3c)



(3d)

Based on the EHT population analysis, Hoffman suggested that the resonance structure bisallene (3c) may contribute significantly to the diradical 1,4-DHB<sup>9</sup>; the total overlap population for the  $C_1-C_2$  (equivalently  $C_3-C_4$ ,  $C_4-C_5$  and  $C_6-C_1$ ) bond is larger than that for the  $C_2-C_3$  (or  $C_5-C_6$ ) bond, and the overlap population for  $C_1-C_4$  is a negative value. All semi-empirical methods and RHF/3-21G yield diradical geometries which seem to reflect this tendency. Recently, Jhonson proposed that the non-planar bisallene (3d) be considered as a possible structure of 1,4-DHB<sup>7</sup>. Even though the GVB/3-21G equilibrium geometry also reflects a

1948

Vol. 1

1948

1948

1948

resonance contribution from a bisallene, the bond length and the  $\pi$ -electron overlap population alternation around the ring are much smaller than those predicted from other calculations. That is, the GVB equilibrium geometry retains the most aromatic character.

The presence of butalene-A has been reported by Dewar and Li<sup>18</sup>. The results of their MINDO/3 calculation show that butalene-A lies 38.5 kcal/mole above the diradical 1,4-DHB with a 4.6 kcal/mole barrier to conversion of (3b) to (3a). Subsequent theoretical results from the MNDOC calculation by Thiel<sup>22</sup>, and from the MNDO calculation by Dewar *et al*<sup>23</sup>, are qualitatively similar to those from the MINDO/3 calculation. A limited geometry optimization at the GVB/4-31G level starting with the MINDO/3 equilibrium geometry yielded an inflection point at the C<sub>1</sub>-C<sub>4</sub> distance of 1.67 Å<sup>20</sup>, which suggests that a complete optimization would lead to butalene-A. As was mentioned earlier, a complete geometry optimization at the GVB/3-21G level indeed obtains butalene-A, and to our surprise, a new species butalene-B. Perhaps the most interesting comparison between butalene-A and butalene-B structures is the reversal of the C<sub>1</sub>-C<sub>4</sub> and C<sub>2</sub>-C<sub>3</sub> bond distances; while the C<sub>1</sub>-C<sub>4</sub> bond length of butalene-B is considerably shortened from that of butalene-A (1.698 → 1.454 Å), the opposite C<sub>2</sub>-C<sub>3</sub> bond is noticeably elongated (1.437 → 1.482 Å).

Table 2.10. Geometrical parameters of 1,4-DHB

species	parameter method	$R_1$	$R_2$	$R_3$	$\alpha_1$	$\alpha_2$	ref.
(3a)	MINDO/3	1.359	1.465	2.720	117.7	126.6	18
	MINDO/3-CI	1.373	1.439	2.724	117.9	124.3	18
	MNDOC/SCF	1.344	1.466	2.604			22
	MNDOC/2x2CI	1.370	1.420	2.624			22
	MNDOC/BWEN1	1.363	1.453	2.653			22
	MINDO/3x3CI	1.37	1.43	2.55			23
	ROHF/3-21G	1.324	1.510	2.674	116.1	127.9	*
	GVB/3-21G	1.369	1.403	2.678	117.7	124.3	*
	GVB/4-31G	1.373	1.439	2.701	117.4	125.3	20
(3b)	MINDO/3-CI	1.393	1.426	1.667	95.0	170.0	18
	MNDOC/SCF	1.388	1.442	1.604			22
	MNDOC/2x2CI	1.389	1.444	1.599			22
	MNDOC/BWEN1	1.397	1.453	1.613			22
	MINDO/3x3CI	1.39	1.45	1.62			23
	GVB/3-21G	1.391	1.437	1.698	95.4	169.2	*
(3b')	GVB/3-21G	1.389	1.482	1.454	89.4	181.2	*
triplet	MINDO/3	1.386	1.410		115.7	126.6	18
	ROHF/4-31G	1.373	1.439	2.677	116.8	126.4	23
	ROHF/3-21G	1.374	1.394	2.654	117.3	125.4	*

$$R_1=C_1C_2, R_2=C_2C_3, R_3=C_1C_3, \alpha_1=\angle C_1C_2C_3, \alpha_2=\angle C_3C_4C_5$$

\* This work

The  $\sigma$ - and  $\pi$ -electron overlap population for butalene-A and butalene-B alternate markedly around the two fused rings, which is indicative of complete loss of aromaticity. While butalene-A and -B form a strong transannular bond, the  $\pi$ -electrons in this bond are quite repulsive. As we squeeze the  $C_1$ - $C_4$  distance of diradical 1,4-DHB to form butalenes, the opposite  $C_2$ - $C_3$  bond length is elongated. On the other hand, the total overlap population for this bond also increases with the elongation; this surprising result may explain how this extremely strained molecule can retain its ring structure. These results are summarized in Table 2.11.

Table 2.11. The overlap population for 1,4-DHB

isomer	bond	overlap population		isomer	bond	overlap population	
		$n(\sigma)$	$n(\pi)$			$n(\sigma)$	$n(\pi)$
(3a)	$C_1C_2$	0.671	0.299	(3b')	$C_1C_2$	0.406	0.353
	$C_2C_3$	0.559	0.277		$C_2C_3$	0.962	0.180
	$C_1C_4$	-0.013	-0.025		$C_1C_4$	1.033	-0.237
(3b)	$C_1C_2$	0.468	0.331	benzene	CC	0.650	0.293
	$C_2C_3$	0.876	0.217				
	$C_1C_4$	0.849	-0.169				

Table 2.12 lists the singlet-triplet separations calculated for 1,4-DHB at various levels of theory. In accord with the GVB/4-31G calculation<sup>20</sup>, we predict that triplet

1941  
1942

1943  
1944



1,4-DHB lies 1.3 kcal/mole below the singlet. While the C-C bond lengths of the triplet 1,4-DHB hexagon are less distorted from an equilibrium benzene geometry, the C<sub>1</sub>-C<sub>4</sub> transannular bond is shorter than that of the singlet structure. This may be explained in terms of the electronic configuration of triplet 1,4-DHB. The HOMO (5b<sub>1u</sub>) of diradical 1,4-DHB approximately corresponds to the antisymmetric combination of the two radical lobe orbitals and the LUMO (6a<sub>g</sub>) to the symmetric combination. Thus, the electronic configuration of triplet 1,4-DHB (~ 5b<sub>1u</sub><sup>1</sup>6a<sub>g</sub><sup>1</sup>) increases the bonding character between the two radical centers.

Table 2.12. Singlet-Triplet separation of 1,4-DHB

method	$\Delta E(S-T)$	comments	ref.
INDO	-42.7	benzene geometry	13
2-Det. CI	- 5.7	benzene geometry ROHF triplet	15
many-Det. CI	- 3.5	benzene geometry	15
MINDO/3	-10.8		18
GVB/ROHF	1.4	4-31G, partially optimized geometry	20
GVB/ROHF	1.3	3-21G	This work

1944-1945  
1946-1947  
1948-1949  
1950-1951  
1952-1953  
1954-1955  
1956-1957  
1958-1959  
1960-1961  
1962-1963  
1964-1965  
1966-1967  
1968-1969  
1970-1971  
1972-1973  
1974-1975  
1976-1977  
1978-1979  
1980-1981  
1982-1983  
1984-1985  
1986-1987  
1988-1989  
1990-1991  
1992-1993  
1994-1995  
1996-1997  
1998-1999  
2000-2001  
2002-2003  
2004-2005  
2006-2007  
2008-2009  
2010-2011  
2012-2013  
2014-2015  
2016-2017  
2018-2019  
2020-2021  
2022-2023  
2024-2025

#### 2.4. Summary and conclusion

The relative energies of three DHBs (1a, 2a and 3a) are in the order: 1,2- (0.0 kcal/mole) < 1,3- (16.0 kcal/mole) < 1,4- (23.9 kcal/mole) at the GVB/3-21G level. This is in good accord with the GVB/4-31G calculation<sup>20</sup>. In contrast to the *ab-initio* calculations, at the 2x2CI level, the semi-empirical MINDO/3, MNDO and MNDOC methods predict that singlet 1,3-DHB is the most stable isomer<sup>18,22,23</sup>. Only the MNDOC/BWEN1 gives the same order as the GVB results<sup>22</sup>. Dewar *et al.*, however, suggested that their MINDO/3 and MNDO results should be reinterpreted based on the following rule-of-thumb<sup>23</sup>: if the difference between the MINDO/3 or MNDO/SCF and their CI energies for a molecule is less than 15 kcal/mole, the former is then to be preferred; if greater, the CI values plus 15 kcal/mole should be taken. According to this rule, the relative energies of three DHBs are given as follow; 1,2- = 1,3- < 1,4- (14 kcal/mole) at the MINDO/3 level<sup>18</sup>, and 1,2- < 1,3- (8 kcal/mole) < 1,4- (9 kcal/mole) at the MNDO level<sup>23</sup>. The main conclusions drawn are that the 1,3-isomer has similar stability to that of 1,2-DHB, and that bicyclic 1,3- and 1,4-DHB are stable intermediates. However, the greatest uncertainty in the semi-empirical results for DHBs arises from the fact that a direct comparison of tabulated numerical values at a given level of calculation (see Table 2.13) does not lead to the same conclusion. As a

1950

1951

1952

1953

1954

1955

1956

1957

1958

1959

1960

1961

1962

1963

1964

result, there has been considerable confusion amongst other researchers concerning the appropriate choice of theoretical values.

Table 2.13. Relative energies (kcal/mole) of DHBs

method \ isomers	(1)	(2a)	(2b)	(3a)	(3b)	(3b')	ref.
INDO	0.0	+ 8.5(T)		+ 9.8(T)			13
2-Det. CI	0.0	+10.8(T)		+ 9.3(T)			15
many-Det. CI	0.0	+11.0(T)		+10.3(T)			15
MINDO/3, SCF	0.0		- 0.7	+15.6			18**
MINDO/3, 2x2CI	0.0	- 7.1		+ 2.6	+38.5		18**
MINDO/2x2CI	0.0	- 6.9		- 3.5	+26.2		22
MINDOC/2x2CI	0.0	-10.4		- 1.3	+31.3		22
MINDOC/BWEN1	0.0	+ 7.4		+17.9	+41.7		22
MINDO/SCF	0.0		+ 8.5	+35.7	+28.8		23**
MINDO/3x3CI	0.0	+ 5.2	+10.9	+ 5.9	+31.9		23**
UMINDO	0.0	+ 6.6		- 2.5	+35.7		23**
GVB/3-21G	0.0	+16.0	+46.0*	+23.9	+105.2	+115.9	This work
GVB/4-31G	0.0	+14.5		+23.3	+100.5*		20

\* Not a local minimum. \*\* See text for reinterpreted values.

(T) indicate the ground state is a triplet.

Since the relative stability of three DHBs has not been established experimentally, it is difficult judge which theoretical results are correct. However, the merits of the

2000  
1000  
500

2000  
1000  
500

*ab-initio* predictions over the semi-empirical results are in their consistency at a given level of calculation.

Various experimental and theoretical results suggest that 1,2-DHB has dual nature in conventional interpretation; while it is an aromatic system with respect to its electronic structure (section 2.1.3 and 2.1.6), its C<sub>1</sub>-C<sub>2</sub> bond closely resembles the *cis*-bent acetylenic bond (sections 2.1.4 - 2.1.6). All known results generally agree that the ground electronic state of 1,2-DHB is a singlet (section 2.1.1). On the other hand, as discussed in section 2.1.2, the first ionization potential and the heat of formation for 1,2-DHB are not yet definitively determined.

While both bicyclic and diradical structures of 1,3-DHB are predicted to correspond to local minima on the MNDO/3x3CI potential surface<sup>23</sup>, only the diradical structure is found at the GVB/3-21G level. The bicyclic structure is located on an inflection point of the GVB potential curve, at a C<sub>1</sub>-C<sub>3</sub> distance of 1.54 Å, thus suggesting that it may not be a stable reaction intermediate.

There are three isomeric species for 1,4-DHB; one diradical and two bicyclic structures. The GVB/3-21G geometry optimization obtains a modestly distorted diradical structure from the equilibrium geometry of benzene, but the extent of

1111-11  
1111-11  
1111-11  
1111-11  
1111-11



this distortion is much less than those obtained by semi-empirical optimizations. The strained bicyclic structures retain their equilibrium geometries by balancing the lengthening of the C<sub>2</sub>-C<sub>3</sub> bond with the increase in its total overlap population. The  $\pi$ -electron overlap population for each C-C bond of bicyclic 1,4-DHBs alternate markedly around the two fused four-membered rings, indicating that the bicyclic 1,4-DHBs are anti-aromatic in character.



## REFERENCES



1. (a) Hoffman, R. W. "*Dehydrobenzene and Cycloalkynes*"; Academic Press: New York, 1967.; (b) Hoffman, R. W. In "*Chemistry of Acetylenes*"; Viehe, H. G., Ed.; Marcel Deckker: New York, 1969; p 1063.
2. Various authors "*Arynes, Carbenes, Nitrenes, and Related Species*" in *Annu. Rep. Progr. Chem., Sect. B.* from 1972 (vol 68) to 1985 (vol 81).
3. (a) Field, E. K. In "*Organic Reactive Intermediates*"; McManus, S. P., Ed.; Academic Press: New York, 1973; Chapter 7.; (b) Field, E. K.; Meyerson, S. *Adv. Phys. Org. Chem.*, 1968, 6, 1.
4. Levin, R. H. *React. Intermed. (Wiley)* 1978, 1, 1; *ibid.* 1981, 2, 1; *ibid.* 1985, 3, 1.
5. Reinecke, M. G. In "*Reactive Intermediates, vol 2.*"; Abramovitch, R. A., Ed.; Plenum Press: New York, 1981; Chapter 5.
6. Gilchrist, T. L. In "*The Chemistry of Triple-Bonded Functional Groups, Supplement C:*" Patai, S.; Rappoport, Z., Eds.; Wiley: New York, 1983; Chapter 11.
7. Johnson, R. P. In "*Molecular Structure and Energetics, vol. 3.*"; Liebman, J. F.; Greenberg, A. Eds; VCH: Deerfield Beach, 1986; Chapter 3.
8. Coulson, C. A. *Chem. Soc. Spec. Publ.* 1961, 12, 100.
9. Hoffmann, R.; Imamura, A.; Hehre, W. J. *J. Am. Chem. Soc.* 1968, 90, 1499.
10. Gheorghiu, M. D.; Hoffmann, R. *Rev. Roum. Chim.* 1969, 14,

- 947.
11. Yonezawa, T.; Konishi, H.; Kato, H. *Bull. Chem. Soc. Jap.* 1969, 42, 933.
  12. Atkin, R. W.; Claxton, T. A. *Trans. Faraday Soc.* 1970, 66, 257.
  13. Olsen, J. F. *J. Mol. Struct.* 1971, 8, 307.
  14. Haselbach, E. *Helv. Chim. Acta* 1971, 54, 210.
  15. (a) Wilhite, D. L.; Whitten, J. L. *J. Am. Chem. Soc.* 1971, 93, 2868.; (b) Whitten, J. L. *Acc. Chem. Res.* 1973, 6, 236.
  16. Mille, P; Praud, L.; Serre, J. *Int. J. Quantum Chem.* 1971, 4, 187.
  17. (a) Newton, M. D.; Fraenkel, H. A. *Chem. Phys. Lett.* 1973, 18, 244. (b) Newton, M. D. In "Applications of Electronic Structure Theory"; Schaefer, H. F., III, Ed.; Plenum Press: New York, 1977; Chapter 6.
  18. (a) Dewar, M. J. S.; Lee, W.-K. *J. Am. Chem. Soc.* 1974, 96, 5569. (b) Dewar, M. J. S. *Pure and Appl. Chem.* 1975, 44, 767.
  19. Yamaguchi, K.; Nishio, A.; Yabushita, S.; Fueno, T. *Chem. Phys. Lett.* 1978, 53, 109.
  20. Newton, M. D.; Noell, J. O. *J. Am. Chem. Soc.* 1979, 101, 51.
  21. Dewar, M. J. S.; Ford, G. P.; Rzepa, H. S. *J. Mol. Struct.* 1979, 51, 275.
  22. Thiel, W. *J. Am. Chem. Soc.* 1981, 103, 1420.
  23. Dewar, M. J. S.; Ford, G. P.; Reynolds, C. H. *J. Am. Chem.*

11. 11. 11.  
12. 12. 12.  
13. 13. 13.  
14. 14. 14.  
15. 15. 15.  
16. 16. 16.  
17. 17. 17.  
18. 18. 18.  
19. 19. 19.  
20. 20. 20.  
21. 21. 21.  
22. 22. 22.  
23. 23. 23.  
24. 24. 24.  
25. 25. 25.  
26. 26. 26.  
27. 27. 27.  
28. 28. 28.  
29. 29. 29.  
30. 30. 30.  
31. 31. 31.  
32. 32. 32.  
33. 33. 33.  
34. 34. 34.  
35. 35. 35.  
36. 36. 36.  
37. 37. 37.  
38. 38. 38.  
39. 39. 39.  
40. 40. 40.  
41. 41. 41.  
42. 42. 42.  
43. 43. 43.  
44. 44. 44.  
45. 45. 45.  
46. 46. 46.  
47. 47. 47.  
48. 48. 48.  
49. 49. 49.  
50. 50. 50.  
51. 51. 51.  
52. 52. 52.  
53. 53. 53.  
54. 54. 54.  
55. 55. 55.  
56. 56. 56.  
57. 57. 57.  
58. 58. 58.  
59. 59. 59.  
60. 60. 60.  
61. 61. 61.  
62. 62. 62.  
63. 63. 63.  
64. 64. 64.  
65. 65. 65.  
66. 66. 66.  
67. 67. 67.  
68. 68. 68.  
69. 69. 69.  
70. 70. 70.  
71. 71. 71.  
72. 72. 72.  
73. 73. 73.  
74. 74. 74.  
75. 75. 75.  
76. 76. 76.  
77. 77. 77.  
78. 78. 78.  
79. 79. 79.  
80. 80. 80.  
81. 81. 81.  
82. 82. 82.  
83. 83. 83.  
84. 84. 84.  
85. 85. 85.  
86. 86. 86.  
87. 87. 87.  
88. 88. 88.  
89. 89. 89.  
90. 90. 90.  
91. 91. 91.  
92. 92. 92.  
93. 93. 93.  
94. 94. 94.  
95. 95. 95.  
96. 96. 96.  
97. 97. 97.  
98. 98. 98.  
99. 99. 99.  
100. 100. 100.

- Soc. 1983, 105, 3162.
24. Bock, C. W.; George, P.; Trachtman, M. J. *Phys. Chem.* 1984, 88, 1467.
25. Radom, L.; Nobes, R. H.; Underwood, D. J.; Lee, W.-K. *Pure and Appl. Chem.* 1986, 58, 75.
26. Apeloig, Y.; Arad, D.; Halton, B.; Randall, C. J. *J. Am. Chem. Soc.* 1986, 108, 4932.
27. Hiller, I. H.; Vincent, M. A.; Guest, M. F.; von Nissen, W. *Chem. Phys. Lett.* 1987, 134, 403.
28. Rigby, K.; Hiller, I. H.; Vincent, M. A. *J. Chem. Soc. Perkin Trans. II.* 1987, 117.
29. Rondan, N. G.; Domelsmith, L. N.; Houk, K. N.; Bowne, A. T.; Levin, R. H. *Tetrahedron Lett.* 1979, 3237.
30. Ng, L.; Jordan, K. D.; Krebs, A.; Rüger, W. *J. Am. Chem. Soc.* 1982, 104, 7414.
31. Schmidt, H.; Schweig, A.; Krebs, A. *Tetrahedron Lett.* 1974, 1471.
32. Krebs, A.; Wilke, J. *Top. Curr. Chem.* 1983, 109, 189.
33. Meier, H.; Peterson, H.; Kolshorn, H. *Chem. Ber.* 1980, 113, 2398.
34. Maier, W. F.; Lau, C. G.; McEwen, A. B. *J. Am. Chem. Soc.* 1985, 107, 4724.
35. Laing, J. W.; Berry, R. S. *J. Am. Chem. Soc.* 1976, 98, 660.
36. Nam, H.-H.; Leroi, G. E. *Spec. Chim. Acta* 1985, 41A, 67.
37. (a) Chapman, O. L.; Mattes, K.; McIntosh, C. L.; Pacansky, J.; Calder, G. V.; Orr, G. J. *Am. Chem. Soc.* 1973, 95,



- 6134.; (b) Chapman, O. L.; Chang, C.-C.; Kolc, J.; Rosenquist, N. R.; Tomioka, H. *ibid.* 1975, 97, 6586.
38. Dunkin, I. R.; MacDonald, J. G. *J. Chem. Soc. Chem. Comm.* 1979, 772.
39. Brown, R. F. C.; Browne, N. R.; Coulston, K. J.; Danen, L. B.; Eastwood, F. W.; Irvine, M. J.; Pullin, D. E. *Tetrahedron Lett.* 1986, 27, 1075.
40. Nam, H.-H.; Leroi, G. E. *J. Mol. Struct.* 1987, 157, 301.
41. Wentrup, C.; Blanch, R.; Briehl, H.; Gross, G. *J. Am. Chem. Soc.* 1988, 110, 1874.
42. (a) Berry, R. S.; Spokes, G. N.; Stiles, M. J. *Am. Chem. Soc.* 1962, 84, 3570.; (b) Schafer, M. E.; Berry, R. S. *ibid.* 1965, 87, 4497.
43. Porter, G.; Steinfeld, J. I. *J. Chem. Soc. (A)* 1968, 877.
44. Kolc, J. *Tetrahedron Lett.* 1972, 5321.
45. Münzel, N.; Schweig, A. *Chem. Phys. Lett.* 1988, 147, 192.
46. Fisher, I. P.; Lossing, F. P. *J. Am. Chem. Soc.* 1963, 85, 1018.
47. Natalis, P.; Franklin, J. L. *J. Phys. Chem.* 1965, 69, 2935.
48. Grützmacher, H. F.; Lohmann, J. *Justus Liebigs Ann. Chem.* 1967, 705, 81.
49. Rosenstock, H. M.; Larkins, J. T.; Walker, J. A. *Int. J. Mass. Spectrom. Ion Phys.* 1973, 11, 309.
50. Rosenstock, H. M.; Stockbauer, R. L.; Parr, A. C. *J. Chim. Phys.* 1980, 77, 745.
51. Pollack, S. K.; Hehre, W. J. *Tetrahedron Lett.* 1980, 21,

1. 1910  
 2. 1911  
 3. 1912  
 4. 1913  
 5. 1914  
 6. 1915  
 7. 1916  
 8. 1917  
 9. 1918  
 10. 1919  
 11. 1920  
 12. 1921  
 13. 1922  
 14. 1923  
 15. 1924  
 16. 1925  
 17. 1926  
 18. 1927  
 19. 1928  
 20. 1929  
 21. 1930  
 22. 1931  
 23. 1932  
 24. 1933  
 25. 1934  
 26. 1935  
 27. 1936  
 28. 1937  
 29. 1938  
 30. 1939  
 31. 1940  
 32. 1941  
 33. 1942  
 34. 1943  
 35. 1944  
 36. 1945  
 37. 1946  
 38. 1947  
 39. 1948  
 40. 1949  
 41. 1950  
 42. 1951  
 43. 1952  
 44. 1953  
 45. 1954  
 46. 1955  
 47. 1956  
 48. 1957  
 49. 1958  
 50. 1959  
 51. 1960  
 52. 1961  
 53. 1962  
 54. 1963  
 55. 1964  
 56. 1965  
 57. 1966  
 58. 1967  
 59. 1968  
 60. 1969  
 61. 1970  
 62. 1971  
 63. 1972  
 64. 1973  
 65. 1974  
 66. 1975  
 67. 1976  
 68. 1977  
 69. 1978  
 70. 1979  
 71. 1980  
 72. 1981  
 73. 1982  
 74. 1983  
 75. 1984  
 76. 1985  
 77. 1986  
 78. 1987  
 79. 1988  
 80. 1989  
 81. 1990  
 82. 1991  
 83. 1992  
 84. 1993  
 85. 1994  
 86. 1995  
 87. 1996  
 88. 1997  
 89. 1998  
 90. 1999  
 91. 2000  
 92. 2001  
 93. 2002  
 94. 2003  
 95. 2004  
 96. 2005  
 97. 2006  
 98. 2007  
 99. 2008  
 100. 2009  
 101. 2010  
 102. 2011  
 103. 2012  
 104. 2013  
 105. 2014  
 106. 2015  
 107. 2016  
 108. 2017  
 109. 2018  
 110. 2019  
 111. 2020  
 112. 2021  
 113. 2022  
 114. 2023  
 115. 2024  
 116. 2025  
 117. 2026  
 118. 2027  
 119. 2028  
 120. 2029  
 121. 2030

- 2483.
52. Moini, M.; Leroi, G. E. *J. Phys. Chem.* 1986, 90, 4002.
53. Dewar, M. J. S.; Tien, T.P. *J. Chem. Soc. Chem. Comm.* 1985, 1243.
54. Leopold, D. G.; Miller, A. E. S.; Linegerger, W. C. *J. Am. Chem. Soc.* 1986, 108, 1379.
55. Brown, R. D.; Godfrey, P. D.; Rodler, M. J. *Am. Chem. Soc.* 1986, 108, 1296.
56. Luibrand, R. T.; Hoffman, R. W. *J. Org. Chem.* 1974, 39, 3887.
57. Jones, M.; Levin, R. H. *J. Am. Chem. Soc.* 1969, 91, 6411.
58. Gassman, P. G.; Benecke, H. P. *Tetrahedron Lett.* 1969, 1089.
59. Wasserman, H.; Soldar, A. J.; Keller, L. S. *Tetrahedron Lett.* 1968, 5597.
60. Jones, M.; Levin, R. H. *Tetrahedron Lett.* 1968, 5593.
61. Tabushi, I.; Oda, R.; Okazaki, K. *Tetrahedron Lett.* 1968, 3743.
62. Campbell, C. D.; Rees, C. W. *Chem. Comm.* 1965, 192.
63. (a) Berry, R. S.; Clardy, J.; Schafer, M. E. *Tetrahedron Lett.* 1965, 1003.; (b) 1965, 1011.
64. Evleth, E. M. *Tetrahedron Lett.* 1967, 3625.
65. (a) Hess, B. A.; Schaad, L. J. *Tetrahedron Lett.* 1971, 17.;  
(b) Hess, B. A.; Schaad, L. J. *J. Am. Chem. Soc.* 1971, 93, 305.
66. (a) Washburn, W. N. *J. Am. Chem. Soc.* 1975, 97, 1615.; (b)

1900  
1901  
1902  
1903  
1904  
1905  
1906  
1907  
1908  
1909  
1910  
1911  
1912  
1913  
1914  
1915  
1916  
1917  
1918  
1919  
1920  
1921  
1922  
1923  
1924  
1925  
1926  
1927  
1928  
1929  
1930  
1931  
1932  
1933  
1934  
1935  
1936  
1937  
1938  
1939  
1940  
1941  
1942  
1943  
1944  
1945  
1946  
1947  
1948  
1949  
1950  
1951  
1952  
1953  
1954  
1955  
1956  
1957  
1958  
1959  
1960  
1961  
1962  
1963  
1964  
1965  
1966  
1967  
1968  
1969  
1970  
1971  
1972  
1973  
1974  
1975  
1976  
1977  
1978  
1979  
1980  
1981  
1982  
1983  
1984  
1985  
1986  
1987  
1988  
1989  
1990  
1991  
1992  
1993  
1994  
1995  
1996  
1997  
1998  
1999  
2000

- Washburn, W. N.; Zahler, R. *ibid.* 1976, 98, 7827.; (c) 1977, 99, 2012.; (d) Washburn, W. N.; Zahler, R.; Chen, I. *ibid.* 1978, 100, 5863.
67. (a) Billups, W. E.; Buynak, J. D.; Butler, D. J. *Org. Chem.* 1980, 45, 4636.; (b) *ibid.* 1979, 44, 4218.
68. Jhonson, G. C.; Stofko, J. J.; Lockhart, T. P., Brown, D. W.; Bergman, R. G. *J. Org. Chem.* 1979, 44, 4215.
69. Bergman, R. G. *Acc. Chem. Res.* 1973, 6, 25.
70. Chapman, O. L.; Chang, C.-C.; Kolc, J. J. *Am. Chem. Soc.* 1976, 98, 5703.
71. (a) Lockhart, T. P.; Comita, P. B.; Bergman, R. G. *J. Am. Chem. Soc.* 1981, 103, 4082.; (b) Lockhart, T. P.; Bergman, R. G. *ibid.* 1981, 103, 4091.
72. (a) Breslow, R.; Napierski, J.; Clarke, T. C. *J. Am. Chem. Soc.* 1975, 97, 6275.; (b) Breslow, R.; Khanna, P. L. *Tetrahedron Lett.* 1977, 3429.
73. Nam, H.-H.; Leroi, G. E. unpublished result
74. Gaviña, F.; Luis, S. V.; Safont, V. S.; Ferrer, P.; Costero, A. M. *Tetrahedron Lett.* 1986, 27, 4779.
75. Borden, W. T. "*Diradicals*"; Borden, W. T. Ed; John Wiley and Sons: New York, 1982; Chapter 1.
76. Wilson, E. B. Jr.; Decius, J.; Cross, P. "*Molecular Vibrations*"; McGraw Hill: New York, N. Y., 1955.

1944  
1945  
1946  
1947  
1948  
1949  
1950  
1951  
1952  
1953  
1954  
1955  
1956  
1957  
1958  
1959  
1960  
1961  
1962  
1963  
1964  
1965  
1966  
1967  
1968  
1969  
1970  
1971  
1972  
1973  
1974  
1975  
1976  
1977  
1978  
1979  
1980  
1981  
1982  
1983  
1984  
1985  
1986  
1987  
1988  
1989  
1990  
1991  
1992  
1993  
1994  
1995  
1996  
1997  
1998  
1999  
2000  
2001  
2002  
2003  
2004  
2005  
2006  
2007  
2008  
2009  
2010  
2011  
2012  
2013  
2014  
2015  
2016  
2017  
2018  
2019  
2020  
2021  
2022  
2023  
2024  
2025

## CHAPTER 3

### Didehydropyridines (DHP)

#### *Introduction*

Didehydroheteroarenes (DHHA) have been proposed as likely intermediates in many organic reactions, principally those involving cycloaddition or cine-substitution. These interesting intermediates have attracted widespread attention, as demonstrated by the many publications, including several reviews, on this subject in the last two decades<sup>1-7</sup>.

Often DHHAs have been generated by dehalogenation of the corresponding halogenated heteroarenes in the presence of strong bases. Dicarboxylic anhydrides, aminotriazoles or diazonium carboxylates of heteroarenes are also well-known precursors of DHHAs. The observation of cine-substituted products, Diels-Alder adducts with some dienes, or tele-substituted products has been taken as evidence of intervening DHHA species. However, this kind of indirect evidence, based on trapping experiments to verify the intermediacy of DHHAs, possesses severe limitations. Other mechanisms, e.g. addition-elimination, transhalogenation, or ANRORC can also account for the formation of the observed

products from a given precursor<sup>5,6</sup>. Mass spectrometric analysis following the electron impact or the pyrolytic fragmentation of some heteroarene dicarboxylic anhydrides has been used to conjecture the structure of DHHAs corresponding to certain  $m/z$  peaks<sup>8-12</sup>. However, no structural information could be obtained from the mass spectrometric analysis. To date, the only direct evidence of any DHHA is the infrared spectrum of 3,4-didehydropyridine (3,4-DHP) generated via near uv photolysis of 3,4-pyridine dicarboxylic anhydride (3,4-PDA) isolated in  $N_2$  or Ar matrices at 13K<sup>19</sup>.

Several theoretical papers have been published which predict the geometries, electronic structures, or heats of formation of some simple DHHAs (didehydro- pyridines, pyridazines, pyrimidines, pyrazines and thiophenes)<sup>13-18</sup>. Some of these calculations are at a rather rudimentary level (EHT<sup>17</sup>, semi-empirical MO<sup>16,18</sup>); others at a more sophisticated level (MNDO<sup>14,15</sup>, ab-initio<sup>13</sup>) fail to report some important information, such as the full structural parameters of optimized geometries, the effect of electron correlation between the two radical centers and the role of the heteroatom lone pair electrons. Thus, more detailed theoretical analyses are necessary to adequately understand the nature of DHHAs.

Didehydropyridines (DHP) have been the most studied of all



1945  
1946  
1947  
1948  
1949  
1950  
1951  
1952  
1953  
1954  
1955  
1956  
1957  
1958  
1959  
1960  
1961  
1962  
1963  
1964  
1965  
1966  
1967  
1968  
1969  
1970  
1971  
1972  
1973  
1974  
1975  
1976  
1977  
1978  
1979  
1980  
1981  
1982  
1983  
1984  
1985  
1986  
1987  
1988  
1989  
1990  
1991  
1992  
1993  
1994  
1995  
1996  
1997  
1998  
1999  
2000  
2001  
2002  
2003  
2004  
2005  
2006  
2007  
2008  
2009  
2010  
2011  
2012  
2013  
2014  
2015  
2016  
2017  
2018  
2019  
2020  
2021  
2022  
2023  
2024  
2025

1945

1946  
1947  
1948  
1949  
1950  
1951  
1952  
1953  
1954  
1955  
1956  
1957  
1958  
1959  
1960  
1961  
1962  
1963  
1964  
1965  
1966  
1967  
1968  
1969  
1970  
1971  
1972  
1973  
1974  
1975  
1976  
1977  
1978  
1979  
1980  
1981  
1982  
1983  
1984  
1985  
1986  
1987  
1988  
1989  
1990  
1991  
1992  
1993  
1994  
1995  
1996  
1997  
1998  
1999  
2000  
2001  
2002  
2003  
2004  
2005  
2006  
2007  
2008  
2009  
2010  
2011  
2012  
2013  
2014  
2015  
2016  
2017  
2018  
2019  
2020  
2021  
2022  
2023  
2024  
2025

1945

known DHHAs<sup>1-7</sup>. There are six possible isomers of DHPs depending on the sites of dehydrogenation. Among the six DHPs, the 3,4- isomer has the most convincing evidence, but the evidence for other isomers is somewhat inconclusive as has been discussed in the previous section<sup>5,6</sup>. Infrared matrix isolation spectroscopy could be a very useful method for the identification of vicinally didehydrogenated pyridines<sup>19</sup>, such as 3,4- and 2,3-DHP, since the two dehydrocarbons are expected to form a partial triple bond which has a characteristic vibrational frequency above 2000 cm<sup>-1</sup>. However, it is quite difficult to identify other isomers by vibrational spectroscopy. Theoretical calculations can provide valuable information regarding the structures and the energetics of DHPs, especially for the isomers whose experimental evidence is inconclusive<sup>13-18</sup>.

EHT (Extended Hückel Theory) calculations on the six possible DHPs have been carried out and the result of their stability sequence is 3,4->2,4->2,5->2,3->3,5->2,6-DHP<sup>17</sup>. However, this calculation used assumed geometries for the DHPs and made no distinction between singlet and triplet states. Energy calculations in the MNDO approximation suggest that all DHPs have singlet ground states with relative energy ordering of 3,4->2,4->2,5->2,6->2,3->3,5-DHP<sup>14</sup>. From these calculations, 3,4-DHP emerges as the most stable isomer and 2,3-DHP is expected to be much less stable than the 2,4- or

1911  
1912  
1913  
1914  
1915  
1916  
1917  
1918  
1919  
1920

2,5- isomer. Early Hückel MO calculations predicted that 2,3-DHP is more stable than the 3,4- isomer because the nitrogen lone pair would be delocalized over the two adjacent radical centers<sup>18</sup>. This argument has not been supported by higher level calculations. EHT calculations showed that the nitrogen lone pair substantially destabilizes the adjacent radical lobes. Recent ab-initio CASSCF/3-21G calculations on 3,4- and 2,3-DHP with the RHF/3-21G optimized geometries favored 3,4-DHP over the 2,3- isomer by 13.9 kcal/mole<sup>13</sup>. However, the influence of the nitrogen lone pair on the equilibrium geometries of DHPs and on the correlation between the two singlet-coupled radical electrons has not been accounted for at a sufficiently high level of theory that reliable predictions can be made.

In this chapter, matrix isolation studies on 3,4- and 2,3-DHP are presented. Theoretical calculations on all six DHP isomers have been carried out at the RHF, GVB and ROHF levels with a 3-21G basis set; these results are also reported and discussed in this chapter.

1944-1945  
1946-1947  
1948-1949  
1950-1951  
1952-1953  
1954-1955  
1956-1957  
1958-1959  
1960-1961  
1962-1963  
1964-1965  
1966-1967  
1968-1969  
1970-1971  
1972-1973  
1974-1975  
1976-1977  
1978-1979  
1980-1981  
1982-1983  
1984-1985  
1986-1987  
1988-1989  
1990-1991  
1992-1993  
1994-1995  
1996-1997  
1998-1999  
2000-2001  
2002-2003  
2004-2005  
2006-2007  
2008-2009  
2010-2011  
2012-2013  
2014-2015  
2016-2017  
2018-2019  
2020-2021  
2022-2023  
2024-2025

### 3.1. 3,4-Didehydropyridine (3,4-DHP)

3,4-DHP is the first DHHA to be proposed in modern times, and the evidence supporting its existence is the most convincing of any DHHA<sup>6</sup>. For example, diazabiphenylene, the dimer of 3,4-DHP, was identified in the time-of-flight mass spectrometric and kinetic uv spectroscopic analysis of the products formed by flash photolysis of pyridine-3-diazonium-4-carboxylate<sup>12</sup>. Our subsequent success in isolating 3,4-DHP in argon or nitrogen matrices has established that this molecule is a true reactive intermediate, not just a transition state<sup>19</sup>.

#### 3.1.1. Infrared Spectrum

As summarized in Scheme I, mild irradiation ( $\lambda > 340\text{nm}$  and less than 100 min duration) of 3,4-PDA in  $\text{N}_2$  or Ar matrices at 13 K readily fragmented the precursor to form  $\text{CO}$ ,  $\text{CO}_2$ , and 3,4-DHP, which has a strong peak at  $2085\text{ cm}^{-1}$  diagnostic of carbon-carbon triple bond formation. Subsequent irradiation with  $\lambda > 210\text{nm}$  light immediately decomposed 3,4-DHP into HCN, diacetylene, acetylene, and cyanoacetylene as a result of alternative two-bond scissions. The infrared spectrum in the  $2050 - 2300\text{ cm}^{-1}$  region prior to and following controlled photolysis (Figure 3.1) clearly demonstrates the formation of 3,4-DHP and its subsequent decomposition. The peak due to



3,4-DHP at  $2085\text{ cm}^{-1}$  disappears upon shorter wavelength irradiation, and new peaks at  $2101\text{ cm}^{-1}$  (HCN),  $2181\text{ cm}^{-1}$  (diacetylene) and  $2236\text{ cm}^{-1}$  (cyanoacetylene) begin to grow. Ten additional peaks below  $2000\text{ cm}^{-1}$  show the same growth and decay pattern as the  $2085\text{ cm}^{-1}$  band and are also attributable to 3,4-DHP (Table 3.1). The IR frequencies of 3,4-DHP indicate that this molecule is remarkably similar to 1,2-didehydrobenzene in character. However, 3,4-DHP decomposes much faster. The wavenumbers observed for both 1,2-DHB and 3,4-DHP in  $\text{N}_2$  matrices are collected in Table 3.1.

Scheme I

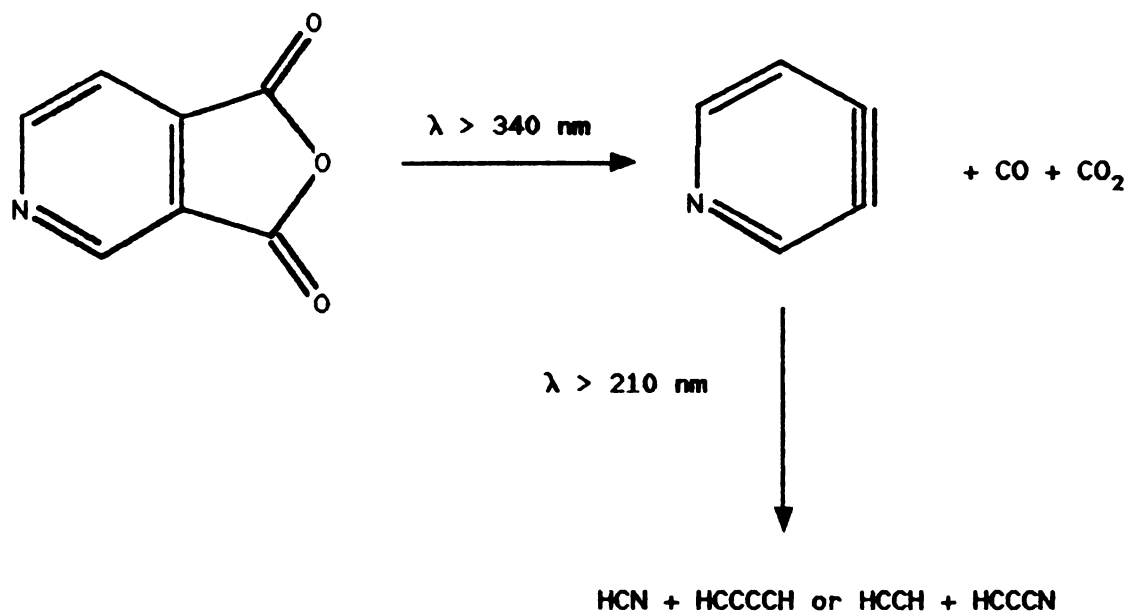






**Table 3.1. Infrared Bands ( $\text{cm}^{-1}$ ) Resulting from Photolysis of 3,4-PDA in an  $\text{N}_2$  matrix at 13 K**

$\lambda > 340 \text{ nm}^a$	$\lambda > 210 \text{ nm}^b$	Photolyzed products	1,2-DHB <sup>c</sup>
	2236	cyanoacetylene	
	2181	diacetylene	
	2101	HCN	
2085		3,4-DHP	2082
1558		3,4-DHP	1596 1448
1387		3,4-DHP	1395
1355		3,4-DHP	1355
	1260	polymer	
1216		3,4-DHP	
1055		3,4-DHP	1055 1038
996		3,4-DHP	
853		3,4-DHP	
848		3,4-DHP	848
802		3,4-DHP	
744	751 744	acetylene acetylene	
	703	polymer	739
	673	cyanoacetylene	
648	648	diacetylene	
635	635	diacetylene	
489		3,4-DHP	470

<sup>a</sup> Photolysis of 3,4-PDA (100 min). <sup>b</sup> Additional 30 min photolysis after a.

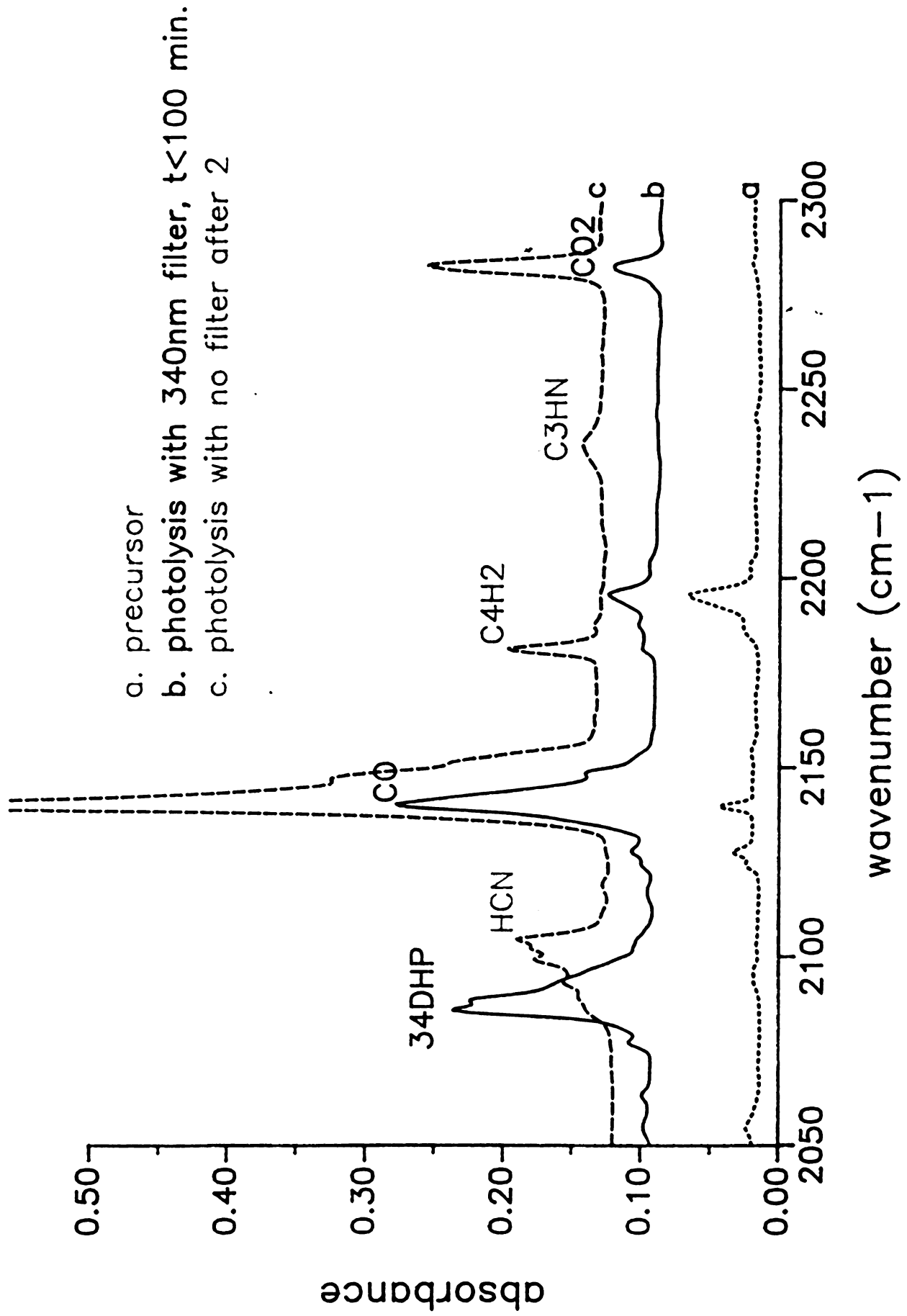
<sup>c</sup> Reference 19

**Fig.3.1** IR spectra of 3,4-PDA and its photolyzed products in the 2050-2300  $\text{cm}^{-1}$  region in an  $\text{N}_2$  matrix at 13 K: (a) 3,4-PDA; (b) after 100 min photolysis through water and  $\lambda > 340\text{nm}$  filter (The peak at  $2281\text{ cm}^{-1}$  is due to  $^{13}\text{CO}_2$ ); (c) following additional 30 min photolysis with  $\lambda > 210\text{nm}$ .

**Fig.3.2** Difference spectrum of 3,4-PDA before and after mild photolysis.

\* indicates a band due to diacetylene.

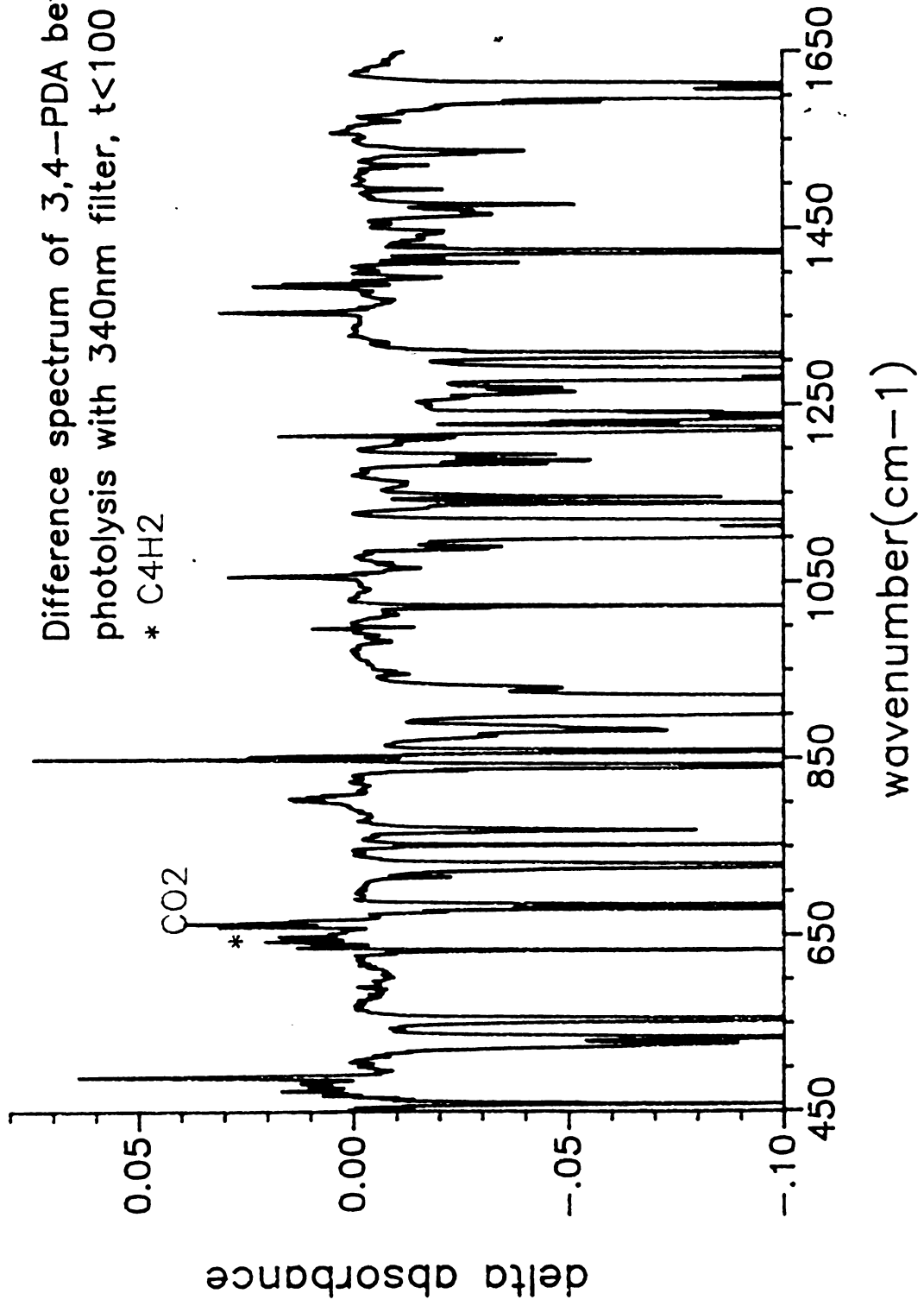
1910  
1911  
1912  
1913  
1914  
1915  
1916  
1917  
1918  
1919  
1920





Difference spectrum of 3,4-PDA before and after  
photolysis with 340nm filter,  $t < 100$  min.

\* C4H2



### 3.1.2. Theoretical Calculation

The predicted geometries of singlet and triplet 3,4-DHP are given in Table 3.2 with their corresponding electronic energies. At the single-determinant SCF level the lowest singlet 3,4-DHP lies 1.6 kcal/mole higher in energy than a triplet. However, consideration of correlation between the two unpaired electrons through a GVB calculation reverses this order, and 3,4-DHP has a singlet ground state with a singlet-triplet energy difference,  $\Delta E(S-T)$ , of 30.7 kcal/mole, which is very similar to that of 1,2-DHB (29.9 kcal/mole) when it is calculated at the same level of theory.

A comparison between the RHF and the GVB optimized structures of singlet 3,4-DHP shows only minor differences, the most significant change in bond distances being the lengthening of the  $C_3C_4$  triple bond (1.229  $\rightarrow$  1.263 Å) as a consequence of the participation of the in-plane  $\pi^*$  anti-bonding character in the GVB description. The occupation number of the acetylenic in-plane  $\pi^*$  natural orbital in the GVB/3-21G optimized structure is 0.11. The same trends are found in the calculation of 1,2-DHB: the same magnitude of  $C_1C_2$  triple bond lengthening (1.225  $\rightarrow$  1.261 Å), and the same in-plane  $\pi^*$  occupation number (0.11). This similarity implies that the physical properties of the bond between the two



Table 3.2. Geometrical parameters of 3,4-DHP

	singlet ( $^1A'$ )		triplet ( $^3A'$ )
	RHF/3-21G	GVB/3-21G	RHF/3-21G
$N_1C_7$	1.337	1.334	1.340
$C_2C_3$	1.386	1.383	1.372
$C_3C_4$	1.229	1.263	1.390
$C_4C_5$	1.378	1.380	1.371
$C_5C_6$	1.403	1.395	1.393
$C_6N_1$	1.341	1.340	1.327
$\angle N_1C_2C_3$	113.5	115.5	121.1
$\angle C_2C_3C_4$	124.2	123.2	119.3
$\angle C_3C_4C_5$	127.0	124.8	120.0
$\angle C_4C_5C_6$	109.0	114.4	117.1
$\angle C_5C_6N_1$	124.5	124.0	123.0
$\angle C_6N_1C_2$	121.8	118.1	119.5
$C_2H_1$	1.065	1.066	1.069
$C_5H_2$	1.067	1.067	1.070
$C_6H_3$	1.070	1.070	1.070
$\angle N_1C_2H_1$	119.2	118.6	121.1
$\angle C_4C_5H_2$	128.3	126.3	116.8
$\angle C_5C_6H_3$	119.3	119.8	120.2
$E_T$	-243.996328	-244.047691	-243.998843

Unit: bond length (Å); bond angle (degree); energy (Hartree)

PROCESSES

---

NO.	DESCRIPTION	AMOUNT
1	...	...
2	...	...
3	...	...
4	...	...
5	...	...
6	...	...
7	...	...
8	...	...
9	...	...
10	...	...
11	...	...
12	...	...
13	...	...
14	...	...
15	...	...
16	...	...
17	...	...
18	...	...
19	...	...
20	...	...
21	...	...
22	...	...
23	...	...
24	...	...
25	...	...
26	...	...
27	...	...
28	...	...
29	...	...
30	...	...
31	...	...
32	...	...
33	...	...
34	...	...
35	...	...
36	...	...
37	...	...
38	...	...
39	...	...
40	...	...
41	...	...
42	...	...
43	...	...
44	...	...
45	...	...
46	...	...
47	...	...
48	...	...
49	...	...
50	...	...
51	...	...
52	...	...
53	...	...
54	...	...
55	...	...
56	...	...
57	...	...
58	...	...
59	...	...
60	...	...
61	...	...
62	...	...
63	...	...
64	...	...
65	...	...
66	...	...
67	...	...
68	...	...
69	...	...
70	...	...
71	...	...
72	...	...
73	...	...
74	...	...
75	...	...
76	...	...
77	...	...
78	...	...
79	...	...
80	...	...
81	...	...
82	...	...
83	...	...
84	...	...
85	...	...
86	...	...
87	...	...
88	...	...
89	...	...
90	...	...
91	...	...
92	...	...
93	...	...
94	...	...
95	...	...
96	...	...
97	...	...
98	...	...
99	...	...
100	...	...

---

dehydrocarbon centers are almost identical for both 1,2-DHB and 3,4-DHP. On the other hand, as depicted in Figure 3.3, the total atomic charges on the dehydrocarbon centers of 3,4-DHP are quite different from those of 1,2-DHB. While the two dehydrocarbon centers of 1,2-DHB have the same negative charges ( $-0.002$ ), those of 3,4-DHP have opposite charges ( $C_3:-0.09$ ,  $C_4:+0.07$ ). This unequal charge distribution in 3,4-DHP would explain the unequal rates of nucleophilic addition at the two ends of the dehydro-bond<sup>7</sup>.

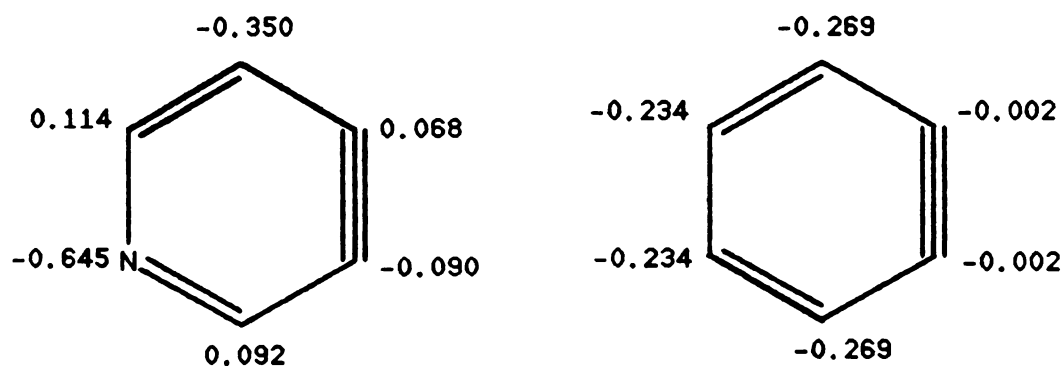


Fig. 3.3 Total atomic charges of 3,4-DHP and 1,2-DHB calculated at the GVB/3-21G//GVB/3-21G level.

Prior to the calculation of the vibrational frequencies of 3,4-DHP at RHF/3-21G level, the performance of the theory was monitored by comparing the calculated and the observed vibrational frequencies of pyridine. The structural parameters of pyridine are listed in Table 3.3, and the calculated and observed vibrational frequencies are listed in

Table 3.3 Geometrical parameters of pyridine

	3-21G <sup>a</sup>	4-21G <sup>b</sup>	4-31G <sup>c</sup>	6-31G <sup>a,d</sup>	Experimental <sup>e</sup>
N <sub>1</sub> C <sub>1</sub>	1.331	1.333	1.329	1.321	1.338
C <sub>2</sub> C <sub>3</sub>	1.383	1.382	1.382	1.385	1.394
C <sub>3</sub> C <sub>4</sub>	1.384	1.384	1.383	1.392	1.392
∠N <sub>1</sub> C <sub>2</sub> C <sub>3</sub>	122.6	122.8	122.4		123.8
∠C <sub>2</sub> C <sub>3</sub> C <sub>4</sub>	118.6	118.5	118.6		118.5
∠C <sub>3</sub> C <sub>4</sub> C <sub>5</sub>	119.0	119.0	119.0		118.4
∠C <sub>6</sub> N <sub>1</sub> C <sub>2</sub>	118.8	118.4	119.0		116.9
C <sub>2</sub> H <sub>1</sub>	1.070	1.071	1.070		1.086
C <sub>3</sub> H <sub>2</sub>	1.070	1.070	1.070		1.082
C <sub>4</sub> H <sub>3</sub>	1.072	1.072	1.072		1.081
∠N <sub>1</sub> C <sub>2</sub> H <sub>1</sub>	116.7	116.4	116.4		116.9
∠C <sub>2</sub> C <sub>3</sub> H <sub>2</sub>	120.7	120.4	120.3		120.1
∠C <sub>3</sub> C <sub>4</sub> H <sub>3</sub>	120.5	120.5	120.5		120.8

<sup>a</sup> This work; <sup>b</sup> Ref. 21; <sup>c</sup> Ref. 22; <sup>d</sup> Ref. 13; <sup>e</sup> Ref. 23

Table 3.4, from which it can be seen that the calculated in-plane (A<sub>1</sub>, B<sub>2</sub>) and out-of-plane (A<sub>2</sub>, B<sub>1</sub>) vibrations of pyridine are overestimated by 10.5% and 20.5% on the average, respectively. Thus, we have applied two different scaling factors (0.905 for in-plane and 0.830 for out-of-plane vibrations) to the calculated vibrations of 3,4-DHP. These results are summarized in Table 3.5. The vibrational



Table 3.4. Vibrational frequencies of pyridine

symmetry	RHF/3-21G	Experimental	Exp/Calc	
A <sub>1</sub>	689	601	0.87	
	1083	991	0.92	
	1138	1032	0.91	
	1199	1072	0.89	
	1354	1218	0.90	
	1654	1483	0.90	
	1749	1583	0.91	
	3364	3030	0.90	
	3378			
3402	3094	0.91	Ave = 0.90	
B <sub>1</sub>	486	403	0.83	
	822	700	0.85	
	875	744	0.85	
	1118	937	0.84	
	1213	1007	0.83	Ave = 0.84
B <sub>2</sub>	749	652	0.87	
	1158	1079	0.93	
	1191	1143	0.96	
	1327	1227	0.93	
	1529	1362	0.89	
	1607	1442	0.90	
	1742	1581	0.91	
	3370	3042	0.90	
	3393	3087	0.91	Ave = 0.91
A <sub>2</sub>	458	373	0.81	
	1039	871	0.84	
	1190	966	0.81	Ave = 0.82

<sup>a</sup> This work; <sup>b</sup> Reference 22

frequencies for the GVB wave functions are given in Table 3.6. However, the RHF scaling factors are not applied to the GVB frequencies since the transferability of an empirical factor between the two different levels of calculation does not seem reasonable<sup>24</sup>.

Table 3.5 Comparison of calculated (RHF/3-21G//RHF/3-21G) and experimental vibrational frequencies ( $\text{cm}^{-1}$ ) for 3,4-DHP

symmetry	RHF/3-21G	scaled	Experimental
A <sup>-</sup>	464	393	
A <sup>+</sup>	535	487	489
A <sup>-</sup>	559	464	
A <sup>+</sup>	745	678	
A <sup>-</sup>	756	627	
A <sup>-</sup>	951	789	802
A <sup>+</sup>	952	866	848
A <sup>-</sup>	1047	869	853
A <sup>+</sup>	1079	982	996
A <sup>-</sup>	1115	925	
A <sup>+</sup>	1146	1043	1055
A <sup>+</sup>	1254	1141	
A <sup>+</sup>	1296	1179	
A <sup>+</sup>	1365	1241	1216
A <sup>+</sup>	1502	1367	1355
A <sup>+</sup>	1525	1388	1385
A <sup>+</sup>	1576	1434	1558
A <sup>+</sup>	2189	1992	2085
A <sup>+</sup>	3392	3086	
A <sup>+</sup>	3433	3124	
A <sup>+</sup>	3441	3131	

1950-1951

1952-1953

---

1954-1955

---

A

A

A

A

A

A

A

A

A

A

A

A

A

A

A

A

A

A

A

A

A

A

A

A

A

A



In general, the agreement between the scaled and the observed frequencies is quite satisfactory. However, the scaled vibrational frequency of the  $C_3C_4$  stretch,  $1992\text{ cm}^{-1}$ , becomes too low compared to the experimental value,  $2085\text{ cm}^{-1}$ . The same tendency also has been found for the  $C_1C_2$  stretch (RHF/3-21G;  $2209\text{ cm}^{-1}$ , scaled (0.91):  $2010\text{ cm}^{-1}$ ) of 1,2-DHB. The GVB method calculates the  $C_3C_4$  stretching at  $1930\text{ cm}^{-1}$ , which is very close to the  $C_1C_2$  stretch of 1,2-DHB,  $1931\text{ cm}^{-1}$ , obtained at the same level of calculation. These data suggest that the bonding between the two dehydrocarbon centers of 1,2-DHB and 3,4-DHP are essentially the same. The harmonic vibrations of the  $^3A'$  state are also listed in Table 3.6. The most noticeable change between the singlet and triplet occurs at the  $C_3C_4$  stretching vibration ( $1703\text{ cm}^{-1}$ ), and its magnitude tells us that the triple bond character of  $C_3C_4$  is essentially lost in the triplet state.

Table 3.6 Calculated vibrational frequencies ( $\text{cm}^{-1}$ ) of 3,4-DHP

symmetry	GVB/3-21G ( $^1A'$ )	ROHF/3-21G ( $^3A'$ )
$A''$	474	463
$A''$	556	515
$A'$	674	668
$A'$	734	728
$A''$	798	806
$A''$	954	937
$A'$	1022	1067
$A''$	1090	1080
$A'$	1091	1129
$A'$	1129	1152
$A''$	1157	1164
$A'$	1264	1194
$A'$	1292	1249
$A'$	1371	1364
$A'$	1517	1530
$A'$	1584	1579
$A'$	1597	1676
$A'$	1930	1703
$A'$	3391	3379
$A'$	3427	3396
$A'$	3431	3402

1911

---

---

---

### 3.2. 2,3-Didehydropyridine (2,3-DHP)

Evidence supporting the generation of 2,3-DHP is neither as extensive nor as convincing as that for 3,4-DHP<sup>5</sup>. For example, the photolysis of 2,3-PDA in N<sub>2</sub> or Ar matrices leads to rupture of the ring structure, and the infrared spectra of the products taken at various time intervals during photolysis provide no evidence for the intermediacy of 2,3-DHP<sup>19</sup>. This isomer seems particularly interesting, however, because of the various possible interactions among three adjacent lobe orbitals.

#### 3.2.1. Infrared Spectra of the photolyzed products of 2,3-PDA

When matrix isolated 2,3-PDA was irradiated with  $\lambda > 300\text{nm}$  light for 14 hours, the plot of a growth-curve for each newly appearing band revealed that at least three products have been formed in the matrix. As shown in Figure 3.4, the first type of compound (Z) grows continuously and remains as the most stable product. The second type of compound (Y) grows faster than the compound Z, but after a certain period of time ( ~ 330 min ) it slowly begins to decay. The third type of compound (X) is very similar to Y, but it begins to decay earlier than Y ( ~ 210 min ). The bands of X, Y and Z are listed in Table 3.7.



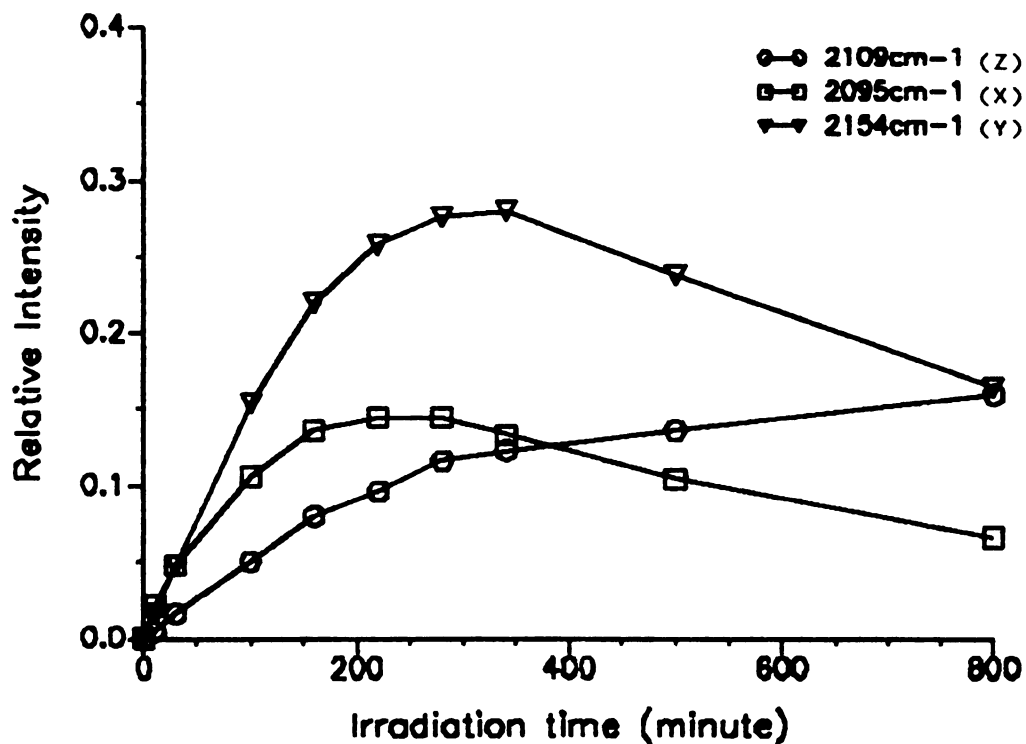


Fig. 3.4 Three types of growth-curve when 2,3-PDA is irradiated with  $\lambda > 300\text{nm}$  light.

As summarized in Scheme II and in Figure 3.5, the compounds X, Y and Z are also distinguished by their photochemical behavior. The spectra (a), (b) and (c) in Figure 3.5 have been obtained respectively from the photolysis of 2,3-PDA in an  $\text{N}_2$  matrix with  $\lambda > 340\text{nm}$  filter for 10 hours, subsequently 2 hours with  $\lambda > 300\text{nm}$  filter and 1.5 hours more with  $\lambda > 210\text{nm}$  filter. The same spectra could be observed when the samples were separately irradiated over each wavelength region mentioned above. While the bands due



Table 3.7 Infrared bands ( $\text{cm}^{-1}$ ) resulting from photolysis of 2,3-PDA  
in an  $\text{N}_2$  matrix at 13 K

compound	irradiation	observed frequencies
X	$\lambda > 340\text{nm}$ $\lambda > 300\text{nm}$	2185, 2095
Y	$\lambda > 300\text{nm}$	2154, 1015, 876
Z	$\lambda > 340\text{nm}$ $\lambda > 300\text{nm}$ $\lambda > 210\text{nm}$	3322, 3317, 3110, 2968, 2257, 2235, 2130, 2118, 2109, 1628, 1607, 1038, 896, 763, 730

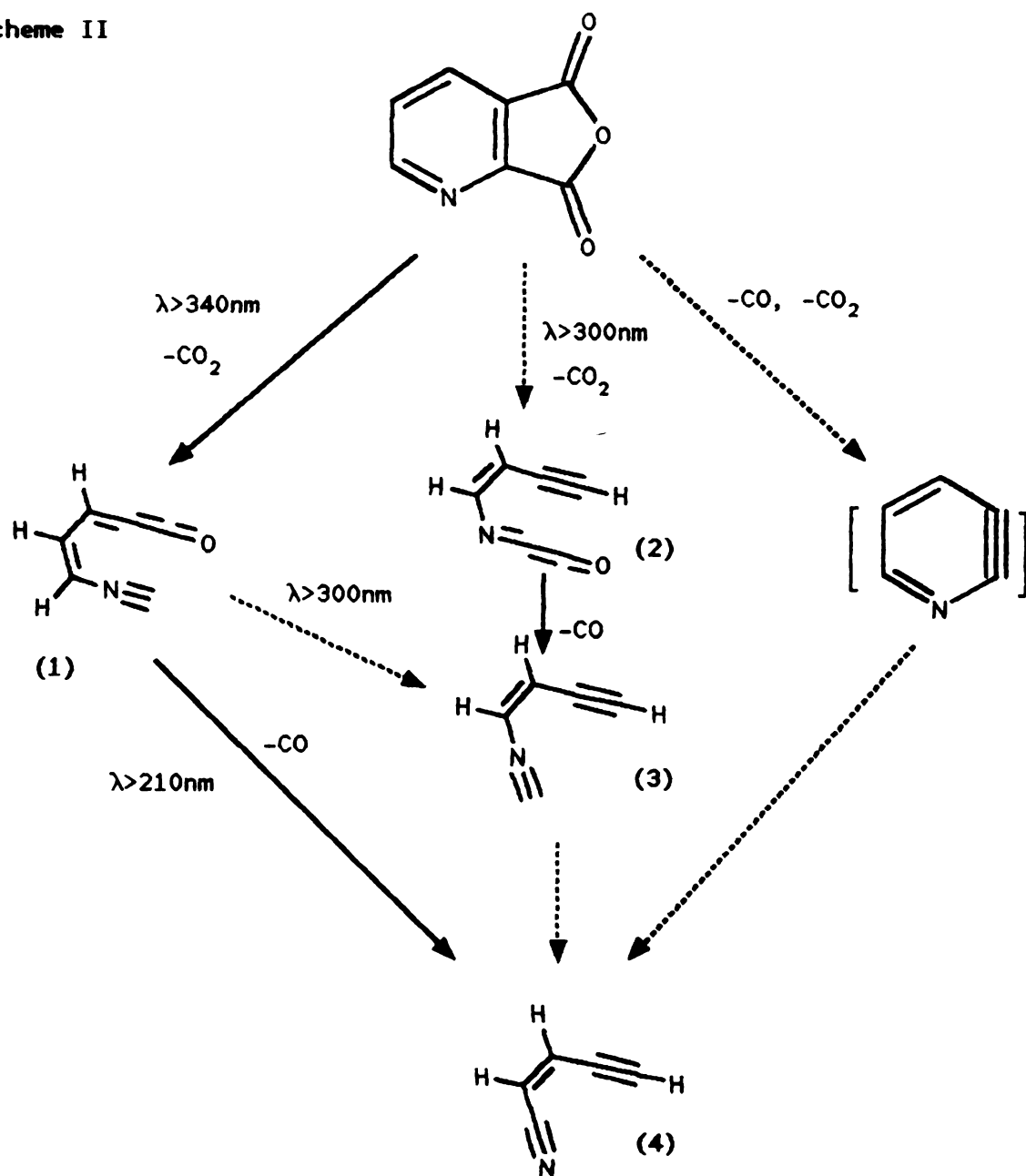
\* Visible when irradiated with  $\lambda > 210\text{nm}$  light

to compound Z appear in all spectra, those due to compound Y are evident only in the spectrum (b). The bands due to compound X occur in both spectra (a) and (b). However, the bands of X and Y completely vanish upon shorter wavelength ( $\lambda > 210\text{nm}$ ) irradiation. On the other hand, the bands due to X and Y do not change their shapes upon annealing of the matrix. The photoproduct Y does not interconvert to X photochemically when the  $\lambda > 300\text{nm}$  filter is replaced with  $\lambda > 340\text{nm}$  filter. Thus, the compounds X and Y are stable photochemical intermediates of Z. However, it is not certain whether compound Y is independently formed from a precursor or photochemically converted from compound X.

The compound Z is readily identifiable as  $\beta$ -ethynylacrylonitrile, (4) in scheme II. Compound X, which has a



Scheme II





characteristic  $\text{=C=C=O}$  band at  $2095\text{ cm}^{-1}$  and  $\text{-N}\equiv\text{C}$  band at  $2185\text{ cm}^{-1}$ , may be attributable to (1)<sup>25</sup>. The interpretation of compound Y is rather difficult. If it has been formed directly from a precursor, (2) is the plausible structure<sup>26</sup>. On the other hand, if it has been formed from compound X, it might have structure (3). In any event, the presence of compounds X and Y preclude the intermediacy of 2,3-DHP in the formation of final product Z.

Characteristics

... ..

...

...

...

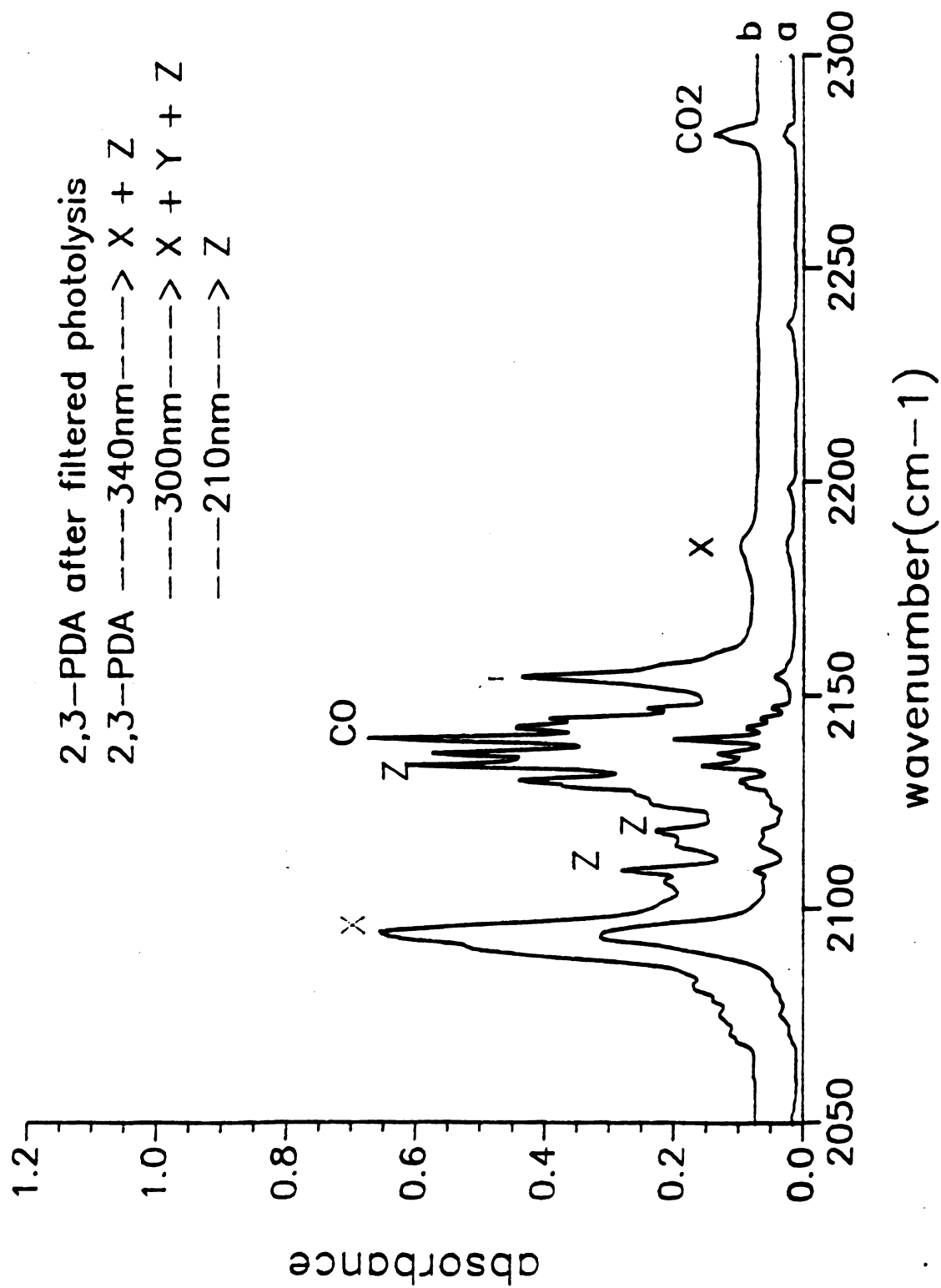
...

...

...

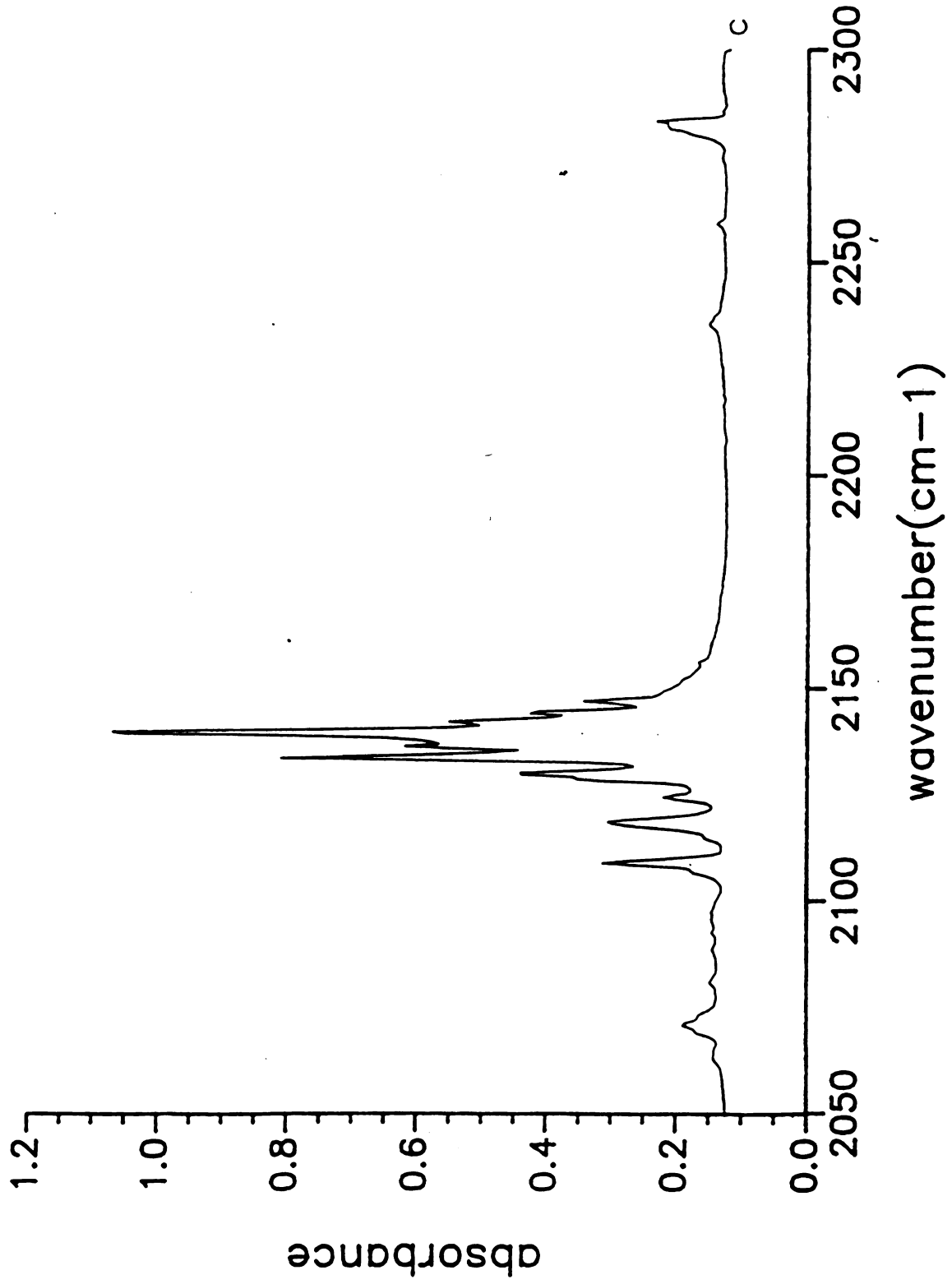
**Fig. 3.5** IR spectra of the photolyzed products of 2,3-PDA in the 2050–2300  $\text{cm}^{-1}$  region in an  $\text{N}_2$  matrix at 13 K; (a) 10 hour photolysis through water and  $\lambda > 340\text{nm}$  filter; (b) 2 hour photolysis after (a) with  $\lambda > 300\text{nm}$  filter; (c) 1.5 hour photolysis after (b) with  $\lambda > 210\text{nm}$  filter.





1850-1851







### 3.2.2. Theoretical Calculation

The total electronic energy of singlet 2,3-DHP at the GVB/3-21G level lies 7.4 kcal/mole higher than that of 3,4-DHP, but 17.5 kcal/mole lower than that of its lowest triplet state. The optimized geometries and total electronic energies of singlet and triplet 2,3-DHP are listed in Table 3.8.

Early Hückel MO calculations predicted that 2,3-DHP is more stable than the 3,4- isomer because the nitrogen lone pair would be delocalized over the two adjacent radical centers<sup>18</sup>. The RHF/3-21G optimized geometry indeed indicates that there is a substantial delocalization of the nitrogen lone pair over the two dehydrogenated carbon centers. This widens the bond angle at C2 (146.4) to allow a maximum overlap among the three lobe orbitals centered on N<sub>1</sub>, C<sub>2</sub> and C<sub>3</sub> at the cost of increased angle strain at N1 (107.0) and C3 (108.1). Thus, the delocalization of the nitrogen lone pair not only negatively contributes to the total electronic energy of 2,3-DHP as was pointed out by Hoffman, but also significantly increases the ring strain.

In order to examine the influence of polarization functions on the equilibrium geometry of 2,3-PDA, the structure has been optimized with a 6-31G\* basis set. As

January 1, 1954

Index card

100-1000

100-1000

100-1000

100-1000

100-1000

100-1000

100-1000

data type

long time

100-1000

100-1000

100-1000

100-1000

100-1000

100-1000

100-1000

100-1000

100-1000

100-1000

100-1000

100-1000

100-1000

100-1000

100-1000

Table 3.8 Geometrical parameters of 2,3-DHP

	singlet ( $^1A'$ )			triplet ( $^3A'$ )
	RHF/3-21G	RHF/6-31G*	GVB/3-21G	RHF/3-21G
$N_1C_2$	1.259	1.244	1.313	1.285
$C_2C_3$	1.253	1.275	1.265	1.393
$C_3C_4$	1.421	1.432	1.383	1.366
$C_4C_5$	1.403	1.402	1.396	1.402
$C_5C_6$	1.393	1.388	1.397	1.375
$C_6N_1$	1.375	1.353	1.351	1.348
$\angle N_1C_2C_3$	146.4	155.5	131.9	122.3
$\angle C_2C_3C_4$	108.1	97.8	120.8	119.4
$\angle C_3C_4C_5$	116.8	122.5	112.6	118.0
$\angle C_4C_5C_6$	121.5	119.7	121.1	118.8
$\angle C_5C_6N_1$	120.2	119.7	123.2	121.3
$\angle C_6N_1C_2$	107.0	104.9	110.4	120.2
$C_4H_1$	1.070	1.077	1.069	1.071
$C_5H_2$	1.070	1.074	1.070	1.070
$C_6H_3$	1.066	1.072	1.069	1.068
$\angle C_3C_4H_1$	122.4	118.9	125.3	121.1
$\angle C_4C_5H_2$	119.8	120.5	120.0	120.6
$\angle C_5C_6H_3$	123.3	123.7	120.6	121.8
$E_T$	-243.987656	-245.381877	-244.035964	-244.008141



noted from Table 3.3, the polarization function preferentially strengthens the NC bond. The same effect is found in the RHF/6-31G\* optimized geometry of 2,3-PDA; the  $N_1C_2$  bond length is considerably shortened with significant increase in its adjacent bond angle (155.5), and the calculation diminishes the interaction between the two radical centers as is reflected by an elongated  $C_2C_3$  bond length (1.275 Å). The resultant geometry is much more strained than that from the RHF/3-21G calculation, which suggests that the use of a polarization function does not necessarily provide improved results for the geometries of DHPs.

The RHF HOMO and LUMO of 2,3-DHP are approximately expressed as linear combinations of three lobe orbitals centered on  $N_1$ ,  $C_2$  and  $C_3$ . When these two orbitals are taken as a pair of initial GVB natural orbitals, the GVB SCF procedure minimizes the magnitude of the nitrogen lobe orbital, and leads to symmetric and antisymmetric combinations of the two radical lobe orbitals. Consequently, the bond length  $N_1C_2$  substantially increases from 1.259 Å to 1.313 Å while the bond angle at  $C_2$  decreases by 14.5°. The GVB optimized geometry of 2,3-DHP is then rather close to other vicinally didehydrogenated aromatic systems. The entries in Table 3.9 show the similarity of the bonds between the two vicinal dehydrocarbon centers of 1,2-DHB, 3,4-DHP and

2,3-DHP.

Table 3.9 C=C bond length (Å) and vibrational frequency of vicinally didehydrogenated aromatic systems

	singlet*	triplet**	$\nu_{C=C}$ (GVB)	$\nu_{C=C}$ (exp.)
1,2-DHB	1.261	1.389	1931 cm <sup>-1</sup>	2082 cm <sup>-1</sup>
3,4-DHP	1.263	1.390	1930	2085
2,3-DHP	1.265	1.393	1894	

\* GVB/3-21G; \*\* RHF/3-21G

Since the GVB method may underestimate the contribution of the nitrogen lobe orbital, we have examined the three-term separated-pair wave function which explicitly includes the nitrogen lobe orbital as the third term in the correlation between the two singlet coupled electrons. However, it turns out that the contribution from the third term to an overall wave function is negligible (~0.04%). Thus, the lone pair electrons are confined to the nitrogen and the bonding between C2 and C3 is determined primarily by the coupling of the two odd electrons.

The RHF/3-21G C<sub>2</sub>C<sub>3</sub> harmonic stretching frequency is predicted to be at 1936 cm<sup>-1</sup>. Considering that RHF/3-21G harmonic frequencies are overestimated by about 11%<sup>26</sup>, an empirical correction of 11% would reduce the calculated C<sub>2</sub>C<sub>3</sub> stretching frequency in 2,3-DHP to 1742 cm<sup>-1</sup>. This value suggests that the C<sub>2</sub>C<sub>3</sub> bond in the RHF optimized geometry of



2,3-DHP is essentially a strained allenic bond. The GVB/3-21G harmonic frequency of the  $C_2C_3$  stretching in 2,3-DHP is calculated to be  $1894\text{ cm}^{-1}$ . Since the GVB method underestimates the vibrational frequency of the strained triple bond in 1,2-DHB or 3,4-DHP by 7.3% (see Table 3.9), the stretching frequency of  $C_2C_3$  in 2,3-DHP may be up-scaled to about  $2044\text{ cm}^{-1}$ . Thus, we expect that the  $C\equiv C$  stretching frequency of 2,3-DHP, if it is ever formed in a matrix isolation experiment, would be observed at least  $40\text{ cm}^{-1}$  below that of 3,4-DHP.

1-1-1952  
National Bureau  
of Standards  
Washington  
D.C.  
10004

### 3.3. 2,4-Didehydropyridine (2,4-DHP)

2,4-DHP has been proposed as a likely intermediate in the tele-substitution of 6-substituted-2-bromopyridines with  $\text{KNH}_2$ <sup>27</sup>. Two previous theoretical calculations predict that 2,4-DHP is the second most stable isomer of DHP<sup>15,17</sup>. The MNDO calculation estimates that the heat of formation of 2,4-DHP is only 0.5 kcal/mole higher than that of 3,4-DHP, but 8.6 kcal/mole lower than that of 2,3-DHP. No theoretical calculation has been published for 2,4-DHP at the ab-initio level.

#### 3.3.1. Theoretical calculation

At the GVB/3-21G level, the lowest singlet state of 2,4-DHP lies 9.6 kcal/mole higher in energy than that of 3,4-DHP. Contradictory to previous calculations<sup>15,17</sup>, 2,4-DHP is less stable than 2,3-DHP by 2.2 kcal/mole. The ground electronic state of 2,4-DHP is a singlet with  $\Delta E(\text{S-T})$  of 14.0 kcal/mole. The optimized geometries of singlet and triplet 2,4-DHP and their corresponding energies are given in Table 3.10.

The RHF calculations on 1,3-DHB yield a bicyclic structure with a  $\text{C}_1\text{-C}_3$  separation of 1.514 Å. Since the two dehydrocarbons of 2,4-DHP are also meta, one might expect the

Table 3.10 Geometrical parameters of 2,4-DHP

	singlet ( $^1A'$ )		triplet ( $^3A'$ )
	RHF/3-21G	GVB/3-21G	ROHF/3-21G
$N_1C_2$	1.220	1.280	1.294
$C_2C_3$	1.357	1.404	1.385
$C_3C_4$	1.414	1.362	1.371
$C_4C_5$	1.411	1.379	1.382
$C_5C_6$	1.381	1.385	1.392
$C_6N_1$	1.372	1.343	1.347
$\angle N_1C_2C_3$	142.6	129.4	126.0
$\angle C_2C_3C_4$	102.0	108.5	113.8
$\angle C_3C_4C_5$	123.2	126.8	123.6
$\angle C_4C_5C_6$	122.2	117.1	116.2
$\angle C_5C_6N_1$	129.8	119.0	122.0
$\angle C_6N_1C_2$	115.6	119.3	118.5
$C_3H_1$	1.060	1.063	1.068
$C_5H_2$	1.071	1.069	1.069
$C_6H_3$	1.067	1.069	1.069
$\angle C_2C_3H_1$	129.8	124.2	122.8
$\angle C_4C_5H_2$	119.5	121.8	122.5
$\angle C_5C_6H_3$	126.4	122.4	121.3
$E_T$	-243.957776	-244.032503	-244.010254

$C_2C_4$  distance: RHF; 2.153, GVB; 2.245, ROHF; 2.308, pyridine(RHF/3-21G);2.378



RHF calculation to predict a bicyclic structure for 2,4-DHP. However, as we have observed from the example of 2,3-DHP, at the RHF level the nitrogen lone pair tends to delocalize over the adjacent dehydrocarbon lobe orbital, which considerably weakens the  $C_2-C_4$  interaction. The total overlap population between the two radical centers is negative, which is indicative of no effective bonding between them.

The GVB SCF procedure restricts the delocalization of nitrogen lone pair to maximize the correlation between the two odd electrons. A comparison between the RHF and the GVB optimized structures of singlet 2,4-DHP shows large differences in the  $N_1-C_2$  bond length (RHF: 1.220, GVB:1.280 Å) and its adjacent bond angle (RHF:142.6, GVB:129.4). The resultant GVB geometry is less strained than the RHF structure with much lower energy ( $\Delta E_T = 46.9$  kcal/mole).

We have examined the three term separate-pair wave function for 2,4-DHP in the same manner as 2,3-DHP. The third term approximately corresponds to the nitrogen lone pair orbital. However, the weight of the third term is less than 0.03%. Thus, the role of the nitrogen lone pair in the correlation between the two odd electrons is negligible.

the level of the  
the adjacent  
level of the  
level of the  
level of the

the level of the

the level of the

the level of the

the level of the

the level of the

the level of the

the level of the

the level of the

the level of the

the level of the

the level of the

the level of the

the level of the

the level of the

the level of the

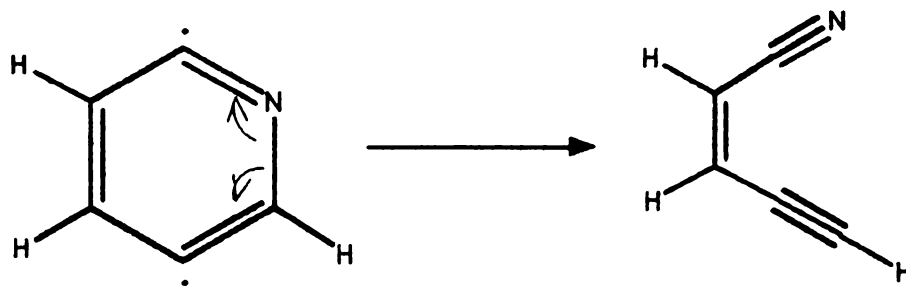
### 3.4. 2,5-Didehydropyridine (2,5-DHP)

The heat of formation of 2,5-DHP calculated by MNDO is 133.5 kcal/mole<sup>15</sup>, which is only 1.6 kcal/mole higher than that of 3,4-DHP. To our knowledge, no definitive experimental evidence of 2,5-DHP has been reported.

#### 3.4.1. Theoretical calculation

RHF geometry optimization of 2,5-DHP leads to the  $\beta$ -ethynylacrylonitrile structure by relocating the bonding electrons of C<sub>6</sub>-N<sub>1</sub> to the bonds N<sub>1</sub>-C<sub>2</sub> and C<sub>5</sub>-C<sub>6</sub> (Scheme III).

Scheme III



On the other hand, GVB geometry optimization does yield a closed ring structure for 2,5-DHP. At the GVB level, the total electronic energy of singlet 2,5-DHP is 9.5 kcal/mole higher than that of 2,4-DHP; singlet 2,5-DHP lies 4.9 kcal/mole lower in energy than the triplet state. Table 3.11 shows the optimized geometry of singlet and triplet 2,5-DHP from our calculation.



1940-1941

1941-1942

1942-1943

1943-1944

1944-1945

1945-1946

1946-1947

1947-1948

1948-1949

1949-1950

1950-1951

1951-1952

1952-1953

1953-1954

1954-1955

1955-1956

1956-1957

Table 3.11 Geometrical parameters of 2,5-DHP

	singlet ( $^1A'$ )		triplet ( $^3A'$ )
	RHF/3-21G	GVB/3-21G	ROHF/3-21G
$N_1C_2$	1.140	1.276	1.295
$C_2C_3$	1.423	1.380	1.386
$C_3C_4$	1.325	1.400	1.385
$C_4C_5$	1.424	1.375	1.382
$C_5C_6$	1.189	1.356	1.368
$C_6N_1$	4.258	1.371	1.349
$\Delta N_1C_2C_3$	179.2	120.0	127.2
$\Delta C_2C_3C_4$	123.9	126.0	115.8
$\Delta C_3C_4C_5$	124.4	115.4	116.9
$\Delta C_4C_5C_6$	179.3	118.2	123.5
$\Delta C_5C_6N_1$		122.9	118.8
$\Delta C_6N_1C_2$		117.5	117.9
$C_3H_1$	1.071	1.068	1.068
$C_4H_2$	1.073	1.071	1.071
$C_6H_3$	1.051	1.066	1.067
$\Delta C_2C_3H_1$	116.0	123.0	121.8
$\Delta C_3C_4H_2$	119.0	119.0	121.6
$\Delta C_5C_6H_3$	179.6	125.3	123.2
$E_T$	-244.073108	-244.017220	-244.009355

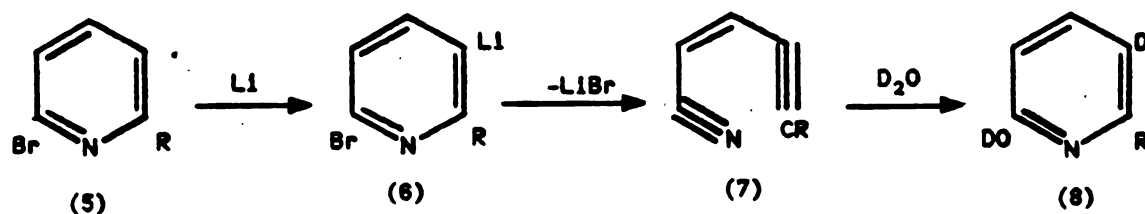
$C_2C_5$  distance: GVB; 2.638, ROHF; 2.613, pyridine(RHF/3-21G);2.715

11.0 11.07

11.07

11.07

The RHF method fails to describe the ring structure of 2,5-DHP because the RHF method tends to strongly bind the nitrogen atom ( $N_1$ ) and its adjacent dehydrocarbon ( $C_2$ ) while it underestimates the interactions between the two dehydrocarbon centers. Nonetheless, the open structure obtained by the RHF calculation corresponds to the global minimum of 2,5-DHP. As we have observed from the examples of 2,3- and 2,4-DHP, the GVB method limits the interaction between  $N_1$  and  $C_2$  to maximize the interaction between the two odd electrons, which results in a local minimum cyclic structure for 2,5-DHP. However, the fact that cyclic 2,5-DHP is a relative minimum at the GVB level tells us nothing about its depth. If the minimum is rather shallow, the cyclic 2,5-DHP will undergo a facile ring opening to form  $\beta$ -ethynylacrylonitrile which corresponds to the global minimum. This conclusion is supported by a related experimental result<sup>28</sup>; the formation of compound (8) from (5) is explained by an unusual ring-opening-cyclization process.



The triplet structure of 2,5-DHP is quite unusual compared to all other isomers of DHP. In general, the triplet DHP ring

structure is less distorted from an equilibrium pyridine geometry than the singlet structure. However, the bond angles at the dehydrocarbon centers of triplet 2,5-DHP ( $C_2$ :  $127.2^\circ$ ,  $C_5$ :  $123.5^\circ$ ) are noticeably larger than those of the singlet ( $C_2$ :  $120.0^\circ$ ,  $C_5$ :  $118.2^\circ$ ), which narrows the  $C_2$ - $C_5$  separation (singlet: 2.638 Å, triplet: 2.613 Å). The same tendency is found for 1,4-DHB, but the extent of distortion for 1,4-DHB (singlet:  $124.3^\circ$  → triplet:  $125.4^\circ$ ) is much less than that of 2,5-DHB.

Figure 3.8 shows approximate MO diagrams for 2,5-DHP and 1,4-DHB. The combinations of the two dehydrocarbon lobe orbitals are antisymmetric for HOMOs and symmetric for LUMOs. Thus, the electronic configuration of the triplet,  $[\{\text{core}\}(\text{HOMO})^1(\text{LUMO})^1]$ , increases the bonding character between the two dehydrocarbon centers, which would narrow the distance between them.

In the cases of 2,3-, 2,4- and 2,6-DHP, the addition of a nitrogen lone pair orbital to a pair of GVB wave functions (three term separate-pair wave function) slightly lowers the GVB energy by 0.2 - 0.6 kcal/mole; the weight of the newly added term is negligibly small (less than 0.04%). The geometry optimization with this wave function converges to the same structure as with the two-configuration (TC) wave function. On the other hand, in the case of 2,5-DHP, the

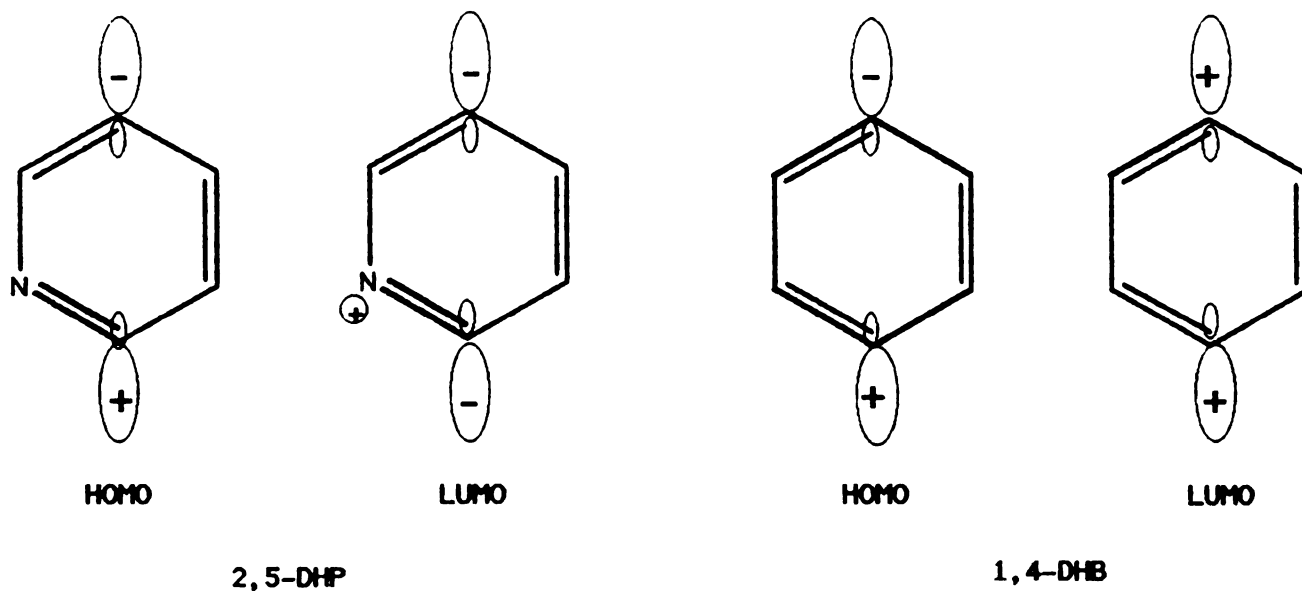


Fig. 3.6. Approximate MOs of 2,5-DHP and 1,4-DHB

addition of the nitrogen lone pair orbital considerably destabilizes the system; it increases the GVB energy by 0.8 kcal/mole and the geometry optimization fails to converge. This result suggests that the cyclic structure of 2,5-DHP is not as rigid as that of the other DHP isomers.



1900  
1901  
1902  
1903  
1904  
1905  
1906  
1907  
1908  
1909  
1910  
1911  
1912  
1913  
1914  
1915  
1916  
1917  
1918  
1919  
1920  
1921  
1922  
1923  
1924  
1925  
1926  
1927  
1928  
1929  
1930  
1931  
1932  
1933  
1934  
1935  
1936  
1937  
1938  
1939  
1940  
1941  
1942  
1943  
1944  
1945  
1946  
1947  
1948  
1949  
1950  
1951  
1952  
1953  
1954  
1955  
1956  
1957  
1958  
1959  
1960  
1961  
1962  
1963  
1964  
1965  
1966  
1967  
1968  
1969  
1970  
1971  
1972  
1973  
1974  
1975  
1976  
1977  
1978  
1979  
1980  
1981  
1982  
1983  
1984  
1985  
1986  
1987  
1988  
1989  
1990  
1991  
1992  
1993  
1994  
1995  
1996  
1997  
1998  
1999  
2000

### 3.5. 2,6-Didehydropyridine (2,6-DHP)

The intermediacy of 2,6-DHP has been proposed for the resin formation which is obtained when 2-halogenopyridines are treated with lithium piperidine<sup>2</sup>; however, the evidence is rather questionable<sup>6</sup>. It has been suggested that 2,6-DHP should be the most stable DHP isomer due to favorable overlap among the three lobe orbitals centered on  $C_2-N_1-C_6$ <sup>18</sup>. However, the results of MNDO and EHT calculations do not support this suggestion. They predict that the 2,6- isomer would have much lower or even the lowest stability<sup>15,17</sup>.

#### 3.5.1. Theoretical calculation

Among the six possible isomers of DHP, only the 2,6- isomer has a triplet ground state, which lies 2.4 kcal/mole lower in energy than the lowest singlet. The details of the optimized structures at the RHF, GVB and ROHF level are summarized in Table 3.12.

Similar to the results for the 2,3- isomer, the RHF method delocalizes the nitrogen lone pair onto the adjacent dehydrocarbons, which shortens the bond between  $N_1$  and  $C_2$  or equivalently  $C_6$  (1.227Å), and widens the bond angle at  $N_1$  (150.2°) to allow the maximum overlap among three lobe orbitals centered on  $C_2-N_1-C_6$ . This causes a large angle



Table 3.12 Geometrical parameters of 2,6-DHP ( $C_{2v}$  structure)

	singlet ( $^1A_1$ )		triplet ( $^3B_2$ )
	RHF/3-21G	GVB/3-21G	ROHF/3-21G
$N_1C_2$	1.227	1.329	1.302
$C_2C_3$	1.436	1.375	1.378
$C_3C_4$	1.398	1.390	1.392
$\angle C_6N_1C_2$	150.6	111.4	117.9
$\angle N_1C_2C_3$	106.6	128.3	124.9
$\angle C_2C_3C_4$	116.1	116.9	116.0
$\angle C_3C_4C_5$	124.1	118.2	120.3
$C_3H_1$	1.065	1.068	1.068
$C_4H_2$	1.072	1.072	1.072
$\angle C_2C_3H_1$	120.7	120.9	122.0
$\angle C_3C_4H_2$	118.0	120.9	119.8
$E_T$	-243.942669	-244.013945	-244.017725

strain at  $C_2$  or  $C_6$  ( $106.6^\circ$ ) and destabilizes the system.

Since the GVB method restricts the delocalization of the nitrogen lone pair, the GVB optimized geometry of 2,6-DHP is rather close to the equilibrium geometry of pyridine. The three-term separate-pair wave function insignificantly improves the GVB energy (0.2 kcal/mole), and the weight of the third term, the nitrogen lone pair orbital, is less than 0.02%.

---

---

1970  
1971  
1972  
1973  
1974  
1975  
1976  
1977  
1978  
1979  
1980

---

---

1981  
1982  
1983  
1984  
1985  
1986  
1987  
1988  
1989  
1990

### 3.6. 3,5-Didehydropyridine (3,5-DHP)

No experimental evidence for 3,5-DHP has been reported. MNDO calculations on 3,5-DHP predict that it would be the least stable DHP isomer<sup>15</sup>.

#### 3.6.1. Theoretical calculation

At the GVB level, 3,5-DHP has a singlet ground state with a predicted  $\Delta E(S-T)$  of 10.0 kcal/mole. Its stability is comparable to singlet 2,5-DHP or triplet 2,6-DHP. Details of the optimized structures are collected in Table 3.13.

3,5-DHP is remarkably similar to 1,3-DHP in many respects. The RHF geometry optimization yields a bicyclic equilibrium structure ( $C_{2v}$ ) with a  $C_3-C_5$  separation of 1.540 Å. The positive  $C_3-C_5$  overlap population indicates the formation of weak bonding between them. The GVB optimized structure increases the  $C_3-C_5$  distance to 2.229 Å, which is 0.061 Å shorter than that of pyridine. The overlap population becomes negative, which is indicative of no effective bonding between the dehydrocarbon centers in the GVB singlet structure.

Introduction

1945-1946

1945-1946

1945-1946

1945-1946

1945-1946

1945-1946

1945-1946

1945-1946

1945-1946

1945-1946

1945-1946

1945-1946

1945-1946

1945-1946

1945-1946

1945-1946

Table 3.13 Geometrical parameters of 3,5-DHP ( $C_{2v}$  structure)

	singlet ( $^1A_1$ )		triplet ( $^3B_2$ )
	RHF/3-21G	GVB/3-21G	ROHF/3-21G
$N_1C_2$	1.357	1.338	1.337
$C_2C_3$	1.381	1.372	1.375
$C_3C_4$	1.349	1.376	1.375
$\angle C_6N_1C_2$	110.9	116.1	120.1
$\angle N_1C_2C_3$	110.0	121.1	120.0
$\angle C_2C_3C_4$	159.8	126.8	122.5
$\angle C_3C_4C_5$	69.6	108.1	115.0
$C_2H_1$	1.062	1.068	1.068
$C_4H_2$	1.063	1.065	1.071
$\angle N_1C_2H_1$	121.6	117.7	117.4
$\angle C_3C_4H_2$	145.2	125.9	122.5
$E_T$	-243.940822	-244.017937	-244.002274

$C_3C_5$  distance: RHF; 1.540, GVB; 2.229, ROHF; 2.319, pyridine; 2.290

$C_3C_5$  overlap pop: RHF; +0.10, GVB; -0.18

考卷之五

五

五

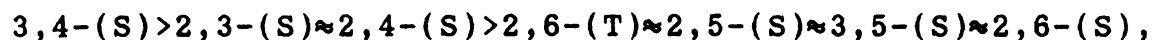
五

五

五

### 3.7. Conclusion and Summary

The results of primary interest are the relative energetics among the six cyclic isomers of DHP. These are summarized in Table 3.14. At the RHF level, the ground states of all DHPs except for the 2,5- isomer are predicted to be triplets. However, at the GVB level the limited electron correlation between the two odd electrons lowers the RHF energies of DHPs by 30 - 48 kcal/mole and the ground state of all DHPs except the 2,6- isomer are predicted to be singlets. Considering the limitations of the small basis set (3-21G) used in this calculation, and attributing little significance to total energy differences less than 5 kcal/mole<sup>29</sup>, the difference in ground state energy between the 2,3- and 2,4- isomer, and between the 2,6- (T) and 2,5- or 3,5- isomers are too small to determine their relative ordering with confidence. However, the splitting between the 3,4- and 2,3-, and between the 2,4- and 2,6- (T) isomers are sufficiently large (7.4 and 9.3 kcal/mole) that their relative stability is probably independent of the level of the computations. Thus, the ground state stabilities of the DHPs decrease in the order:



where S and T in parentheses represent singlets and triplets, respectively.

U. S. Copyright

The Author

Copyright

Copyright

Copyright

Copyright

Copyright

Copyright

Copyright

Copyright

Copyright

Copyright

Copyright

Copyright

Copyright

Copyright

Copyright

Copyright

Copyright

Copyright

Copyright

Copyright

Copyright

Copyright



Table 3.14 Relative  $\Delta E$  (kcal/mole) values of DHPs with respect to the ground state energy of 3,4-DHP

	RHF (singlet)	GVB (singlet)	ROHF (triplet)
3,4-	32.2	0.0	30.7
2,3-	37.7	7.4	24.8
2,4-	56.4	9.5	23.5
2,5-	-15.9*	19.1	24.1
2,6-	65.9	21.2	18.8
3,5-	67.1	19.1	28.5

\*  $\beta$ -ethynylacrylonitrile, the global minimum of 2,5-DHP

The GVB optimized geometries of 2,4-, 2,5-, 2,6- and 3,5-DHP strongly suggest that their singlet structures are not bicyclic, but rather are monocyclic with significant diradical character. All attempts to find bicyclic geometries for those compounds at the GVB level have failed. On the other hand, MNDO calculations predicted bicyclic structures for these isomers. Does this mean that the strained bicyclic structures cannot be dealt with by the GVB method, or that they exist because the MNDO method underestimates their ring strain energies? No definitive answer can be given at this time.

The structure of a DHP isomer depends critically on the extent of interaction between the nitrogen lone pair and the

Table 1.1.1

Year	Value
1950	1.0
1951	1.1
1952	1.2
1953	1.3
1954	1.4
1955	1.5

Table 1.1.2

Table 1.1.2.1  
Table 1.1.2.2  
Table 1.1.2.3  
Table 1.1.2.4  
Table 1.1.2.5  
Table 1.1.2.6  
Table 1.1.2.7  
Table 1.1.2.8  
Table 1.1.2.9  
Table 1.1.2.10

Table 1.1.3  
Table 1.1.4

two odd electrons on dehydrocarbon centers. When the dehydrocarbons are non-adjacent to the nitrogen atom ( $N_1$ ), such as 3,4- or 3,5-DHP, the nitrogen lone pair does not play a significant role in determining the structures. When one of the dehydrocarbon centers is adjacent to  $N_1$ , we have two contradictory descriptions: at the RHF level the nitrogen lone pair and the adjacent radical lobe are delocalized; on the other hand, at the GVB level they are localized on their own atoms and the nitrogen lone pair has limited interaction with the adjacent radical center. This difference between the two methods is well illustrated in the optimized structures of the 2,n-DHPs ( $n=3,4,5,6$ ); while the RHF method strongly binds  $N_1$  and  $C_2$  and obtains an extremely strained ring or open acyclic structure, the GVB method obtains modestly distorted cyclic structures. When the nitrogen lone pair orbital is included as the third term of the GVB wave function the total electronic energies are slightly improved (by 0.2 - 0.6 kcal/mole), except for 2,5-DHP for which the energy is increased by 0.8 kcal/mole. The weight of the third term is less than 0.04% for all 2,n-DHPs. Geometry optimization of each 2,n-DHP with this wave function converged to the same geometry as with the TC wave function, except for the 2,5- isomer which did not retain its cyclic structure. Thus, it is apparent that the interaction between the nitrogen lone pair and the adjacent radical center contributes negatively to the stability of these systems.

## REFERENCES



1. den Hertog, H. J.; van der Plas, H. C. *Advan. Het. Chem.* 1965, 4, 121.
2. Kauffmann, Th. *Angew. Chem. (Intern. Ed. Engl.)* 1965, 4, 543.
3. Hoffmann, R. W. "*Dehydrobenzene and cycloalkynes*" Academic Press, New York 1967.
4. Kauffmann, Th.; Wirthwein, R. *Angew. Chem. (Intern. Ed. Engl.)* 1971, 10, 20.
5. Reinecke, M. G. in "*Reactive Intermediates, vol. 2*" Abramovitch, R. A. ed., Plenum Press, New York 1981.
6. Reinecke, M. G. *Tetrahedron* 1982, 38, 427.
7. van der Plas, H. C.; Roeterdink, F. in "*The Chemistry of Functional Groupes, Supplement C: The Chemistry of Triple Bonded Functional Groups*" Patai, S.; Rapport, Z. eds. John Wiley and Sons, New York 1983.
8. Brown, R. F. C.; Crow, W. D.; Solly, R. K. *Chem. Ind. (London)* 1966, 343.
9. Cava, M. P.; Mitchel, M. J.; Dejongh, D. C.; van Fossen, R. Y. *Tetrahedron Letters*, 1966, 2947.
10. Reinecke, M. G.; Newsom, J. G.; Chen, L.-J., *J. Am. Chem. Soc.* 1981, 103, 2706.
11. Sio, F.; Chimichi, S.; Nesi, R. *Heterocycles*, 1982, 19, 1427.
12. Krammer, J.; Berry, R. S. *J. Am. Chem. Soc.* 1972, 94, 8336.
13. Radom, L.; Nobes, R. H.; Underwood, D. J.; Lee, W.-K. *Pure*

1. der Herrsch...
2. 1900, 4. 1901
3. Kautsky, 1. 1902, 2. 1903
4. Kautsky, 1. 1904, 2. 1905
5. Kautsky, 1. 1906, 2. 1907
6. Kautsky, 1. 1908, 2. 1909
7. Kautsky, 1. 1910, 2. 1911
8. Kautsky, 1. 1912, 2. 1913
9. Kautsky, 1. 1914, 2. 1915
10. Kautsky, 1. 1916, 2. 1917
11. Kautsky, 1. 1918, 2. 1919
12. Kautsky, 1. 1920, 2. 1921
13. Kautsky, 1. 1922, 2. 1923

- & *Appl. Chem.* 1986, 58, 75.
14. Dewar, M. J. S.; Kuhn, D. R. *J. Am. Chem. Soc.* 1984, 106, 5256.
  15. Dewar, M. J. S.; Ford, G. P. *J. Chem. Soc. Chem. Comm.* 1977, 539.
  16. Yonezawa, T.; Konishi, H.; Kato, H. *Bull. Chem. Soc. Jap.* 1969, 42, 933.
  17. Adam, W.; Grimison, A.; Hoffmann, R. *J. Am. Chem. Soc.* 1969, 91, 2590.
  18. Jones, H. L.; Beveridge, D. L. *Tetrahedron Letters* 1964, 1577.
  19. H.-H. Nam; Leroi, G. E. *J. Am. Chem. Soc.* 1988, 110, 4096.
  20. Theoretical calculations (RHF, GVB and ROHF with 3-21G basis set) on 1,2-, 1,3-, and 1,4-DHB have been carried out independently for this dissertation.
  21. Pang, F.; Pulay, P.; Boggs, J. E. *J. Mol. Struct. (THEOCHEM)* 1982, 88, 79.
  22. Wiberg, K. B.; Walters, V. A.; Wong, K. N.; Colson, S. D. *J. Phys. Chem.* 1984, 88, 6067.
  23. Sorensen, G. O.; Mohlen, L.; Rastrup-Andersen, N. *J. Mol. Struct.* 1974, 20, 119.
  24. Rigby, K.; Hiller, I. H.; Vincent, M. *J. Chem. Soc., Perkin Trans. II* 1987, 117.
  25. Wentrup, C.; Lorenčak, P. *J. Am. Chem. Soc.* 1988, 110, 1880.
  26. Rapi, G.; Sbrana, G. *J. Am. Chem. Soc.* 1971, 93, 5213.



27. den Hertog, H. J.; Boer, H.; Streef, J. W.; Vekemans, F. C. A.; van Zoest, W. J. *Rec. Trav. Chim. Pays-Bas.* 1974, 93, 195.
28. Newkome, G. R.; Sauer, J. D.; Staires, S. K. *J. Org. Chem.* 1977, 42, 3524.
29. Noell, J. O.; Newton, M. D. *J. Am. Chem. Soc.* 1979, 101, 51.







MICHIGAN STATE UNIV. LIBRARIES



31293005820364